

ICE FORMATION IN SALINE SOILS

Report Submitted

to

SUPPLY AND SERVICES CANADA

HULL, QUEBEC

(DSS File No. 63SS.23233-7-1080)

Prepared by

**J.- M. Konrad, Ph.D., P.Eng.
Dept. of Earth Sciences
University of Waterloo
Waterloo, Ontario, N2L-3G1**

March, 1989

DISCLAIMER

The Waterloo Research Institute, University of Waterloo, assumes no liabilities for the use of, or damages resulting from the use of any information, apparatus, method or process resulting from the work described in this report.

EXECUTIVE SUMMARY

This report presents the results of an experimental study conducted at the Watfrost laboratory of the University of Waterloo under the supervision of Dr. J.- M. Konrad in order to determine the freezing characteristics of a saline clayey silt subjected to various overburden pressures. An understanding of the frost-heave and ice-segregation behaviour of soils that contain saline pore water is important to the development of offshore petroleum and gas resources, especially with respect to transport of chilled gas from offshore to onshore, where a transition zone of variable salinity will have an impact on pipeline performance during its lifespan.

The report provides a description of equipment used at UW, soil sample properties before freezing, (i.e. the unfrozen consolidated soil), actual test conditions, test results, post-freezing data and comments with respect to the test results.

The report has been separated in three volumes. Volume 1 contains the main findings of the study and some typical examples of interpretation of test data. Volume 2 contains all data of test Series 1 which comprised a total of 27 samples frozen under zero applied surcharge but at different initial pore water salinities. Volume 3 contains all the data of test Series 2 which comprised a total of 13 samples frozen under applied surcharges of 50, 100 and 130 kPa and different salinities. The maximum surcharge is equivalent of about 7 m overburden.

The concept of segregation potential introduced by Konrad and Morgenstern (1980-84) for clayey silts with negligible salinity appears to be applicable to clayey silts with pore water salinities approaching 35 g/l, which is the salinity of sea water. Segregation Potential is defined as the ratio of water intake rate and temperature gradient in the frozen soil near the frost front, both quantities being obtained from a well-controlled freezing test.

In order to develop a predictive frost heave model for field conditions, it was shown by Konrad and Morgenstern that representative values of SP must be used in a coupled heat and mass transfer formulation. The relevant value of SP can be obtained from step-freezing test at the onset of the formation of the final ice lens where the rate of cooling is close to field conditions and the freezing still in transient conditions, similarly to the field. Solute concentration near the final ice lens must therefore also be determined at the onset of its formation, which requires correction of the salinity determined at the end of testing, owing to solute enrichment during the growth of the final ice lens.

A set of constitutive equations characterizing frost heaving in saline soils were established as a function of pore water salinity, applied surcharge and segregation potential. To be consistent, each of these parameters must correspond to the onset of formation of the final ice lens. The relationship between SP_{t0} and pore water salinity, S , was of the form:

$$SP_{t0} = E(P_e) - F(P_e) \ln S$$

where E and F are soil constants for a given applied surcharge, P_e .

The relationship between SP_{t0} and applied surcharge can be expressed as:

$$SP_{t0} = G(S_w) \exp -H(S_w).P_e$$

where G and H are soil constants for a given pore water salinity.

The constitutive equations are shown in figures A and B, with the respective values of the soil constants.

This study has also led to the following observations. Although these observations are well supported by the experimental data, no systematic study was undertaken to fully explore the mechanisms involved in each phenomenon.

1. Solute rejection appears to be dependent upon rate of cooling. For high rates of cooling, (i.e. in the early phase of transient freezing) salinity profiles in the frozen soil after freezing revealed that there was little change in pore water salinity with respect to the initial pore water salinity of the unfrozen soil. More tests are required to determine the relationship between rate of cooling and degree of solute exclusion as water freezes.

2. It was also observed that solute migration occurred in the frozen soil when the samples were subjected to large temperature gradients. Furthermore, it appears that this phenomenon was also dependent upon the initial pore water salinity. Higher pore water salinities led to significant solute redistribution in the frozen soil whereas for lower initial pore water salinities, redistribution was almost negligible over the duration of freezing. This observation may be significant for field conditions where temperature gradients across the frozen soil may be sustained for tens and even thousands of years. More studies are required to establish the constitutive equations governing solute transfer in low permeability frozen saline soils.

3. Similarly to the freezing point depression in saline water, segregation-freezing temperatures in a saline clayey silt are also dependent on pore water salinity. In general, it was observed that the temperature of ice lens initiation decreased with increasing pore water salinity. Further research is required in order to develop a mechanistic model of rhythmic ice lens initiation and limited growth in saline soils.

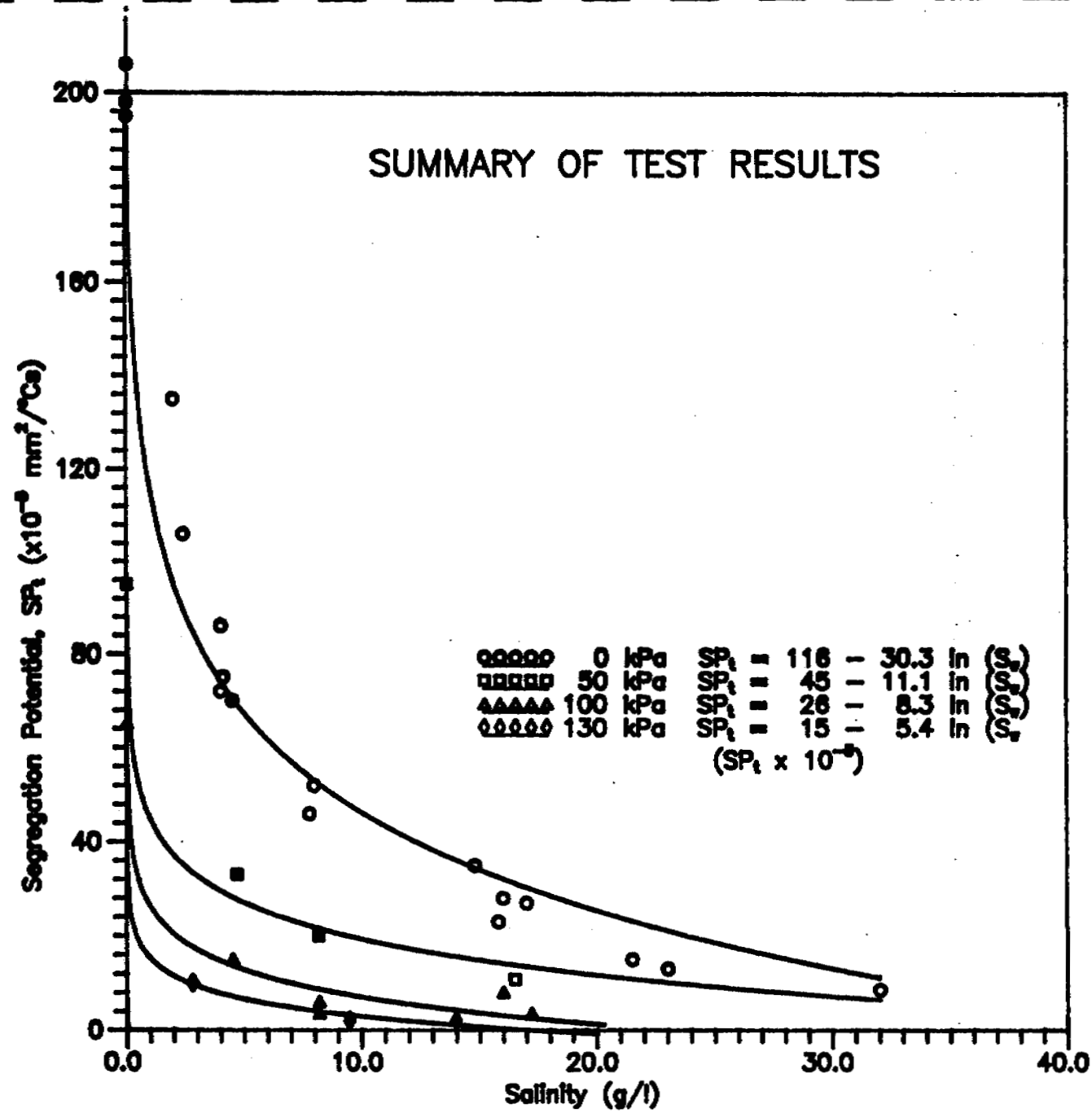
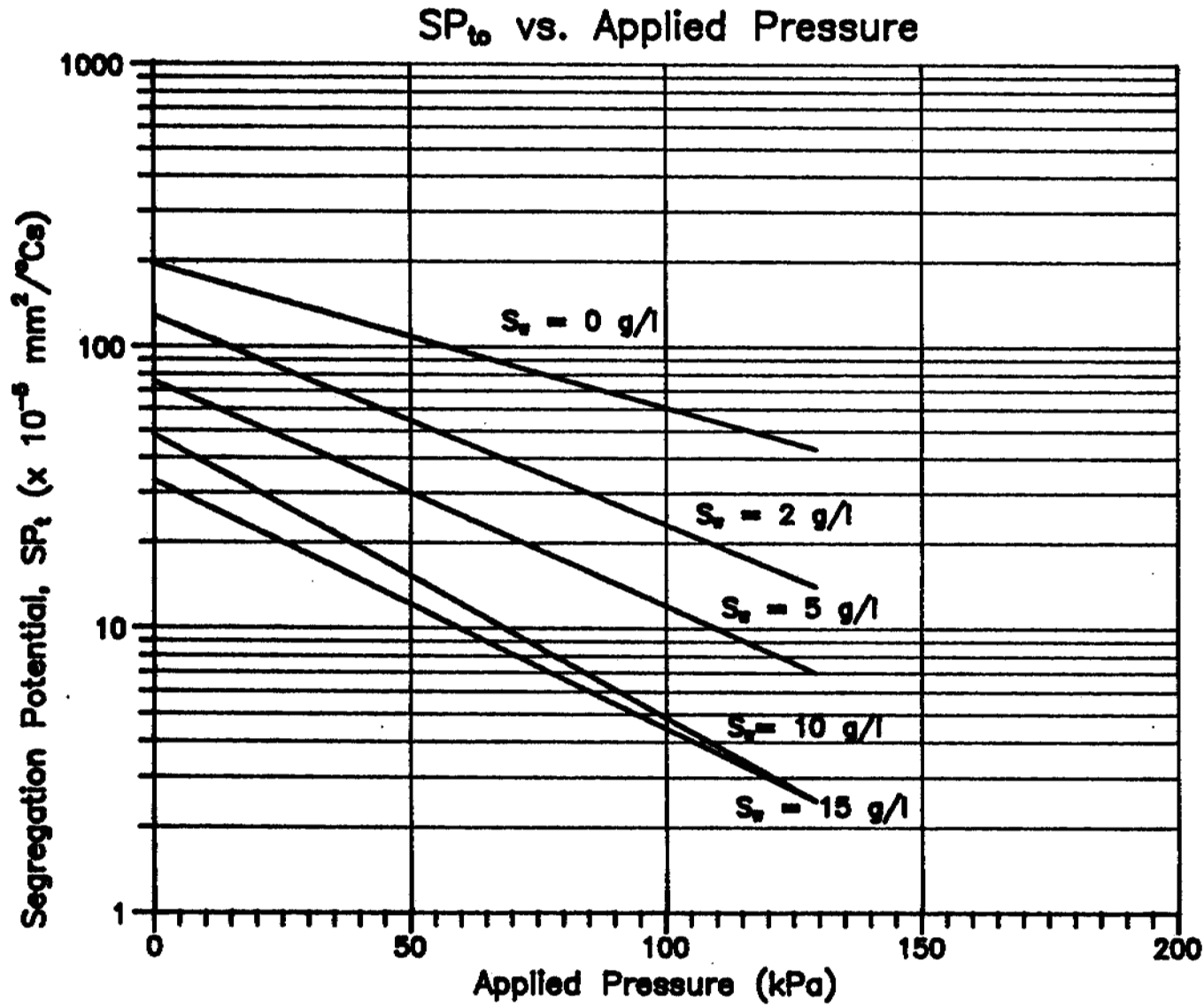


Fig. A



S_v (g/l)	SP_t ($\text{mm}^2/^\circ\text{Cs}$)
0	$195 \times 10^{-5} e^{-.0117P}$
2	$128 \times 10^{-5} e^{-.0171P}$
5	$75 \times 10^{-5} e^{-.0184P}$
10	$48 \times 10^{-5} e^{-.0229P}$
15	$33 \times 10^{-5} e^{-.0200P}$

FIG. B

ACKNOWLEDGEMENTS

The principal investigator gratefully acknowledges the conscientious efforts and dedication of the Waterloo Co-op students who conducted laboratory tests as well as data interpretation. Mr. R. Coutts deserves special mention for being responsible for establishing Watfrost and its fully automatic data acquisition system. He also programmed the various software needed for data interpretation in terms of segregation potential and derived parameters. This report was ready in time owing to the tremendous organization skills of Mr. J.T.C. Seto who was able to process the data and prepare all the figures as well as conducting most of the tests of Series 2. Thanks are also extended to Mr. A. Mc Cammon, Graduate student, who participated in the research program and provided invaluable data on solute redistribution from his one-dimensional model. The author would also like to express his sincere thanks to Mr. C.W. Flowers, Watfrost technician, who assisted in the laboratory work.

Devon clayey silt was kindly provided by Dr. D. Segó (U. of Alberta) and the clay mineralogy analyses were performed by Dr. J. Locat (U. Laval). Invaluable discussions with Dr. E. Reardon (UW) were greatly appreciated. Advice and continuous encouragement of Dr. D. Harry (EMR) and Mr. S. Dallimore (EMR), scientific advisors for this contract, facilitated the communication between the parties involved and ensured the success of this research. Dr. P. Kurfurst (EMR) participated also in many discussions during the different review meetings. Finally, I would like to thank Mr. A. Heggibottom (GSC/EMR) for his support during the last years.

TABLE OF CONTENTS

EXECUTIVE SUMMARY

ACKNOWLEDGEMENTS

1.	INTRODUCTION	1
	1.1 General	1
	1.2 Objectives	1
	1.3 Scope of Work	2
2.	TEST PROCEDURES	2
	2.1 Sample Preparation	2
	2.2 Freezing Tests	3
	2.3 Analysis of Frost Heave Data	3
	2.4 Geochemical Analysis	6
	2.5 Testing Program	7
3.	EXPERIMENTAL RESULTS	10
	3.1 Freezing Tests with Zero Applied Surcharge	10
	3.2 Freezing Tests with Applied Surcharge	12
4.	DISCUSSION	17
	4.1 Rate of Ice Lens Growth in the Field	17
	4.2 Problems with Frost Heave Testing in Saline Soils	18
5.	CONCLUSIONS	19
6.	REFERENCES	21

APPENDIX 1 - Soil Properties

APPENDIX 2 - Freezing Cells

APPENDIX 3 - Salinity Measurements

APPENDIX 4 - Freezing Test Results (Series 1) in Volume 2

APPENDIX 5 - Freezing Test Results (Series 2) in Volume 3

1. INTRODUCTION

1.1 General

In the Arctic Coastal Plain of North America, massive ground ice is frequently encountered both near the surface and at depths extending well below 20 m. Most of this material is attributed to ice segregation following the emergence of the sites above sea level. Recent information has shown that saline soils are far more widespread in Northern Canada communities than had been expected. Furthermore, Permafrost, often thought to be found only on land, can be found at some locations beneath the sea bed of the Beaufort Sea.

The mechanics of formation of Permafrost in saline soils under natural conditions or induced by operating offshore chilled pipelines buried in unfrozen soils may differ substantially from that of segregated ice formation in soils in fresh water environments. On one hand, the salinity of the pore water depresses the freezing point of the water. On the other hand, solutes are excluded from the ice at two locations: (a) from the pore ice which freezes at the T_i isotherm (the warmest temperature at which ice can form) and (b) from the segregated ice lens at the T_s isotherm (the segregation-freezing temperature). This solute exclusion process leads to significant increases in solute concentrations below these isotherms, affecting the pore ice content and depressing the freezing point of the pore water even further.

The physics of freezing in saturated saline soils is thus complex. An understanding of the frost-heave and ice-segregation behaviour of soils that contain saline pore water is important to the development of offshore petroleum and gas resources, especially with respect to transport of chilled gas from offshore to onshore, where a transition zone of variable salinity will have an impact on pipeline performance over its lifespan.

1.2 Objectives

Despite extensive research in recent years such as Chamberlain (1983), Hallet (1978), Mahar et al. (1983), little is known of ice segregation processes in saline soils that would lead to the development of a frost heave model for pipeline design. Chamberlain (1983) speculated that, from a mechanistic point of view, the effect of seawater in a clayey soil would cause the formation of a thick active freezing zone with many ice lens growth sites, each with its own brine concentration. However, no systematic study was undertaken to determine the engineering characteristics needed as an input to a coupled heat and mass transfer model leading to the prediction of frost heave or ice content in saline soils subjected to freezing.

The primary objective of this project is to obtain a complete and consistent data bank of frost heave characteristics of a clayey silt saturated with water at different initial salt contents. The frost heave data are obtained from one-dimensional freezing tests on reconstituted soil samples in the laboratory. Konrad and Morgenstern (1980,81,82,83,84) and Konrad (1987,89) established that the segregation potential, SP, defined as the ratio of water intake rate to temperature gradient in the frozen soil near the frost front, is a suitable parameter which appears to incorporate the major factors controlling the process of frost heave in soils saturated with fresh water.

It is proposed to characterise frost heaving in saline soil using the concept of the segregation potential. A number of factors, however, influence segregation potential (void ratio, soil structure, mineralogy, freeze-thaw history, rate of cooling, applied surcharge,...). This project investigates solely ice lens formation in a clayey silt with different pore water salinities and subjected to different applied surcharges in order to simulate various environments at different depths.

1.3 Scope of Work

The result of the present research will be used to extend the concept of segregation potential to saline soils in order to develop in a later phase a predictive model for field problems which can be readily used by design engineers. The knowledge of the laws of ice formation in saline environments can also be used by geologists to investigate the nature of shallow and deep subsea Permafrost as well as the climatic conditions required for its formation.

2. TEST PROCEDURES

In order to address Canadian issues near the coastal zone of the Beaufort Sea, frost-susceptible soil was obtained from Devon, Alberta. The characteristics of Devon clayey silt are very similar to the fine-grained soils found in the Mackenzie delta.

2.1 Sample Preparation

The soil bags were thoroughly mixed to obtain uniform conditions. Soil properties are as follows: liquid limit = 31 %, plastic limit = 24 %, specific gravity = 2.80. The grain size distribution (App. 1) indicates that the amount of clay size particles is approximately 26 % by dry weight. X-ray diffraction analyses reveal that the clay size fraction is composed of quartz and feldspar particles and that the clay minerals consist mainly of smectite and dolomite with some traces of chlorite, illite and calcite. The influence of saline water at different NaCl concentrations on the liquid and plastic limits of Devon soil is negligible as shown in App. 1. Appendix 1 summarizes the physical properties of Devon clayey silt.

The clayey silt samples were prepared by consolidating under static load a slurry at an initial water content of about 1.5 times the liquid limit. The slurry, which is a mixture of air-dried Devon clayey silt and deionized water mixed with NaCl salt at given initial concentrations, is allowed to stand overnight.

Consolidation of the slurry to 130 kPa (simulating a maximum overburden of about 7 m) was performed in three stages as shown in Fig. 1, of 30, 80 and 130 kPa, respectively. The axial deformation was monitored automatically with a displacement transducer. The settlement is readily converted into vertical strain by dividing it by the initial height of the sample (prior to the first load increment application).

Depending on the testing conditions, the samples were allowed to rebound under a constant applied pressure of 0, 50, 100 and 130 kPa with free access of water at both ends.

2.2 Freezing Tests

The samples were allowed to reach thermal equilibrium prior to freezing. The initial temperature corresponded to the warm plate temperature controlled by the refrigerated bath within ± 0.02 °C.

The samples were then subjected to a step-freezing condition where the temperature of the bottom plate was lowered below the freezing temperature of the pore water, while the top plate was maintained at the original temperature, i.e. the initial temperature of the sample after thermal conditioning. The cold plate temperature was also maintained constant with time. In such freezing tests a period of decelerating frost penetration prevails during transient freezing followed by a period during which a major ice lens is growing.

The samples were frozen from the bottom up. This freezing procedure results in a reduction of side friction with time that is proportional to the reduction in the thickness of the unfrozen soil column pushed upwards during heaving when frost heave tests are conducted with an applied surcharge. Free access to water was permitted at the top. The intake water was at the same salinity than the water used to mix the initial slurry.

Total heave recorded by a displacement transducer (LVDT) is automatically stored by the acquisition system and personal computer. Readings are taken every hour. Water intake is recorded manually, thus at a much lower frequency as total heave. Water intake measurements were used to verify that water was available and that no leaks occurred during freezing. The water level in the burette was maintained between 5 and 15 cm above the sample's top. Finally, thermistors embedded in the freezing cell's wall (see Plates in Appendix 2) were monitored continuously and recorded every hour.

At the end of the freeze test, the sample was probed to determine the thawed length. Photographs were taken on both sides of the sample. The thickness of the final ice lens was measured.

Water contents were obtained for horizontal slices of about 5 to 10 mm thickness in both frozen and unfrozen parts of the samples.

Pore water salinity was determined from horizontal slices using the procedure described in Section 2.4 and Appendix 3.

2.3 Analysis of Frost Heave Data

One-dimensional step-freezing tests conducted on saturated fine-grained soil consolidated from slurries obtained by adding distilled water to dry soil have shown that the migration rate of the intake water at the onset of the formation of the warmest ice lens, v_0 , was proportional to the temperature gradient in the frozen fringe (Grad T). This relationship was valid provided that the same suction exists at the frozen-unfrozen interface (Konrad and Morgenstern, 1980-84). The relationship was established theoretically and confirmed by experiments as shown on Fig. 2. This linear relationship can be expressed as:

$$v_0 = SP_0 \text{ Grad } T$$

where

SP_0 is a constant for a given suction at the frost front and is termed the segregation potential near thermal steady state.

The advantage of using SP to characterize any freezing soil is that no assumptions on the segregation-freezing temperature, the hydraulic conductivity of the frozen soil, and the osmotic pressure due to solutes are required. It is simply the ratio of two measurable quantities: Water intake rate and temperature gradient derived from thermistor output. Another important advantage is that the thermal boundary conditions do not have to be the same in each test, since water intake rate is normalized with respect to the temperature gradient. This is especially of value when dealing with saline soils where the freezing point depression caused by the solutes may require different cold plate temperatures in order to achieve similar length of unfrozen soil near thermal steady state.

Because water intake was not automatically monitored, it is proposed to calculate the segregation potential based on total heave measurements as:

$$dh/dt = SP_t \text{ Grad } T$$

where dh/dt = total heave rate
 SP_t = SP derived from total heave measurements

At the onset of the final ice lens, there is no further frost penetration and total heave is then equal to the heave resulting from the growth of the final ice lens. Therefore:

$$SP_0 = SP_{t0}/1.09$$

Since total heave and temperature data are stored on a floppy disk every hour, software developed at the University of Waterloo readily permits calculation of these derived parameters over time. The software used for the interpretation of the freezing test data calculates all slopes using a 7 point polynomial regression approach. It is noteworthy to mention that the shape of these curves is very sensitive to the frequency of data acquisition. Higher recording frequency will result in more variation in the derived parameters if consecutive data points (i.e. heave and temperature) display some variations. The variation in derived parameters would be worse if the slope was obtained from two consecutive points only.

Figs. 3 to 7 present the frost heave data for test S10 which was prepared from a slurry obtained with water at a salinity of 1.72 g/l (0.03 mol/l). Fig. 3 presents the temperature across the sample with elapsed freezing time and Fig. 4 shows the resulting total heave with time.

Figs 5 and 6 show the position of the frost front with elapsed freezing time and present the interpretation of these frost heave data in terms of SP_t , respectively.

Fig. 5 gives the length of unfrozen soil (T_i °C isotherm from Fig. 11) and the position of the top of the sample with elapsed time. While this plot does not represent the laboratory conditions where the unfrozen soil is pushed upwards, it is still showing the actual thickness of frozen and unfrozen soil except that the warm side is considered as a reference. This type of plot is similar to the actual frost penetration in the field where the ground is frozen from the surface downwards. The main advantage of Fig. 5 is that a stable frost front with time is characterized by a horizontal line. Therefore, one can readily see that thermal steady state conditions were reached after about 26 hours of freezing.

Fig. 6 shows the variation of SP_t during transient freezing (first 26 hours) and during the growth of the final ice lens. The value of interest is that corresponding to the onset of the formation of the final ice lens, which occurs slightly before thermal steady state is reached. The actual time corresponding to the onset of the formation of the final ice lens can be inferred from the measured thickness of this lens at the end of the

test. The time at which the warmest ice lens was initiated is then obtained by subtracting its thickness from the maximum total heave. For sample S10, the thickness of this ice lens was 2.5 mm, which suggests that the time of its formation was approximately 24 hours. This is in close agreement with the temperature data. Thus the segregation potential at the formation of the final ice lens for test S10 is equal to $106.10^{-5} \text{ mm}^2/\text{s} \cdot ^\circ\text{C}$.

It should be noted that for an elapsed freezing period less than 26 hours, heat flow through the sample is transient (unsteady conditions). During transient freezing, SP_t from total heave comprises both heave from in-situ pore water and from migratory water freezing. Since the rate of frost penetration decreases steadily with time in step freezing tests, the contribution of in-situ pore water freezing decreases also with time. At the onset of the formation of the final ice lens, (i.e. near thermal steady state) migratory water solely contributes to frost heaving. During transient freezing, it is therefore expected that there is a significant decrease in SP_t with time.

After 26 hours of freezing, thermal steady state is reached and the final ice lens grows. For these conditions, Konrad (1987) showed that the rate of ice lens growth was solely related to the rate of net heat extraction. Since the temperature boundary conditions are constant in step freezing tests, the rate of net heat extraction decreases as the sample heaves. Furthermore, the freezing system is then extremely sensitive to variation in lateral heat flow into the sample, which results in a variation in net heat extraction rate. It is thus expected that SP_t continues to decrease during the growth of the final ice lens. In some cases, cell insulation was insufficient and caused fluctuations in wall thermistor readings, which, in turn, produced wavy SP curves.

It must be emphasized that the concept of segregation potential is only applicable during transient freezing and should not be used to predict the rate of growth of the final ice lens.

Fig. 7 shows the temperature gradient across the sample and compares the position of the frost front to the observed position of the warmest side of the final ice lens. The close agreement confirms the adequacy of the thermistor's calibrations.

The salinity in the unfrozen soil was obtained by squeezing the pore water out of the soil using a hydraulic squeezer. The measured pore water salinity (see Section 2.4) was 2.4 g/l, which is an average salinity in the unfrozen soil. It is higher than the salinity of the water used to mix the slurry since there has been an enrichment of solutes near the final ice lens caused by solute rejection at the ice lens. The squeezing technique was lengthy and produced an average salinity in the unfrozen soil. A different technique was used for other samples, which permitted the determination of a detailed salinity profile in both the frozen and unfrozen zones of the samples. This technique is described in the next Section.

2.4 Geochemical Analysis

A brief general procedure for determining soil pore water salinity will be presented here. A detailed procedure is given in Appendix 3.

It has long been known that the electrical conductivity or conductance (the inverse of electrical resistance) of an electrolyte solution varies with the concentration and nature of the dissolved solutes. The electrical conductivity of a solution was measured using a YSI Model 35 Conductance meter with a probe featuring a 10 mm electrode spacing.

Fig. 8 shows the relationship between conductance and actual salinity of a solution obtained by mixing a known quantity of NaCl salt to a known volume of distilled water. In order to readily obtain the pore water salinity from conductance measurements, the following equation was fitted to the experimental data:

$$S = S_0 (C/C_0)^A$$

where
 S = Salinity (g/l)
 C_0 = conductance at a salinity equal to S_0
 A = constant

For the salt used in the present experiments, $C_0 = 1.0$ mmho, $S_0 = 0.52808$ g/l and $A = 1.12586$.

One method to obtain pore water from a consolidated soil sample is by subjecting the sample to further consolidation using a squeezer. A major limitation of this technique is that rather small volumes of water are produced, even when the samples are fully saturated. Furthermore, pore water is extracted from the whole unfrozen part and is thus an average value.

Another possible method to determine the salinity of pore water of a given soil is to immerse a given mass of soil into a given volume of distilled water and allow solutes of the pore water to diffuse into the surrounding fluid until equilibrium is attained. The measurement of the conductivity of the diluted water mixture can then be related to its concentration using the above mentioned simplified conductance equation. The initial pore water salinity is then back-calculated, knowing the initial water content, the dilution ratio (i.e. the ratio of total volume of water to the volume of pore water) and the salinity of the diluted water. This is expressed by:

$$S_w = D.S_d$$

where:
 S_w = Salinity of pore water
 S_d = Salinity of diluted water
 $D = (V_w + V_a)/V_w$, dilution ratio
 V_w = volume of pore water in soil sub-sample
 V_a = volume of distilled water added

The total amount of background dissolved solids in the Devon soil is slightly in excess of 0.1 g/l (see Appendix 3) and was neglected in the salinity analysis.

In order to obtain the salinity profile after freezing, the following steps were taken:

1. Determine C_d (diluted solution)
2. Calculate salinity of diluted solution, S_d , from conductance function
3. Calculate salinity of pore water : $S_w = S_d \cdot D$

All the salinity profiles incorporate the error introduced by the dilution ratio considering an accuracy of conductance measurements of ± 0.05 mmho. The salinity profiles present therefore the lower and upper values corresponding to the actual value of the dilution ratio. Typically, for a dilution ratio of 25, the absolute error in salinity associated with an accuracy of ± 0.05 mmho is ± 0.40 g/l (see Appendix 3).

Figs. 9 and 10 show the water content profile and the salinity profile of sample S34 mixed with water at a salinity of 0.15 mol/l or 8.65 g/l. Fig. 9 indicates that the water content is uniform throughout the sample, suggesting that the consolidation procedure is adequate for reconstituting samples from slurries. Fig. 10 shows that the salinity profile is also uniform throughout the sample and that the minimum value of the pore water salinity is 8.0 g/l and the maximum value 9.0 g/l, suggesting an average value for the pore water salinity of 8.5 g/l. The close agreement between the measured salinities and the input salinity demonstrate clearly that the solute extraction method can be used to adequately monitor the salinity profile across the sample after freezing. Furthermore, this technique permits the determination of the pore water salinity every 5 mm in the unfrozen soil and every 1 cm in the frozen soil. Identical conclusions were obtained for samples S22 and S48, mixed at initial salinities of 3.44 and 16.5 g/l, respectively. The inferred average pore water salinity of these samples (App. 3) was 3.5 and 17.0 g/l for S22 and S48, respectively.

2.5 Testing Program

In order to obtain the relationship between segregation potential at the onset of the formation of the final ice lens, SP_{to} , applied surcharge, P_e , and pore water salinity, S_w , the following laboratory testing program was performed in two Series.

Series 1 comprised a total of 27 tests in which samples at different pore water salinities were frozen under zero applied surcharge. It is well known that an applied surcharge reduces frost heave. Consequently, test Series 1 yields an upper bound of the frost heave characteristics of Devon clayey silt at a water content of about 26 to 28 % of dry weight. The conditions of each freezing test of Series 1 are summarized in Table 1.

Series 2 comprised a total of 13 tests in which samples at different pore water salinities were also subjected to various applied surcharges. During a single freezing run, the applied surcharge was maintained constant. The conditions of each test of Series 2 are given in Table 2.

These tables give the dimensions of each sample prior to consolidation and at the end of primary consolidation and rebound under the testing surcharge. The temperature boundary conditions are also indicated. The salinity of the water used for the slurry can be compared to the pore water salinity S_w measured in the unfrozen soil near the warm plate at the end of freezing. The difference in salinity gives an estimate of the accuracy in the salinity measurements. In general, the difference is very small, but may, in some cases, reach 1.0 g/l. This is consistent with the effects of dilution ratio and accuracy in conductance measurements on pore water salinity as discussed in Section 2.4.

Table 1. Summary of Testing Conditions of Series 1. (No Applied Surcharge)

Test #	Height(mm)		Diam. (cm)	T cold Deg. C	T warm Deg. C	Salinity g/l	S _w g/l	Remarks
	Ini.	End						
S1	112	90	5	NA	NA	0	0	Preliminary Run
S2	110	88	5	NA	NA	0	0	Preliminary Run
S3	130	103	5	-2.75	+0.85	0	0	
S4	166	133	10	-4.20	+1.00	0	0	
S5	159	124	10	-4.60	+1.80	0	0	
S10	140	112	5	-2.75	+1.10	1.72	2.4	end of test
S11	118	94	5	-3.20	+2.50	1.72	2.2	
S12	158	125	10	-5.20	+1.10	3.44	3.5	
S20	145	116	5	-2.90	+0.80	3.44	4.0	end of test
S21	133	101	5	-4.70	+2.25	3.44	3.7	
S30	144	111	5	-2.90	+0.60	8.25	7.8	end of test
S31	137	106	5	-3.25	+0.80	8.65	8.2	
S32	148	114	5	-9.50	+5.00	8.65	8.0	
S33	110	86	5		Melted during testing			
S40	131	103	5	-2.70	+0.40	17.3	17.0	end of test
S41	131	104	5	-3.50	+0.90	16.5	15.1	
S42	130	108	5	-9.80	+5.30	17.3	17.0	
S43	132	108	5	-4.60	+2.20	16.5	16.2	
S44	145	113	5	-4.60	+2.90	16.5	15.6	
S45	100	78	5	NA	NA	16.5	NA	Power Failure
S46	128	107	5	-4.50	+2.50	16.5	15.0	
S50	157	118	5	-2.90	+0.80	26.1	NA	
S52	144	108	5	-5.90	+1.90	26.1	25.6	
S60	145	105	5	Var.	Var.	33.0	29.0	Several steps
S62	146	106	5	-5.60	+1.75	33.0	29.0	
S70	125	100	5	-5.20	+1.95	0.9	1.5	
S71	129	104	5	-5.90	+1.90	2.6	3.0	

Table 2. Summary of Testing Conditions of Series 2. (Applied Surcharge)

Test #	Height(mm)		Diam. (cm)	T cold Deg. C	T warm Deg. C	Salinity g/l	S _w g/l	Surcharge kPa
	Ini.	End						
SAP1	120	100	10	- 5.65	+ 2.80	8.0	7.2	50
SAP2	133	109	10	- 5.90	+ 2.40	8.0	7.5	100
SAP2R	126	106	10	- 6.10	+ 2.45	8.0	8.0	100
SAP3	128	107	10	- 5.75	+ 2.50	8.0	7.7	130
SAP4	133	103	5	- 4.30	+ 1.50	16.5	15.7	60
SAP5	134	106	5	- 4.60	+ 2.10	16.5	15.2	100
SAP6	130	110	10	- 5.90	+ 2.00	15.0	13.5	130
SAP5R	131	105.4	10	- 5.90	+ 2.00	16.5	15.7	100
SAP7	139	117	10	- 5.80	+ 2.40	2.0	2.4	130
SAP8	151	120	10	- 5.40	+ 1.00	3.34	3.2	50
SAP9	156	123	10	- 5.65	+ 1.20	3.34	3.5	100
SAP10	168	124	10	- 4.40	+ 1.10	0	NA	50
SAP11	167	120	10	- 4.20	+ 2.00	0	NA	100

3. EXPERIMENTAL RESULTS

3.1 Freezing Tests with Zero Applied Surcharge.

3.1.1 Typical Test Results

The results of the freezing tests of Series 1 are presented in this Section. They are interpreted in terms of the segregation potential prevailing at the onset of the formation of the final ice lens and as a function of salinity. Each test is supported by a comprehensive set of graphically presented data as follows:

- a. Consolidation data
- b. Temperature vs time
- c. Total heave vs time
- d. T_i isotherm vs time
- e. SP_t vs time
- f. Temperature profile at the onset of formation of the warmest ice lens and observed location of the ice lens
- g. Water content profile at the end of test
- h. Salinity profile at the end of test

T_i is the warmest temperature at which ice can exist in the soil pores. T_i is thus a function of pore size and pore water salinity. The freezing point depression is very sensitive to salinity as shown in Fig. 11. The computer program takes the value of T_i corresponding to the salinity of the pore water after consolidation.

Typical results for Sample S12 are given in Figs. 12 to 19. The cold plate was maintained at a temperature of $-5.2\text{ }^\circ\text{C}$ and the warm plate was at $+1.1\text{ }^\circ\text{C}$ for a freezing period of 93 hours. Thermal steady state was reached after 37 hours of freezing. The final ice lens is always initiated while the system is still in transient freezing, i.e. slightly before reaching thermal steady state. This is confirmed by the observation of the thickness of the final ice lens (plate 1). It should be noted that the final ice lens is not always a compact body of ice. Depending on soil variability, heat flux and pore water salinity on a microscopic scale, the final ice lenses may engulf some soil. This was the case for sample S12 where the final ice lens contained some soil. Its thickness is then taken as the sum of each lens. For sample S12, the total thickness was approximately 4.0 mm. The total heave plot shown in Fig. 13 suggests then that the time of ice lens initiation was 32 hours. Plot 16 yields thus a value for SP_{t0} of $70.10 \cdot 10^{-5}\text{ mm}^2/\text{s} \cdot ^\circ\text{C}$

The interpretation of frost penetration with time (Fig. 15) suggests that the length of unfrozen soil at the end of test should be 27 mm. Plate 1 shows that the distance between the warm plate and the base of the warmest ice lens is 30 mm, which suggests that the thickness of the frozen fringe is approximately 3 mm. According to the temperature profile, the segregation-freezing temperature, T_s , is thus about $-0.24\text{ }^\circ\text{C}$.

To successfully predict frost heave in the field using the segregation potential concept, SP must be determined from laboratory tests with representative values of suction at the frost front, rate of cooling and overburden pressure (Konrad and Morgenstern, 1983). In the field, frost penetration rates are usually small (less than 1 cm/day), and the average temperature gradients in the frozen soil are also small (less than $0.1\text{ }^\circ\text{C}/\text{cm}$). These conditions result in rates of cooling in the field of about $0.01\text{ }^\circ\text{C}/\text{day}$.

Such low rates of cooling are obtained near thermal steady state in step-freezing tests, at the onset of the formation of the final ice lens. The relationship that we are seeking to use as input in a coupled heat and mass transfer formulation in saline soils is consequently between SP_{T0} and salinity.

Since SP_T corresponds to the onset of the formation of the final ice lens, one must also obtain the salinity in the frozen fringe at the same time. This is not always possible since it means stopping a freezing test as soon as the final ice lens is initiated and determining a salinity profile immediately thereafter. If, however, the test continues and the final ice lens is allowed to grow to a given thickness, saline water is attracted to the ice lens and solutes are excluded at the ice. This, in turn, causes an enrichment in solutes in the frozen fringe and unfrozen soil, which is a function of the diffusivity of NaCl in the pore water. Assuming a given distribution of NaCl concentration with distance from the ice lens, it is possible to calculate the salinity at the base of the final ice lens when it formed. At the end of a freezing test, the salinity profile in the unfrozen zone indicates the maximum salinity at the base of the warmest ice lens, $S(\text{lens})$. Computer simulations using the diffusion equation and a constant rate of solute enrichment at the ice lens show that the increase in solute concentration with time is nearly the same at different distances from the ice lens (Fig. 20). The salinity at the onset of formation of the final ice lens can therefore be calculated as outlined below:

The mass of salt released at the ice lens per unit area during its growth is obtained as:

$$M_{\text{NaCl}} = (e/1.09) \cdot S_{wi}$$

where e = thickness of final ice lens
 S_{wi} = average salinity of pore water near the ice lens

The maximum increase in salinity per unit area at the ice lens during its growth is thus given by:

$$\Delta S = M_{\text{NaCl}} / (n \cdot l_u)$$

where l_u is the length of unfrozen soil corresponding to changes in salinity and n is the porosity.

The salinity at the onset of ice lens formation is thus obtained from:

$$S_{wo} = S_w - \Delta S$$

In order to minimize the error associated with this back-calculation of salinity at the formation of the final ice lens, freezing tests were conducted over a shorter period. The final ice lens was allowed to grow to a thickness of less than 1 mm. The salinity profile at the end of freezing is thus closer to that existing at the onset of the formation of the final ice lens.

Fig. 18 shows the salinity profile obtained at the end of freezing for sample S12. As anticipated, the salt concentration increased in the vicinity of the warmest ice lens. The salinity at the lens was 6.3 g/l. Data points too close to the final ice lens will show lower pore water salinities since the ice is essentially salt-free water. For this reason, the extrapolation of salinity in the unfrozen soil often neglects the data point closest to the ice lens. The backcalculated salinity at the formation of the final ice lens was then found to be 4.5 g/l.

Test S70 is typical of a test in which the final ice lens was readily identifiable as shown on Plate 2. The thickness of the final ice lens was 3.0 mm and the time of its formation was 14 hours after the beginning of freezing. This is in agreement with the frost penetration data shown in Fig. 23. The corresponding SP_{T0} was thus $135 \cdot 10^{-5} \text{ mm}^2/\text{s} \cdot \text{C}$. The extrapolated salinity at the ice lens at the end of freezing was 5.0 g/l (Fig. 26). The back-calculated salinity at the onset of formation of the final ice lens was thus 2.0 g/l. It should be noted that because the temperature boundary conditions are maintained constant during the whole freezing test, thermistor readings along the sample will display a slight but steady decrease in temperature with time since the sample heaves continuously as the ice lenses grow. This, in turn, results in a steady decrease in the overall temperature gradient. Therefore, Fig. 21 shows sloping trends of each thermistor output but Fig. 23 shows a stable frost front, consistent with step-freezing.

3.1.2 Segregation potential vs. Salinity

Table 3 is a summary of the frost heave tests of Series 1 interpreted similarly to tests S12 and S70. All the results are presented in Appendix 4, Volume 2 of this report. Fig. 28 shows segregation potential near thermal steady state, (i.e. extremely small rate of cooling) of fully saturated Devon clayey silt at a water content between 26 and 28 % for various pore water salinities of the frozen fringe. The reduction in SP_{T0} increases with increasing salinities. For example, a salinity of 5 g/l reduces frost heaving by 63 % and a pore water salinity of 15 g/l causes a reduction of SP_{T0} of about 85 %. This figure also indicates that there is no effect of size of the freezing cell. In Fig. 28, open symbols represent tests conducted in the 5-cm diameter cell and full symbols indicate tests in the 10-cm diameter freezing cell.

A best-fit using a logarithmic function was performed on the data points and yielded the following equation, valid for salinities in excess of 0.5 g/l and less than 40 g/l and for Devon clayey silt at water contents between 26 and 29 %, frozen under zero applied surcharge:

$$SP_{T0} = 10^{-5}(116 - 30.3 \ln S)$$

where the units of SP_{T0} are $\text{mm}^2/\text{s} \cdot \text{C}$ and those of salinity g/l.

3.2 Freezing Tests with Applied Surcharge

3.2.1 Typical Test Results

Typical results of test Series 2, referred to as SAP, are given for test SAP1 for an applied surcharge of 50 kPa and an initial pore water salinity of 7.2 g/l as well as for test SAP3 conducted with an applied surcharge of 130 kPa and an initial salinity of 7.7 g/l. The complete results of test Series 2 are given in Appendix 5, Volume 3 of this report.

Typical results for Test SAP1 are given in Figs. 29 to 33. The cold plate was maintained at a temperature of $-5.65 \text{ }^\circ\text{C}$ and the warm plate was at $+2.8 \text{ }^\circ\text{C}$ for a freezing period of 68 hours. Thermal steady state was reached after 23 hours of freezing. The thickness of the final ice lens was 1.3 mm, suggesting that the time of its formation was 21 hours. Plot 32 yields thus a value for SP_{T0} of $20 \cdot 10^{-5} \text{ mm}^2/\text{s} \cdot \text{C}$.

The interpretation of frost penetration with time (Fig. 31) suggests that the length of unfrozen soil at the end of the test ($T_1 = -0.5$ °C for a salinity of 8.0 g/l) should be 37 mm. Plate 3 shows that the distance between the warm plate and the base of the warmest ice lens is 38 mm, which is in close agreement with the thermistor's data.

The salinity profile (Fig. 33) shows that the salinity increased near the ice lens from 7.2 g/l to about 10 g/l at the end of freezing. The back-calculated salinity at the onset of formation of the final ice lens was thus 8.2 g/l. Fig. 33 shows also that the salinity profile in the frozen zone is fairly uniform and is close to the initial pore water salinity. This, in turn, indicates that there is no solute rejection for high rates of frost advance. When the frost front stabilizes and ice lenses form, the overall salinity will show a marked decrease since the water of the ice lenses is essentially salt-free. The salinity profile in the unfrozen soil indicates that solute diffusion occurred only over about 25 mm of soil, which took place for about 40 hours. This appears to be in agreement with theoretical calculations assuming a value for the diffusion coefficient of NaCl in porous media of about 10^{-4} mm²/s.

Sample SAP3 was frozen under an applied surcharge of 130 kPa. In order to minimize temperature fluctuations caused by temperature changes in the environmental chamber, additional insulation was put around the cell. As shown in Fig. 34, the procedure was successful since the temperatures within the sample do not fluctuate with time, despite temperature changes in the cold room. As expected, water was first expelled from the draining end before being sucked into the sample after about 24 hours of freezing. The total amount of water expelled during the first 24 hours of freezing was only about 10 cc, which is equivalent to a change in sample height of approximately 1.3 mm as shown on Fig. 35. Water was also expelled in test SAP1, but only during the first 5 hours of freezing. Thermal steady state was reached after about 26 hours of freezing and the thickness of the final ice lens was 0.4 mm. The segregation potential, SP_{T_0} , was thus $2.0 \cdot 10^{-5}$ mm²/s.°C and the corresponding salinity was 9.5 g/l.

3.2.2 Segregation potential vs. Salinity

Table 4 is a summary of the frost heave tests of Series 2 interpreted similarly to tests SAP1 and SAP3. All the results are presented in Appendix 5, Volume 3 of this report. Fig. 39 shows segregation potential near thermal steady state, (i.e. extremely small rate of cooling) of fully saturated Devon clayey silt at a water content between 23 and 26 % for various pore water salinities of the frozen fringe and for different applied surcharges. For comparison, the results obtained in Series 1, i.e. zero applied surcharge, are also shown on Fig. 39.

As expected, SP_{T_0} is strongly controlled by salinity and applied surcharge. For a given surcharge, SP_{T_0} decreases with increasing salinities. For example, under an applied surcharge of 50 kPa, a salinity of 5 g/l reduces frost heaving by 70 % and a pore water salinity of 15 g/l causes a reduction of SP_{T_0} of about 85 % when compared to a salt free soil freezing under similar conditions. At a surcharge of 100 kPa, the reduction in SP_{T_0} is 80 % and 94 %, respectively. This figure also indicates that there is no effect of size of the freezing cell. In Fig. 39, open symbols represent tests conducted in the 5-cm diameter cell and full symbols indicate tests using the 10-cm diameter freezing cell. The open symbol for the 50 kPa test Series was in fact performed under an applied surcharge of 60 kPa, because the small freezing cell was loaded by dead weights. This slightly higher surcharge will cause a slight reduction in SP_{T_0} as shown on Fig. 39.

A best-fit using a logarithmic function was performed on the data points and yielded the following equations:

$$SP_{t0} = 10^{-5}(45 - 11.1 \ln S)$$

for Devon clayey silt at water contents between 26% and 25%.

Applied surcharge of 50 kPa. This equation is valid for $0.5 < S < 40$ g/l.

$$SP_{t0} = 10^{-5}(26 - 8.3 \ln S)$$

for Devon clayey silt at water contents between 25% and 24 %.

Applied surcharge = 100 kPa. Valid for $0.5 < S < 24$ g/l

$$SP_{t0} = 10^{-5}(15 - 5.4 \ln S)$$

for Devon clayey silt at a water content of 23 %.

Applied surcharge = 130 kPa. Valid for $0.5 < S < 15$ g/l

where the units of SP_{t0} are $\text{mm}^2/\text{s} \cdot ^\circ\text{C}$ and those of salinity, S , g/l.

In order to express the results as a function of applied surcharge, the following best-fit equations were obtained as shown on Fig. 40.

$$SP_{t0} = 195 \cdot 10^{-5} \exp(-0.0117 \cdot P_e) \text{ mm}^2/\text{s} \cdot ^\circ\text{C} \text{ for } S_w = 0 \text{ g/l}$$

$$SP_{t0} = 128 \cdot 10^{-5} \exp(-0.0171 \cdot P_e) \text{ mm}^2/\text{s} \cdot ^\circ\text{C} \text{ for } S_w = 2 \text{ g/l}$$

$$SP_{t0} = 75 \cdot 10^{-5} \exp(-0.0184 \cdot P_e) \text{ mm}^2/\text{s} \cdot ^\circ\text{C} \text{ for } S_w = 5 \text{ g/l}$$

$$SP_{t0} = 48 \cdot 10^{-5} \exp(-0.0229 \cdot P_e) \text{ mm}^2/\text{s} \cdot ^\circ\text{C} \text{ for } S_w = 10 \text{ g/l}$$

$$SP_{t0} = 33 \cdot 10^{-5} \exp(-0.0200 \cdot P_e) \text{ mm}^2/\text{s} \cdot ^\circ\text{C} \text{ for } S_w = 15 \text{ g/l}$$

Graphs 39 and 40 clearly demonstrate that the rate of ice lens formation in a saline fine-grained soil for conditions similar to field freezing where the rate of cooling is small and the suctions at the frost front are small can be related to applied surcharge and salinity by a set of constitutive equations as outlined above. Many tests with different thermal boundary conditions yielded identical values of segregation potential, which indicates that the concept of segregation potential developed for essentially salt-free soils can be used for saline soils. It is, however, of paramount importance to relate the segregation potential at the onset of the formation of the final ice to the salinity of the frozen fringe at the same time. The application of these findings to the prediction of ice lens formation in the field will be briefly discussed below.

Table 3. Summary of Test Results of Series 1. (No Applied Surcharge)

Test #	Height(mm)		Diam. (cm)	Heave (mm)	SP _{to} (P _e) 10 ⁻⁵ mm ² s.C	S(lens) g/l	S _{wo} g/l	Onset Final Lens (hours)
	Ini.	End						
S3	103	115	5	11.63	206	0	0	30 (e = 5.6)
S4	133	145.5	10	12.5	195	0	0	42 (e = 1.5)
S5	124	156.5	10	32.5	198	0	0	40 (e = 18.3)
S10	112	118	5	6.1	106	2.4	NA	27 (e = 2.5)
S11	94	101.5	5	7.5	72	5.0	4.0	24 (e = 2.2)
S12	125	137.5	10	12.0	70	6.3	4.5	30 (e = 4.0)
S20	116	126	5	9.5	86	4.0	NA	30 (e = NA)
S30	111	117	5	5.8	46	7.8	NA	40
S31	106	110.5	5	4.4	52	9.4	8.0	27 (e = 1.0)
S40	103	107	5	3.8	27	17.0	NA	56 (e = 0.3)
S41	104	107	5	3.05	28	17.5	16.0	30 (e = 0.6)
S42	108	112	5	4.2	15	25.5	21.5	18 (e = 1.5)
S43	108	113	5	4.6	23	18.7	15.8	29 (e = 2.0)
S46	107	111	5	3.8	35	16.2	14.8	20 (e = 1.8)
S52	108	114	5	6.3	13	26.7	23.0	52 (e = 1.0)
S62	106	112	5	5.60	8.6	32.2	32.0	104 (e = 0.3)
S70	100	109	5	8.9	135	5.0	2.0	14 (e = 3.0)
S71	104	111.5	5	7.5	75	5.2	4.1	16 (e = 2.0)

Table 4. Summary of Test Results of Series 2. (Applied Surcharge)

Test #	Height(mm)		Diam. (cm)	Heave (mm)	SP _{to} (P _e) 10 ⁻⁵ mm ² s.C	S(lens) g/l	S _{wo} g/l	Onset Final Lens (hours)
	Ini.	End						
SAP1	100	103	10	3.0	20.0(50)	10.0	8.2	21 (e = 1.3)
SAP2	109	110	10	0.9	6.0(100)	8.8	8.2	40 (e = 0.5)
SAP2R	106	107	10	0.98	3.6(100)	9.2	8.2	32 (e = 0.8)
SAP3	107	107.5	10	0.40	2.0(130)	10.1	9.5	30 (e = 0.4)
SAP4	103	107.2	5	4.20	10.8(60)	18.2	16.5	32 (e = 1.0)
SAP5	106	107.4	5	1.35	8.0(100)	16.7	16.0	36 (e = 0.5)
SAP6	110	110.5	10	0.30	2.0(130)	14.5	14.0	20 (e = 0.3)
SAP5R	105	105.8	10	0.9	3.5(100)	18.2	17.2	30 (e = 0.5)
SAP7	117	119	10	2.1	10.0(130)	3.1	2.8	40 (e = 1.0)
SAP8	120	131.5	10	11.5	33.0(50)	5.9	4.7	34 (e = 2.0)
SAP9	123	130	10	6.5	15.0(100)	5.5	4.5	44 (e = 2.0)
SAP10	124	139.6	10	15.6	95.0(50)	0	0	50 (e = 3.0)
SAP11	120	132	10	12.0	65.0(100)	0	0	56 (e = 3.9)

4. DISCUSSION

4.1 Rate of Ice lens Growth in the Field.

In the field, although the rate of cooling is extremely small, frost penetration occurs steadily owing to a constant heat flux boundary condition rather than a fixed temperature one. Considering that any given freezing soil can be characterized by the constitutive equations, $C.E. = fct(SP_{10}, S, P_e)$, the rate of ice lens growth can be predicted using the following approach:

1. At a given time and for a given time step, determine the salinity profile in the unfrozen soil as a function of time and position of the frost front. The unfrozen soil can be regarded as a finite or a semi-infinite medium. The key inputs are the diffusion coefficient of salt in a saturated soil at a given porosity and the boundary conditions. At the ice lens, the rate of solute exclusion will be related to the rate of water migration, i.e. the rate of ice lens growth, and the salinity of the pore water.

2. The rate of water migration is related to salinity and applied surcharge by virtue of the constitutive equations. At the same time step, use the C.E. to calculate the rate of water migration and use as input for the next time step.

3. Advance one time-step, calculate new position of frost front and repeat steps 1 and 2.

The steady decrease in rate of ice lens growth will essentially cause a sudden increase in frost penetration rate in order to maintain heat flow balance through the system. The new ice lens will be initiated at a location dictated by the salinity and temperature conditions in the unfrozen soil. This sudden advance of the frost front may also lead to layers of unfrozen soil owing to high salt concentrations sandwiched between frozen soil layers. These unfrozen layers in frozen soil may have significant consequences for engineering works in saline soils.

In order to verify if such an approach yields adequate results, ramped freezing tests must be performed. Solute redistribution in the unfrozen soil will influence the ice lens pattern and confirm the interaction between pore water salinity and segregation potential during transient freezing.

4.2 Problems with Frost Heave Testing in Saline Soils

Conducting freezing tests in saline soils is a complex task. Temperatures must be cold enough to ensure ice nucleation in the frozen soil. As the salinity increases, the minimum temperature require for ice nucleation decreases exponentially as shown on Fig. 11. Tests are thus not always carried out at the same temperature gradient and the use of Segregation Potential which normalizes water flux and temperature gradient is very useful. Test S50 (initial pore water salinity of 26 g/l which produces a freezing point depression of about 1.5 °C) was characterized by an event of spontaneous crystallization after 50 hours of freezing as shown in Fig. 41. The release of latent heat associated with phase change was sensed by all the thermistors which recorded an increase in temperature. Ice was most likely formed near the cold plate since thermistor #2 recorded the highest increase in temperature.

Test S62 had an initial salinity of 33.0 g/l. It is well-known that pore water salinity affects also the unfrozen water content of a given soil. Test S60 was conducted for a period of 123 hours. The salinity profile obtained at the end of freezing (Fig. 42) suggests that there is solute movement in the frozen zone induced by the temperature gradient. This phenomenon was not observed in tests with lower pore water salinity and shorter duration. It is an interesting observation worth further study but it is not within the scope of the present report to cover this aspect of ice formation in saline soils.

5. CONCLUSIONS

The objectives of the present research were to obtain a complete characterization of a saline clayey silt subjected to one-dimensional freezing under various applied surcharges and for different pore water salinities. In order to achieve these objectives, an extensive laboratory testing program was undertaken at the Watfrost laboratory of the University of Waterloo. The test program was comprised of two Series, consisting of a total of 27 tests frozen with free access to saline water under zero applied surcharge and of 13 tests frozen with free access to saline water but subjected to applied surcharges simulating various overburden pressures in the field. The maximum applied surcharge was 130 kPa, which corresponds to an overburden of about 7 m.

The study has led to the following conclusions:

1. The concept of segregation potential introduced by Konrad and Morgenstern (1980-84) for clayey silts with negligible salinity appears to be applicable to clayey silts with pore water salinities approaching 35 g/l, which is the salinity of sea water. In order to develop a predictive frost heave model for field conditions, it was shown by Konrad and Morgenstern that representative values of SP must be used in a coupled heat and mass transfer formulation. The relevant value of SP can be obtained from step-freezing test at the onset of the formation of the final ice lens where the rate of cooling is close to field conditions and the freezing still in transient conditions, similarly to the field.

2. Solute rejection during phase change has been observed during the growth of the final ice lens, i.e. for quasi thermal steady state. Considerable increases in solute concentration were measured close to the ice lens at the end of freezing for all tests. Detailed salinity profiles in the unfrozen soil showed also that solutes were transported away from the phase change interface by the diffusion mechanism, which is proportional to the concentration gradient and the magnitude of the mass diffusion coefficient.

3. Solute enrichment in the vicinity of the final ice lens is directly related to the time of testing since as saline water freezes at the ice lens, solutes are rejected, contributing to the enrichment of pore water in adjacent layers to the ice lens.

4. A set of constitutive equations characterizing frost heaving in saline soils were established as a function of pore water salinity, applied surcharge and segregation potential. To be consistent, each of these parameters must correspond to the onset of formation of the final ice lens. The relationships between SP_{T0} and pore water salinity, S , was of the form:

$$SP_{T0} = E(P_e) - F(P_e) \ln S$$

where E and F are soil constants for a given applied surcharge, P_e .

The relationship between SP_{T0} and applied surcharge can be expressed as:

$$SP_{T0} = G(S) \exp[-H(S).P_e]$$

where G and H are soil constants for a given pore water salinity.

This study has also led to the following observations. Although these observations are well supported by the experimental data, no systematic study was undertaken to fully explore the mechanisms involved in each phenomenon.

1. Solute rejection appears to be dependent upon rate of cooling. For high rates of cooling, (i.e. in the early phase of transient freezing) salinity profile in the frozen soil after freezing revealed that there was little change in pore water salinity with respect to the initial pore water salinity of the unfrozen soil. More tests are required to determine the relationship between rate of cooling and degree of solute exclusion as water freezes.

2. It was also observed that solute migration occurred in the frozen soil when the samples were subjected to large temperature gradients. Furthermore, it appears that this phenomenon was also dependent upon the initial pore water salinity. Higher pore water salinities led to significant solute redistribution in the frozen soil whereas for lower initial pore water salinities, redistribution was almost negligible over the duration of freezing. This observation may be significant for field conditions where temperature gradients across the frozen soil may be sustained for tens and even thousands of years. More studies are required to establish the constitutive equations governing solute transfer in low permeability frozen saline soils.

3. Similar to the freezing point depression in saline water, segregation-freezing temperatures in a saline clayey silt are also dependent on pore water salinity. In general, it was observed that the temperature of ice lens initiation decreased with increasing pore water salinity.

While the knowledge of constitutive equations involving SP_{10} , S , and P_e are sufficient to predict average ice enrichment during freezing, the knowledge of the relationship between segregation-freezing temperature, rate of cooling and pore water salinity is necessary to predict the actual pattern of ice lenses in freezing soils. This, however, requires that ramped freezing tests be conducted in association with X-ray photography in order to determine the segregation freezing temperature for given rates of cooling.

6. REFERENCES

- Chamberlain, E.J., 1983. Frost heave in saline soils. Proc. 4 th Int. Conf. on Permafrost, Fairbanks, pp 121-126.
- Fuoss, R.M. and Accascina, F., 1959. Electrolytic Conductance. New York Interscience Publishers. pp. 191-205.
- Hallet, B., 1978. Solute redistribution in freezing ground. 3rd ICOP Edmonton, PP 86-91.
- Konrad, J.-M., 1989. The influence of overconsolidation of the freezing characteristics of a clayey silt. In press Can. Geot. J.
- Konrad, J.-M., 1988. Influence of freezing mode on frost heave characteristics. Cold Regions Science and Technology 15, 15 pages.
- Konrad, J.-M., 1987. The influence of heat extraction rate in freezing soils. Cold Regions Science and Technology, 14, pp. 120-137.
- Konrad, J.-M., 1987. Procedure for determining the segregation potential of freezing soils. Geotechnical Testing Journal; Vol. 10, No. 2, pp. 51-58.
- Konrad, J.-M., and N.R. Morgenstern, 1982. Prediction of frost heave in the laboratory during transient freezing. Canadian Geotechnical Journal, 19, pp. 250-259.
- Konrad, J.-M., and N.R. Morgenstern, 1981. The segregation potential of freezing soil. Canadian Geotechnical Journal, 18, pp. 482-491.
- Konrad, J.-M., and N.R. Morgenstern, 1980. A mechanistic theory of ice lens formation in fine-grained soils. Canadian Geotechnical Journal, 17, pp. 473-486.
- Konrad, J.-M., 1980. Frost heave mechanics Ph.D. thesis, U. of Alberta.
- Mahar, L.J., R.M. Wilson and T.S. Vinson, 1983. Physical and numerical modelling of uniaxial freezing in a saline gravel. Proc. 4 th. ICOP, Fairbanks, pp 773-778.
- Nixon, J.F. 1987. Ground freezing and frost heave- A review. Proc. of the Am. Soc. Mech. Eng. Int. Symp. on Cold Regions Heat Transfer., Dept. Mech. Eng. Univ. of Alberta Edmonton, Alta. pp 1-10.
- Penner, E., 1986. Aspects of ice lens growth in soils. Cold Regions Science and Technology, Vol. 13, pp.91-100.
- Robinson, R.A. and Stokes, R.H. 1959. Electrolyte Solutions. Butterworths Scientific Publications. pp 133-161.

CONSOLIDATION TEST S10

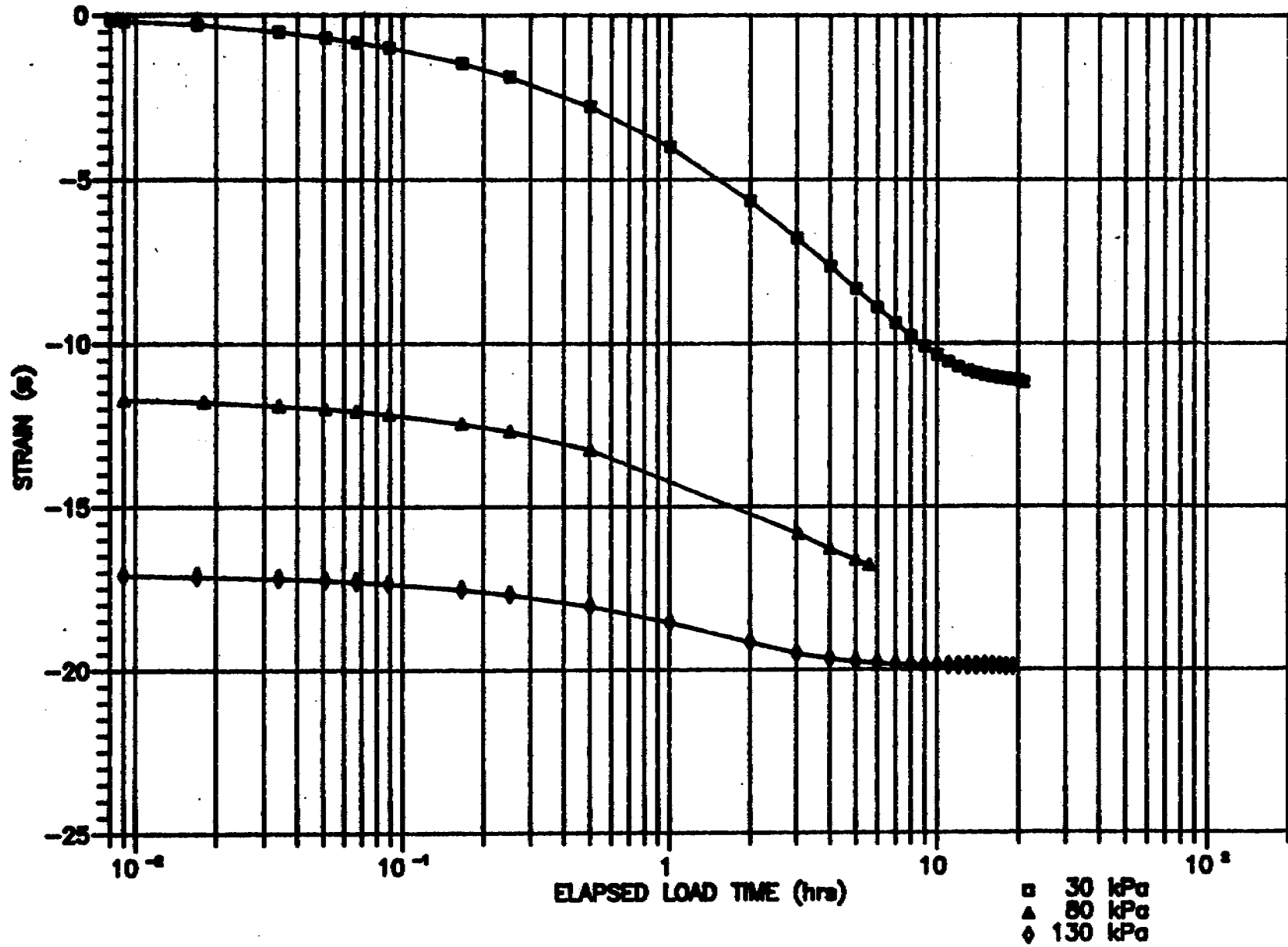


FIG. 1

Fig. 2

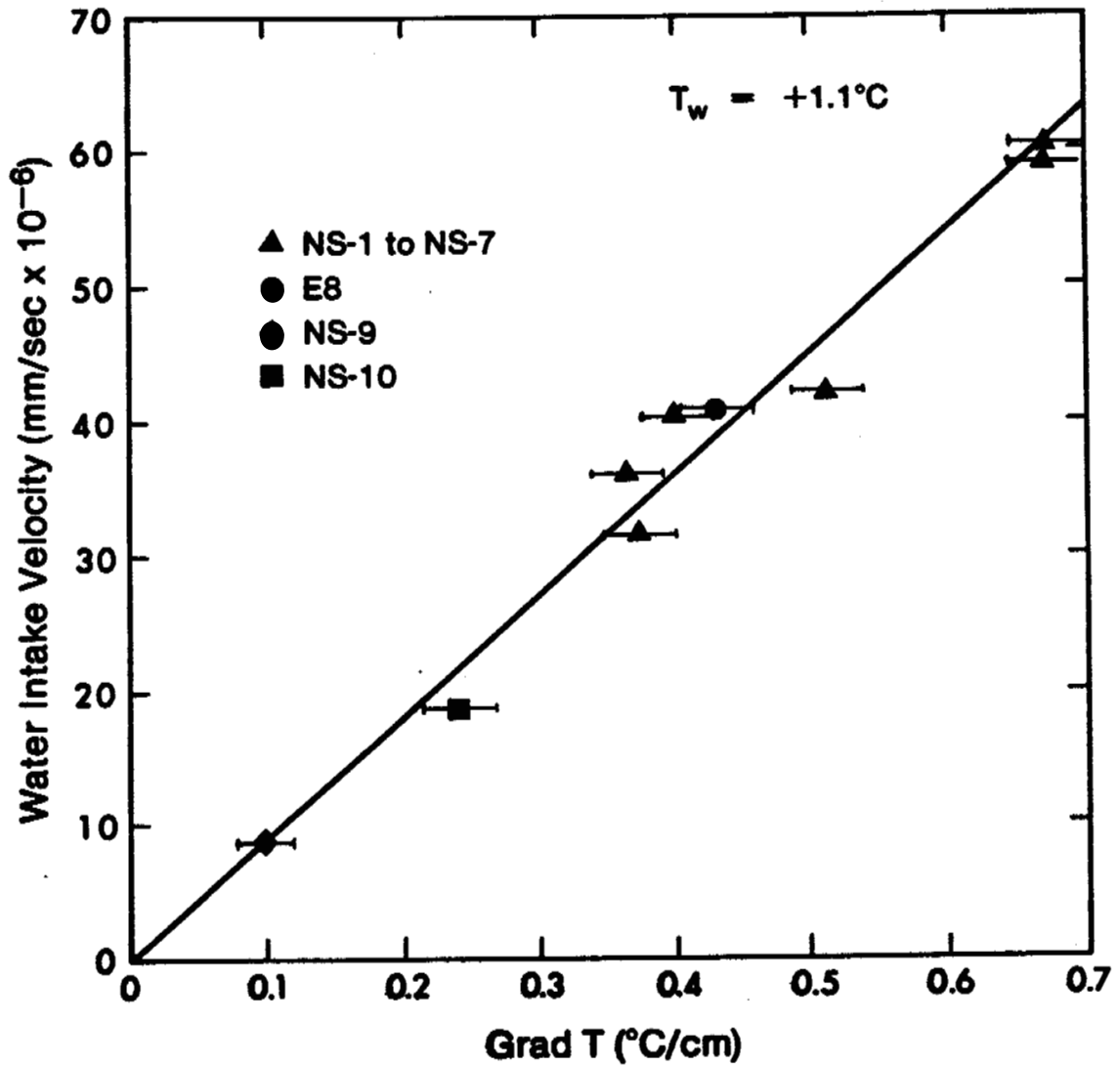


Figure 2. Relation Between Water Intake Velocity and Temperature Gradient Across the Active System at the Beginning of Steady State.

FREEZING TEST S10

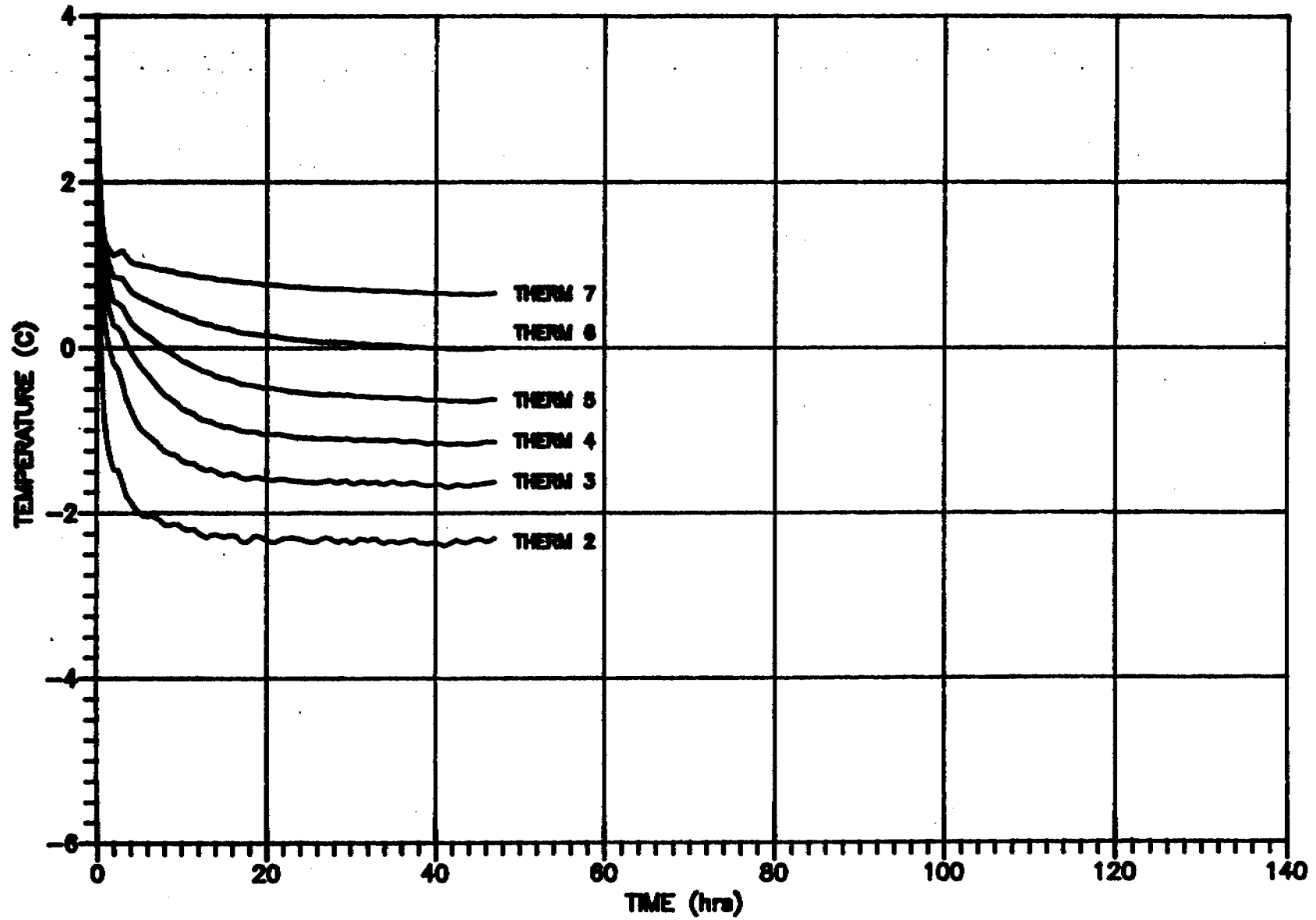


Fig. 3

FREEZING TEST S10

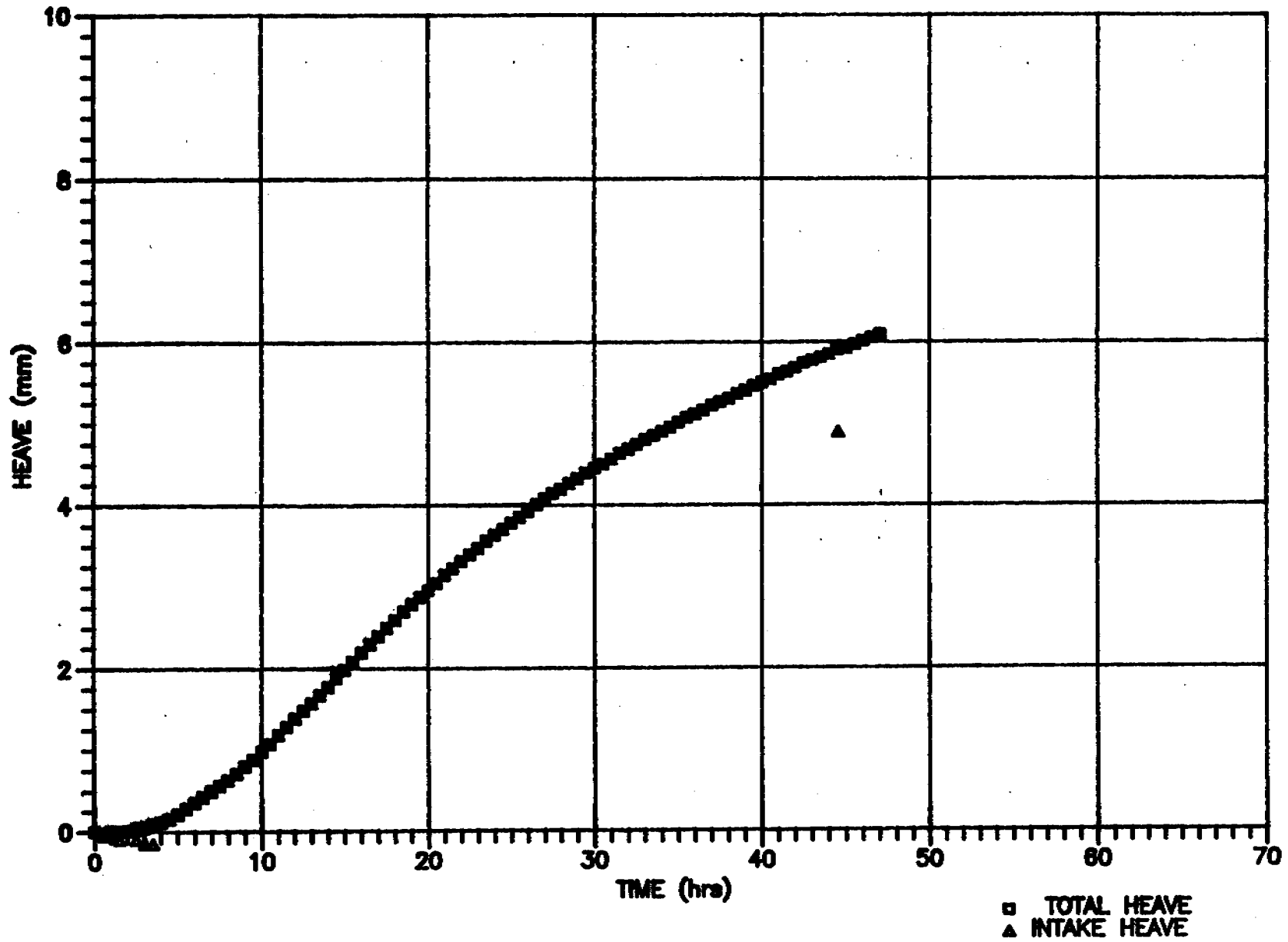


Fig. 4

TEST S10 FROST FRONT LOCATION

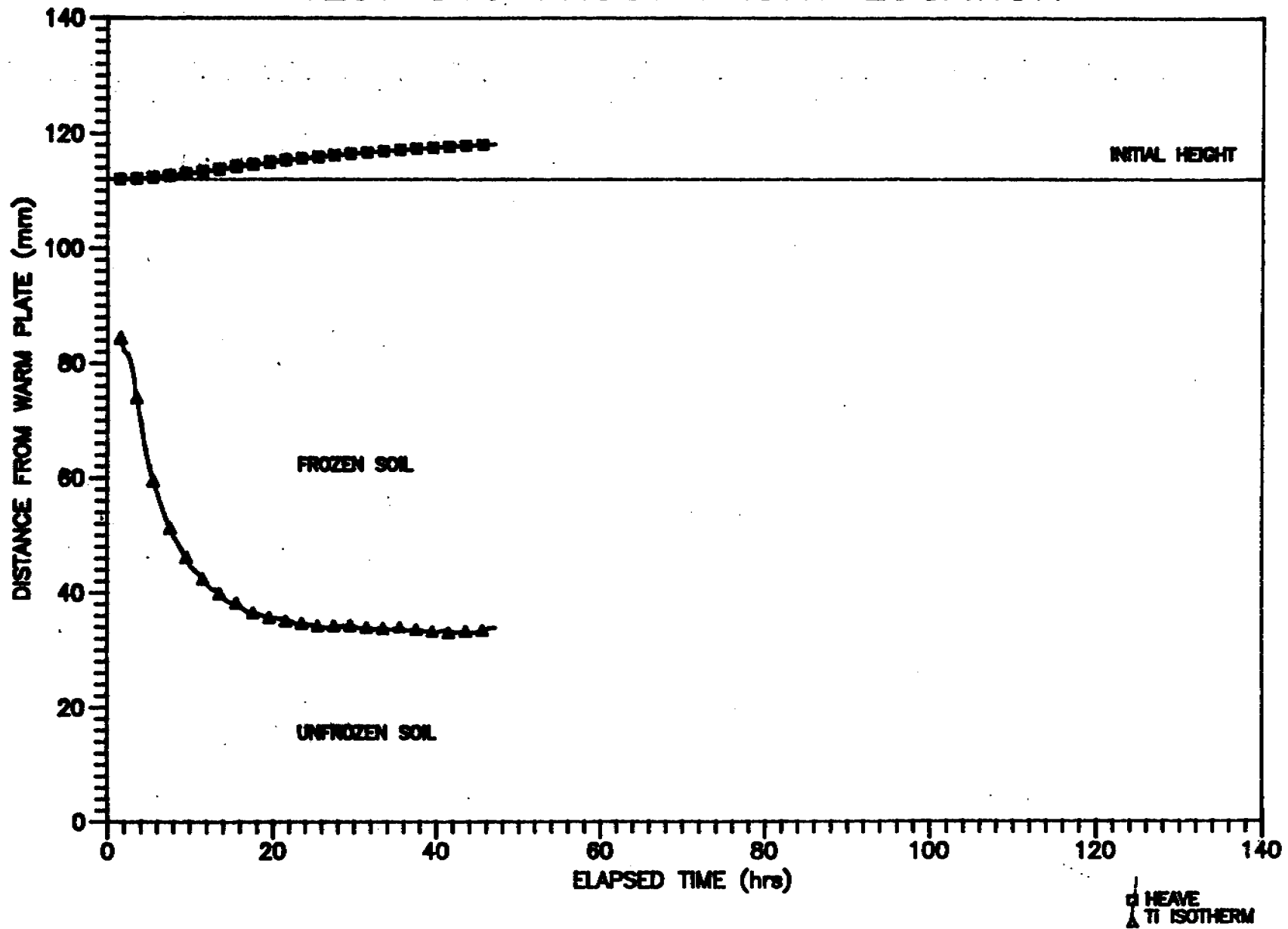


Fig. 5

FREEZING TEST S10

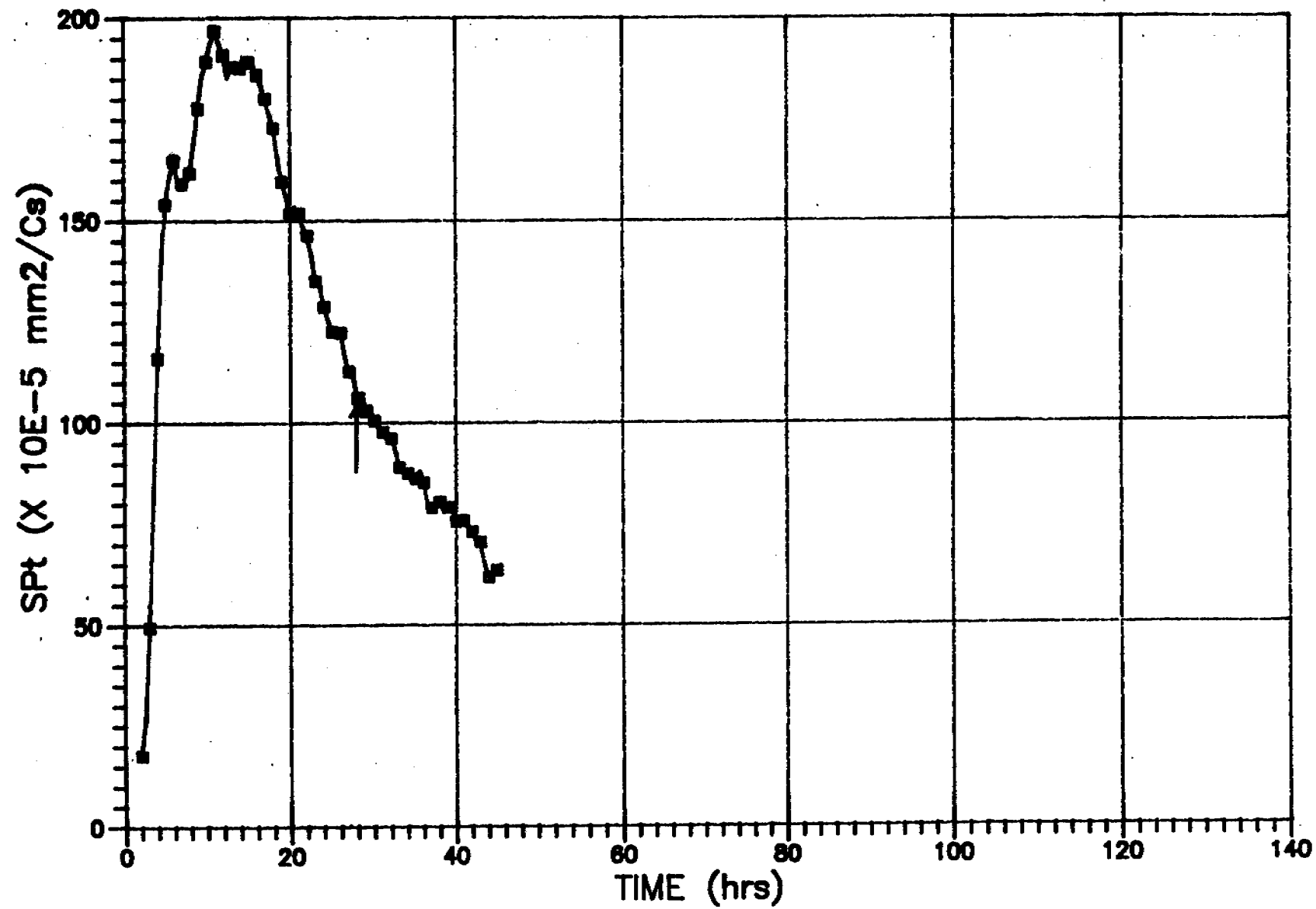
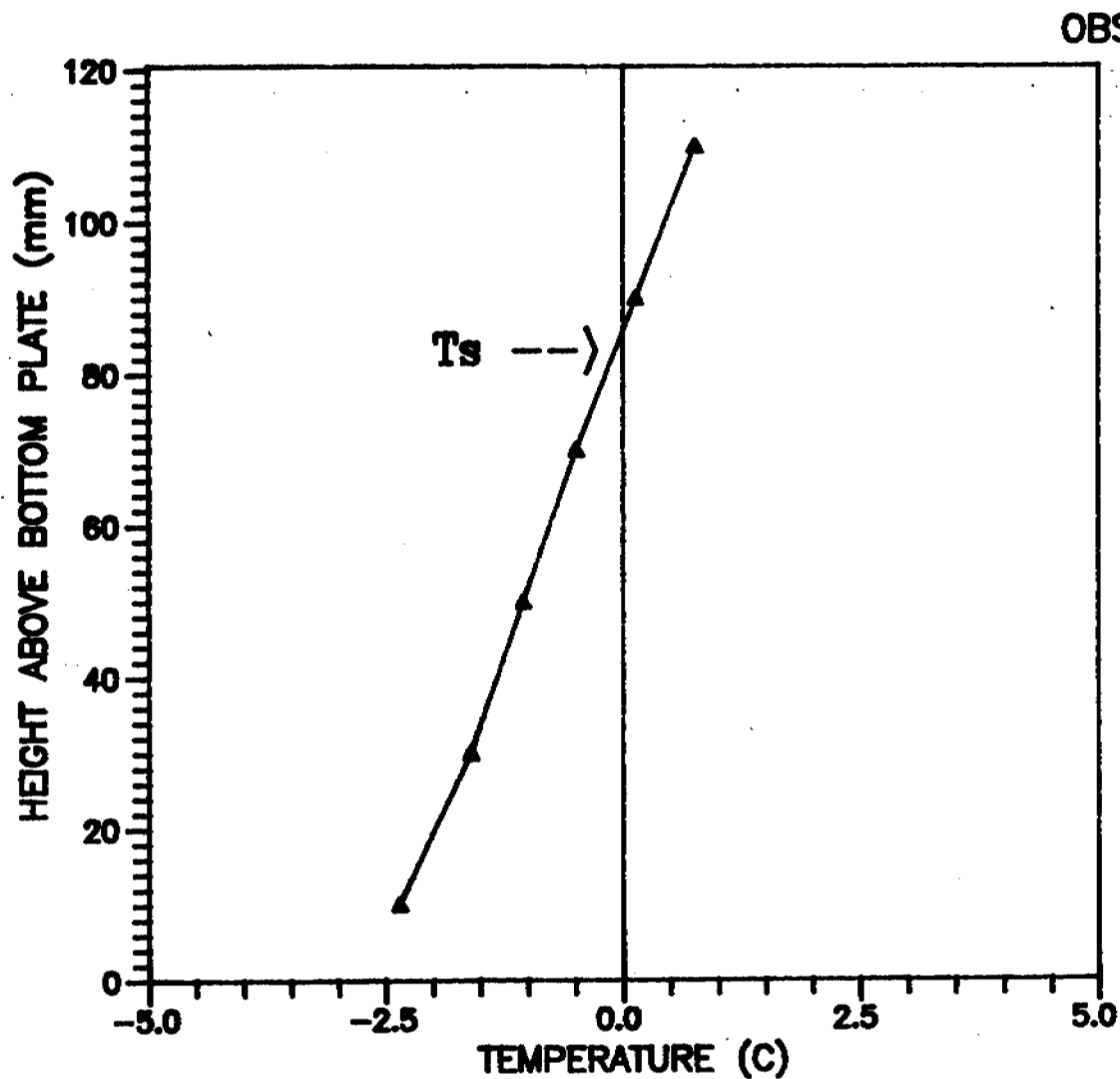
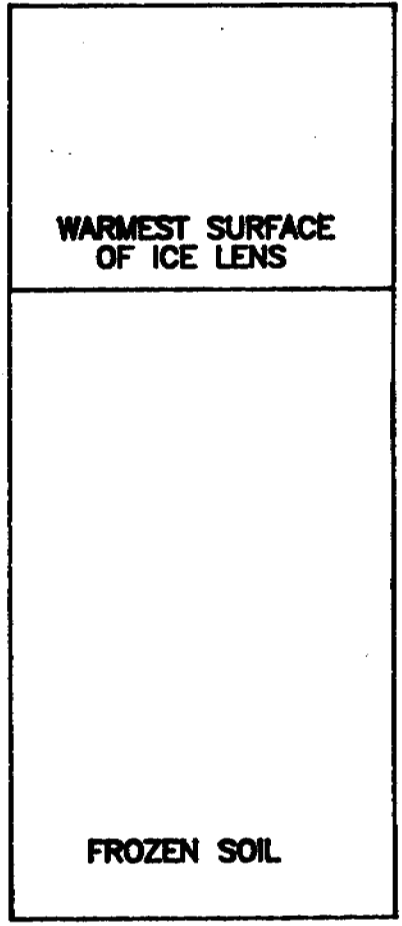


Fig. 6



OBSERVED POSITION OF ICE LENS



TEMPERATURE PROFILE AT ONSET OF WARMEST ICE LENS -- S10

SALINITY vs. CONDUCTANCE (NaCl)
T = 25 C, (UW, 1989)

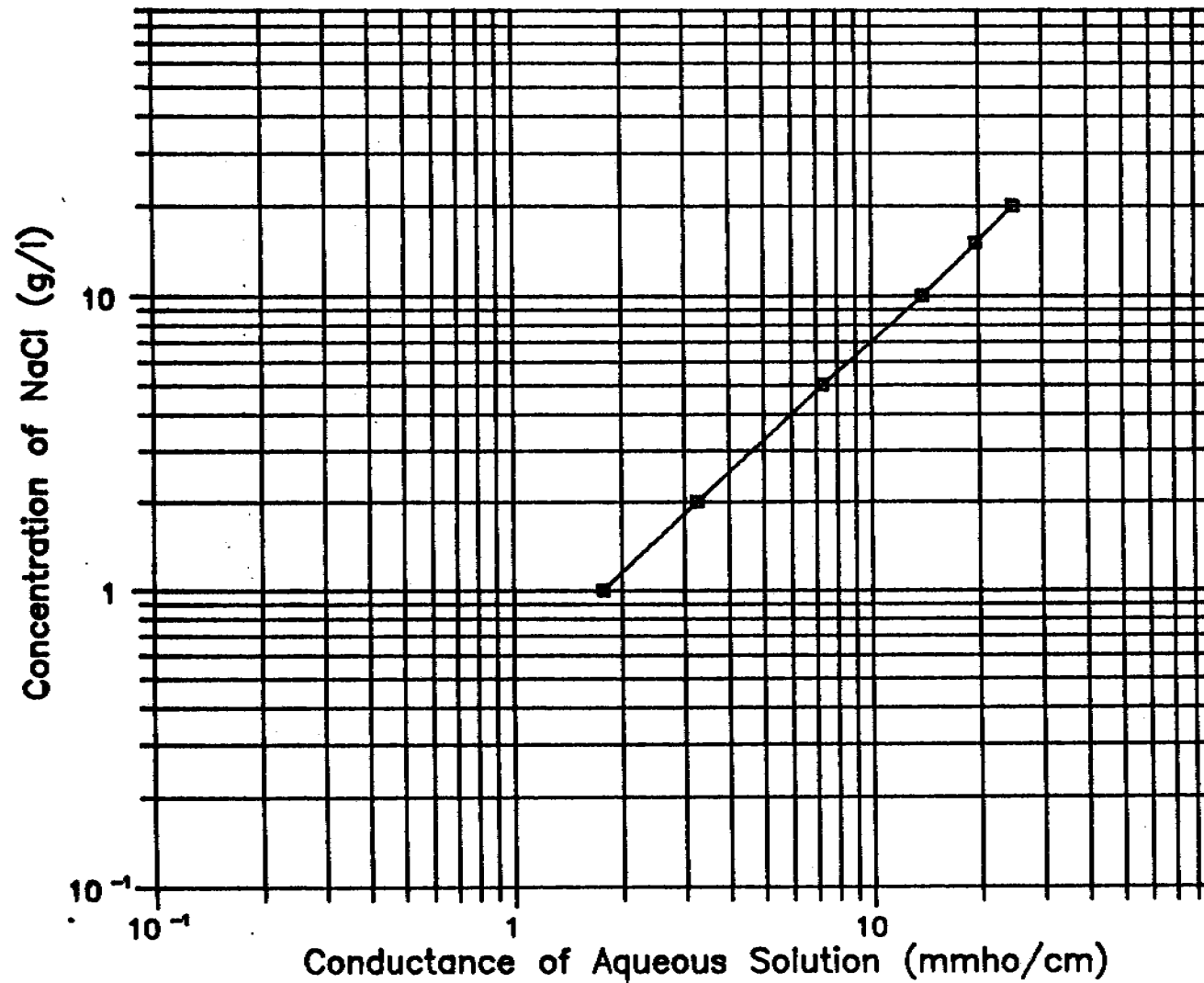


Fig. 8

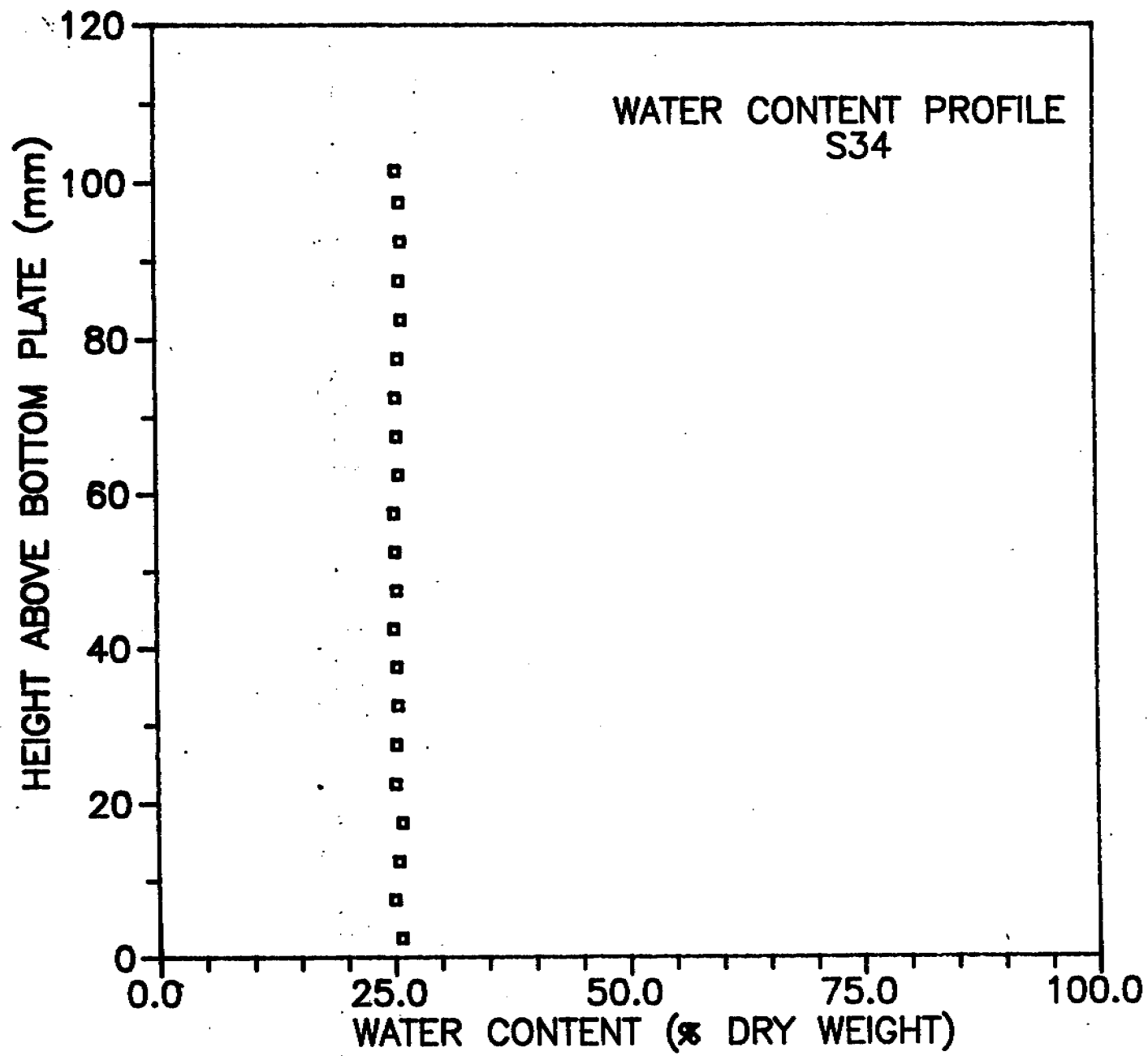


Fig. 9

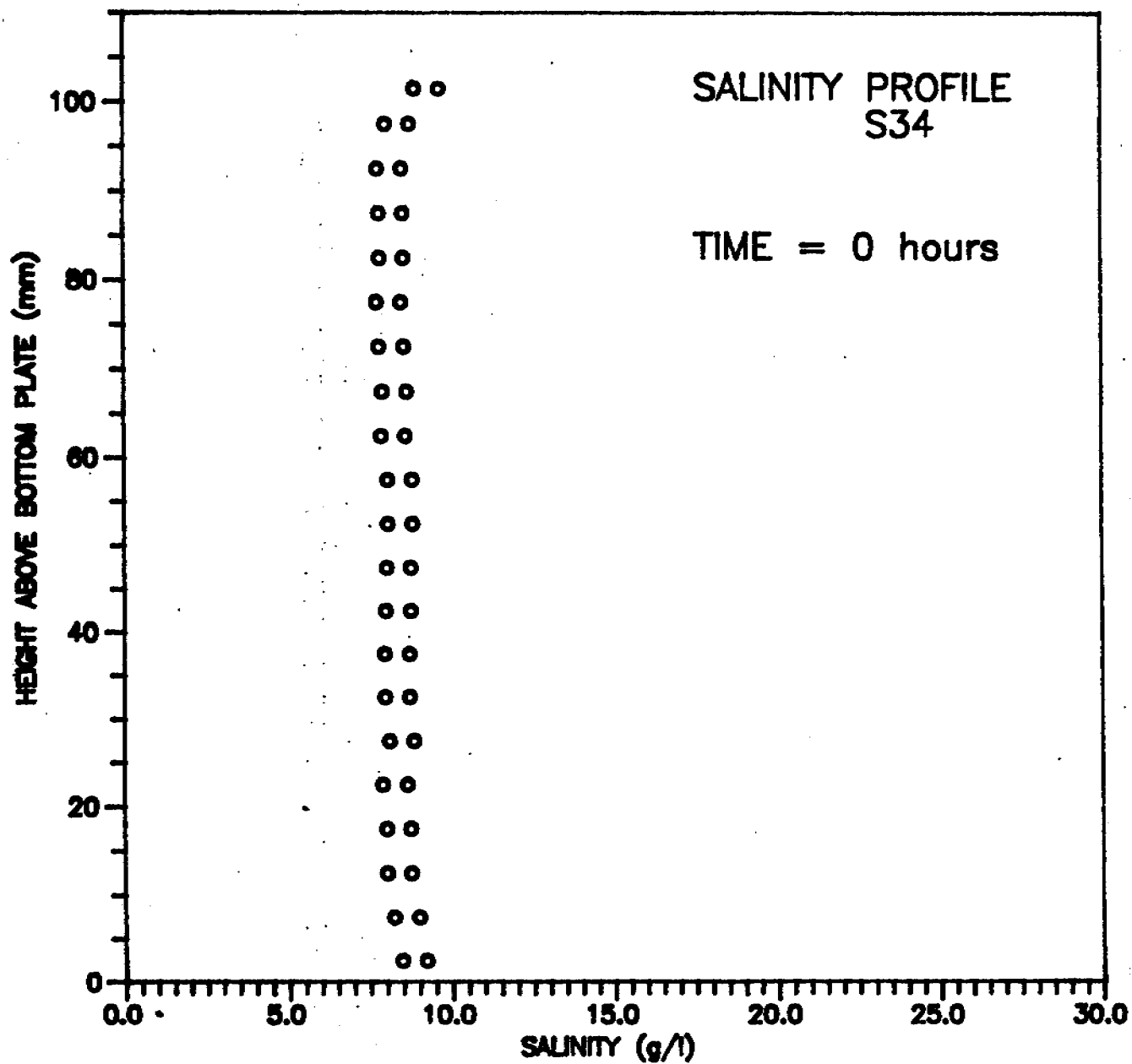


Fig. 10

Freezing Point Depression as a
Function of Salinity

T_f from Landolt-Bornstein-
Meyerhoffer's Physikalisch-
chemische Tabellen

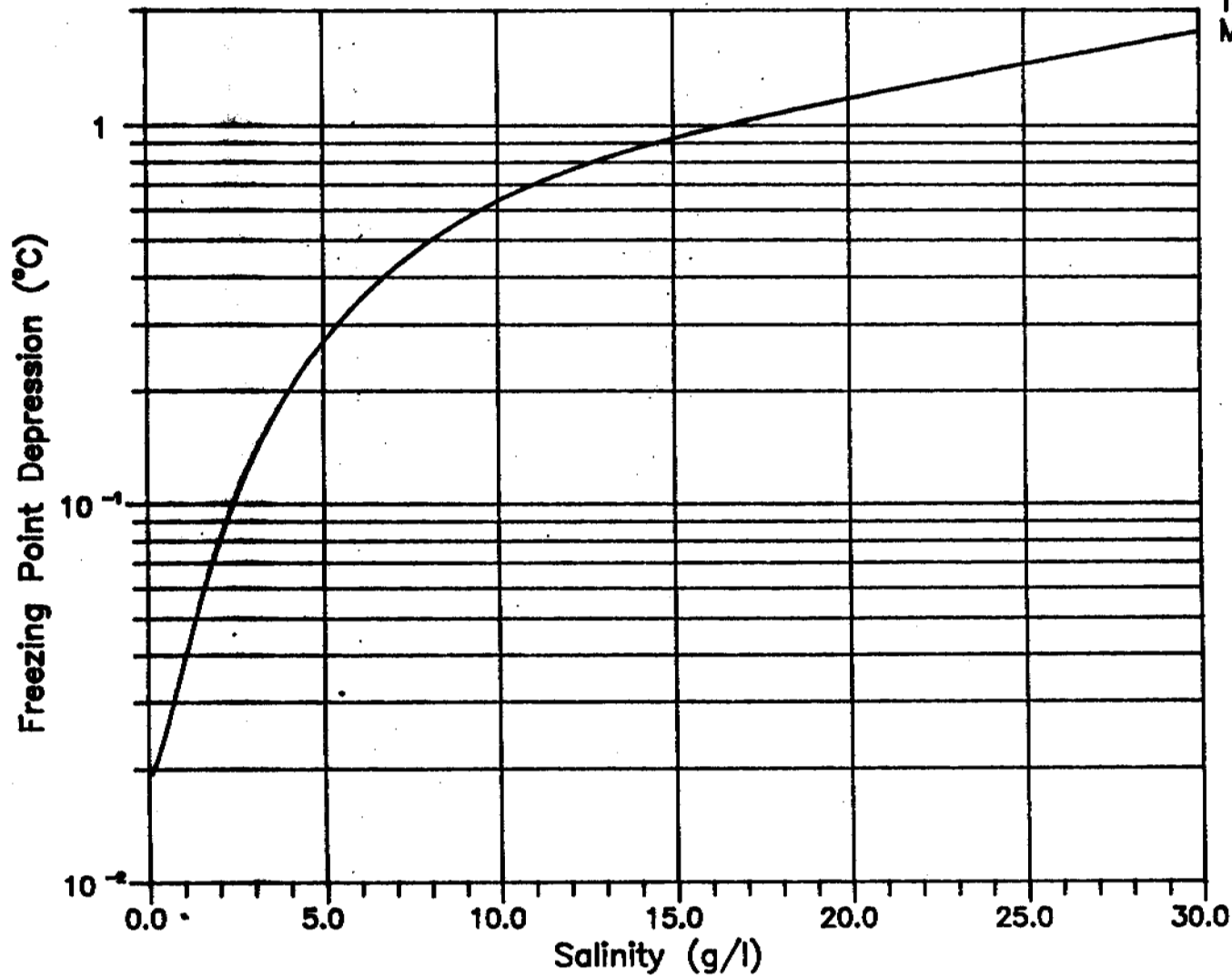


Fig. 11

CONSOLIDATION TEST S12

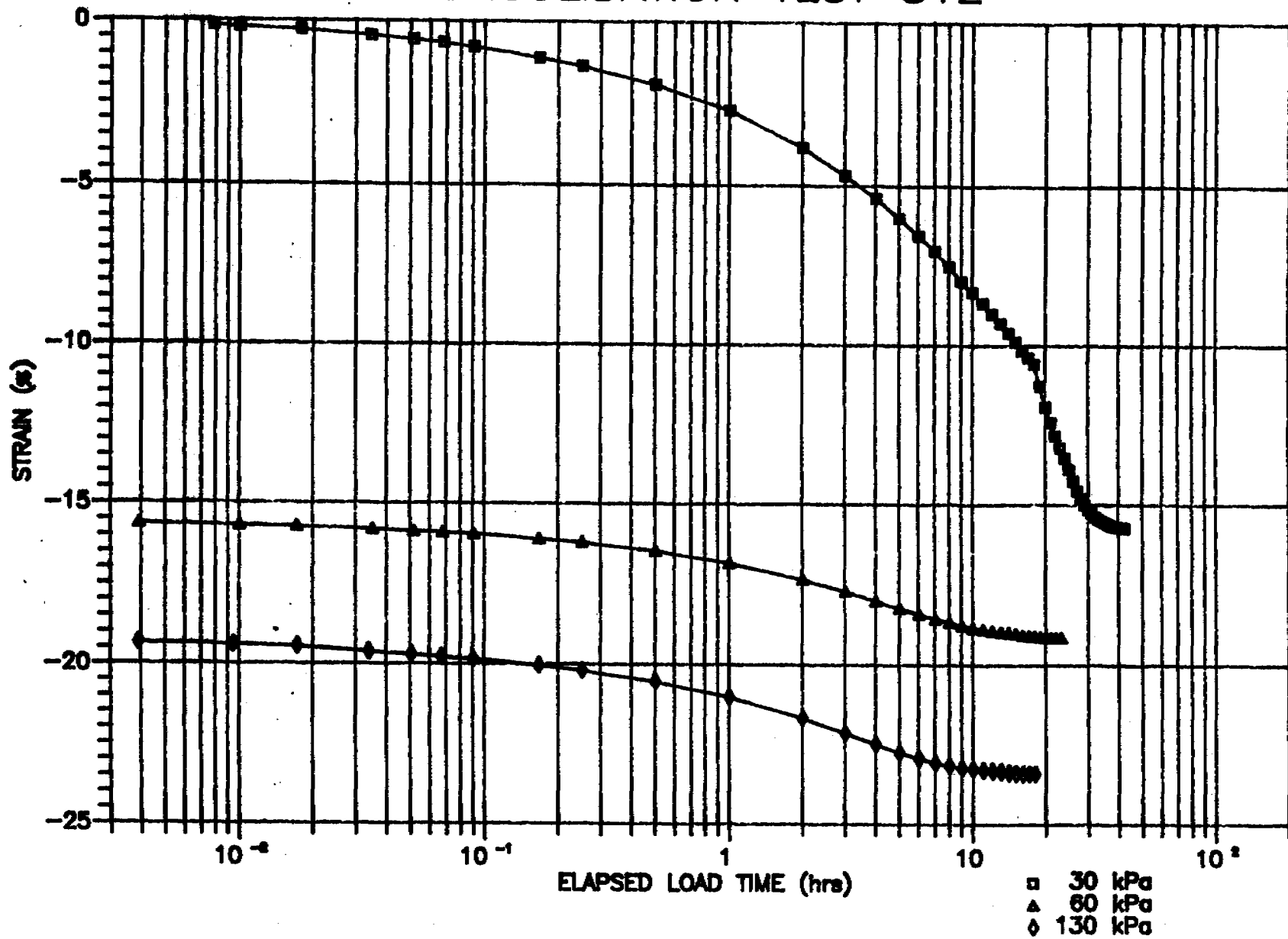
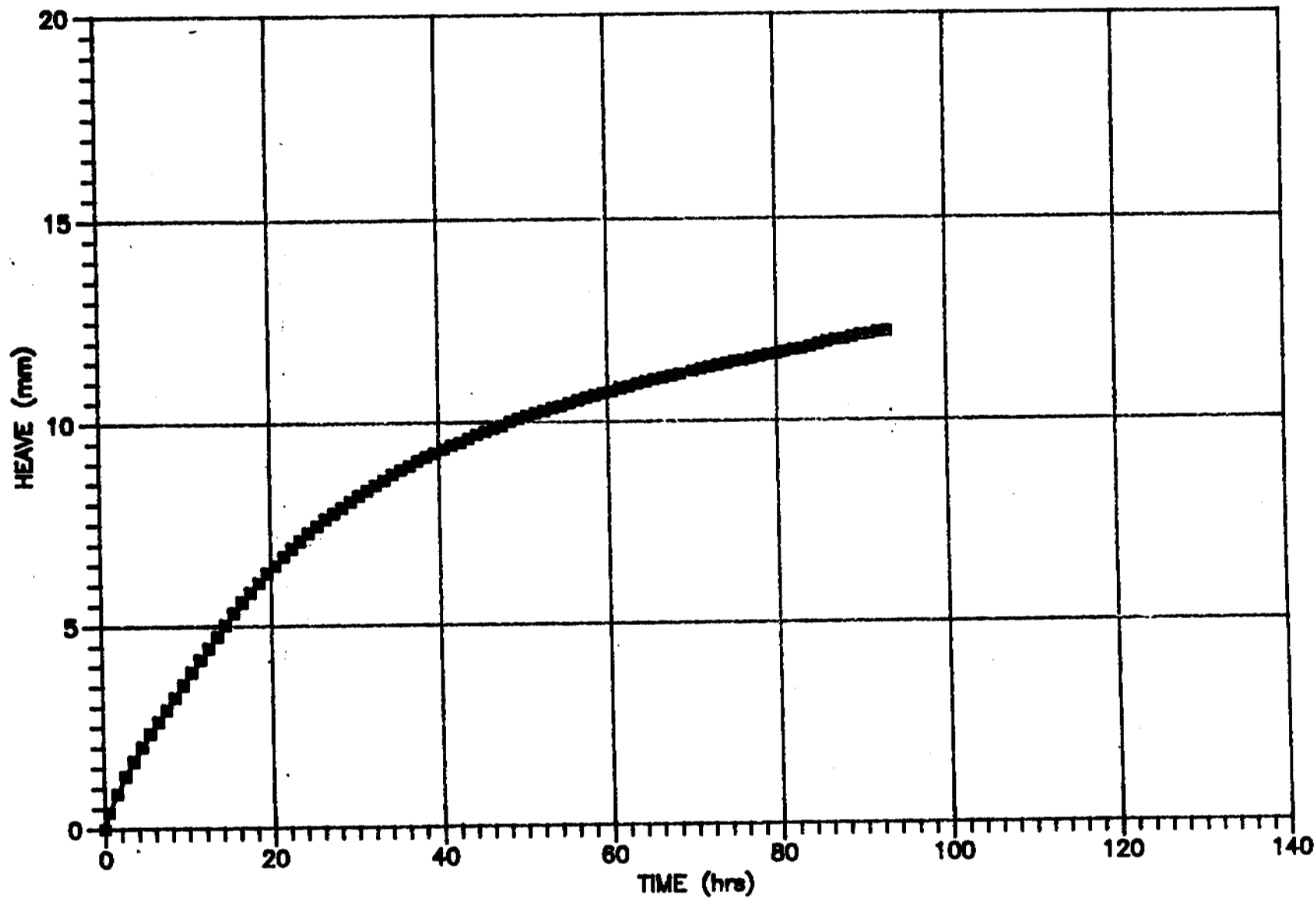


Fig. 12

FREEZING TEST S12



□ TOTAL HEAVE

Fig. 13

FREEZING TEST S12

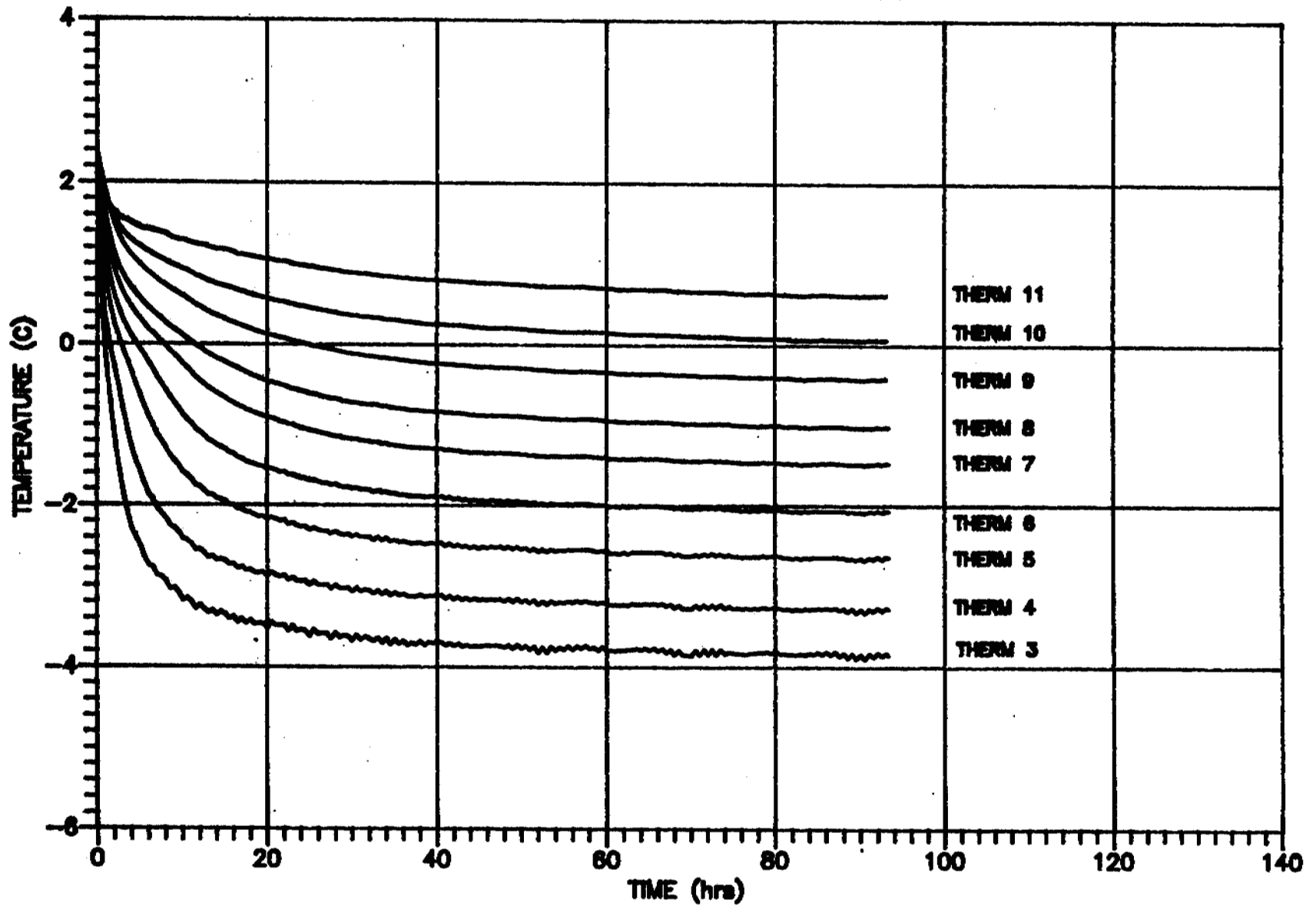


Fig. 14

TEST S12 FROST FRONT LOCATION

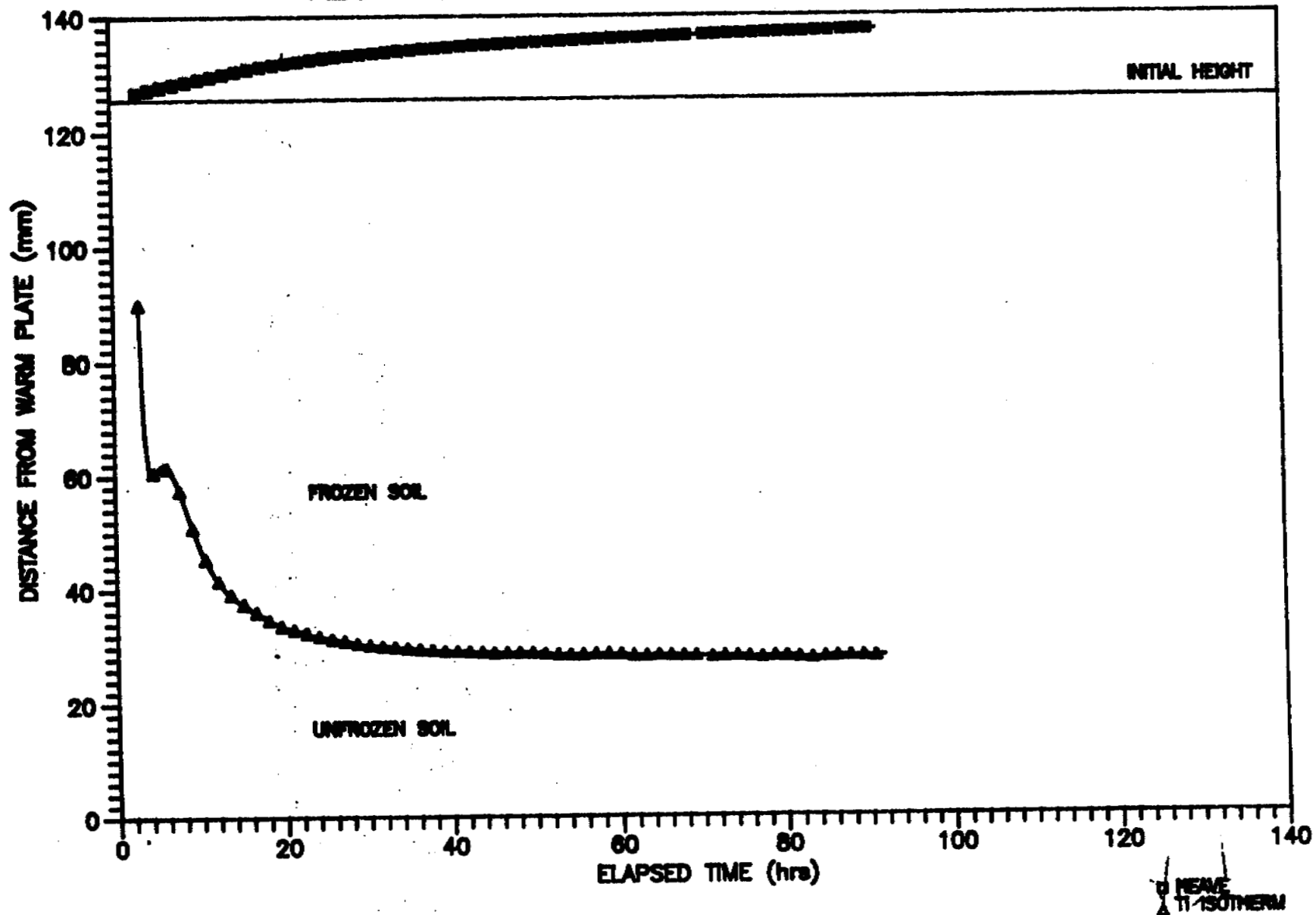


Fig. 15

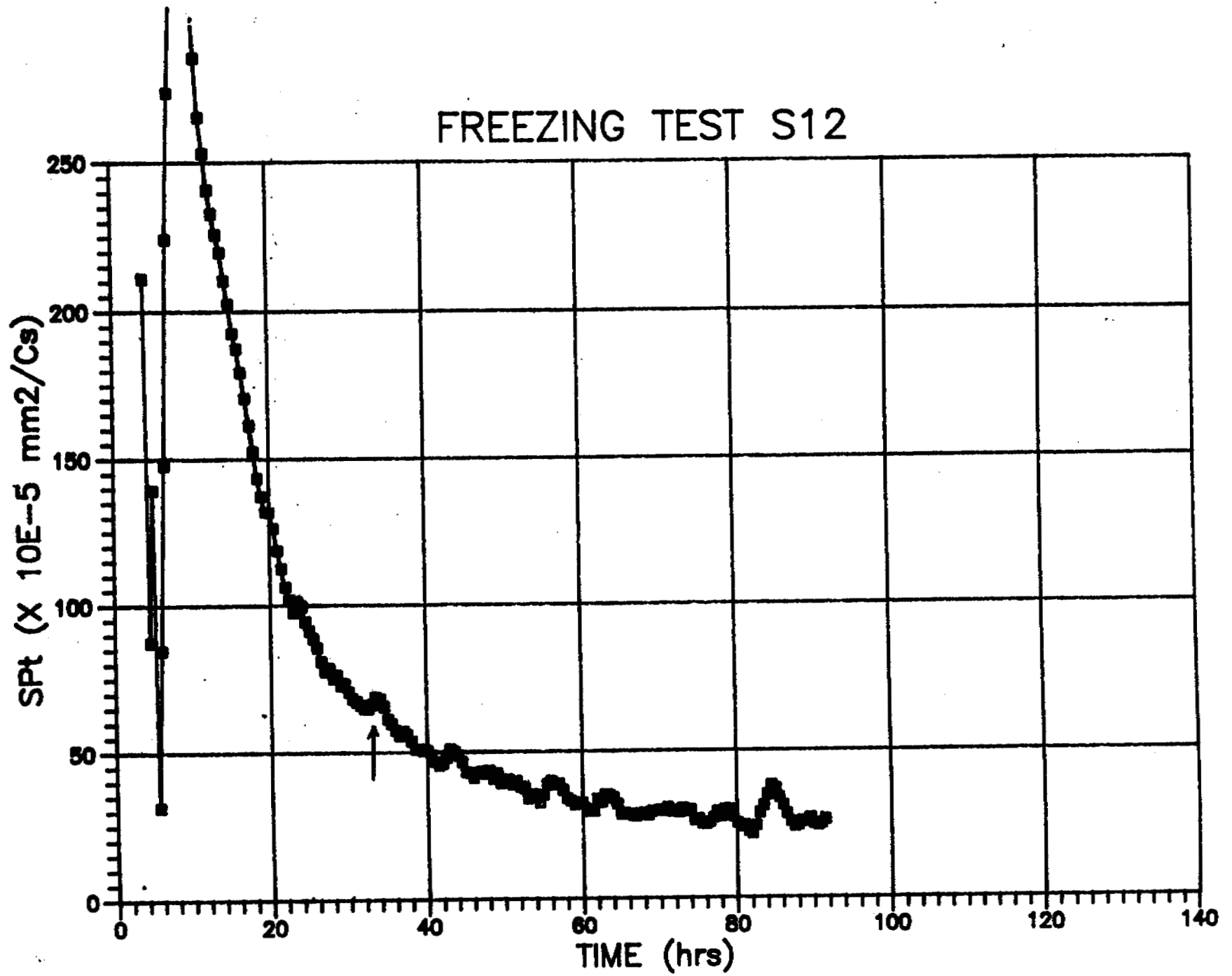


Fig. 16

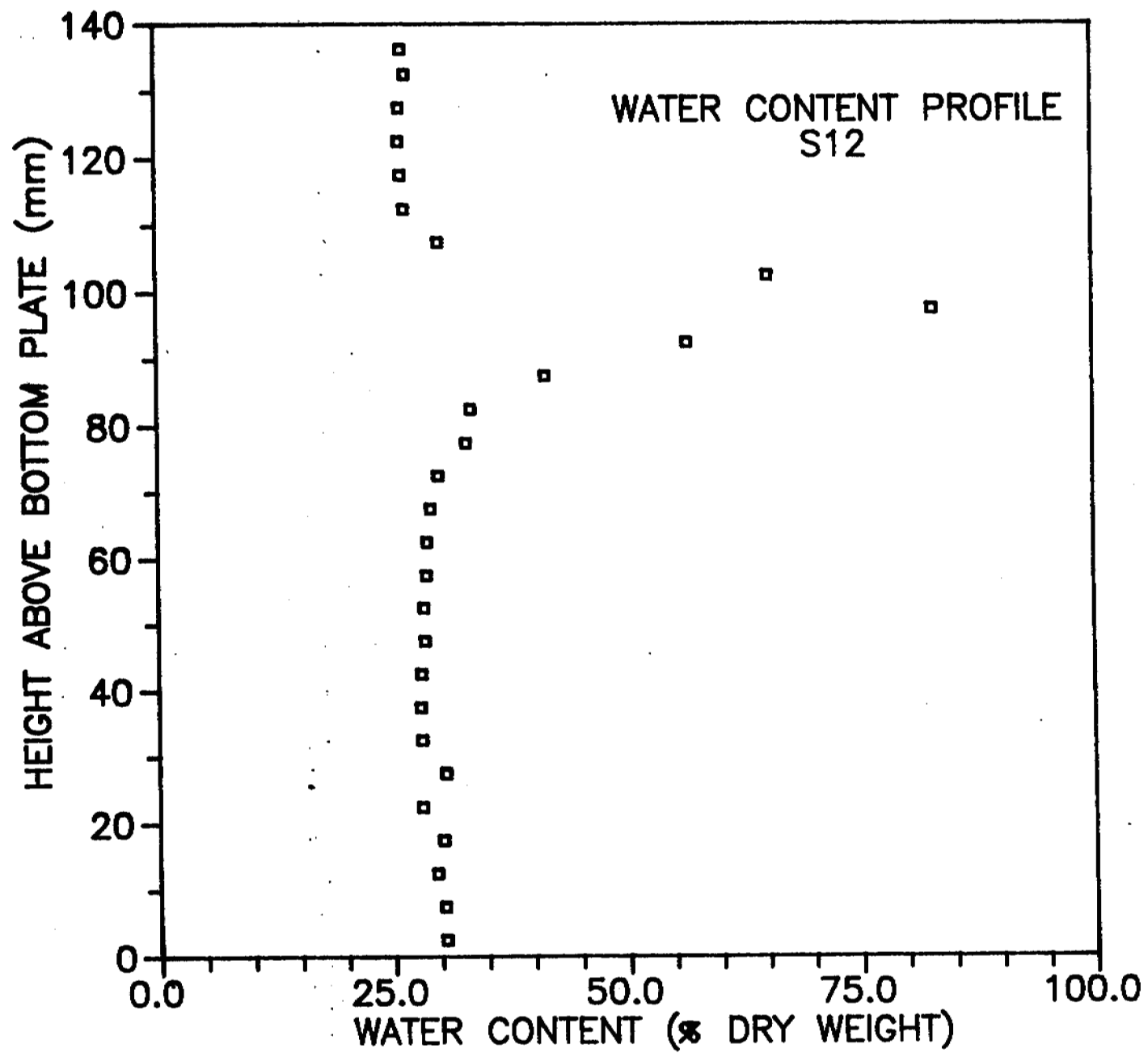


Fig. 17

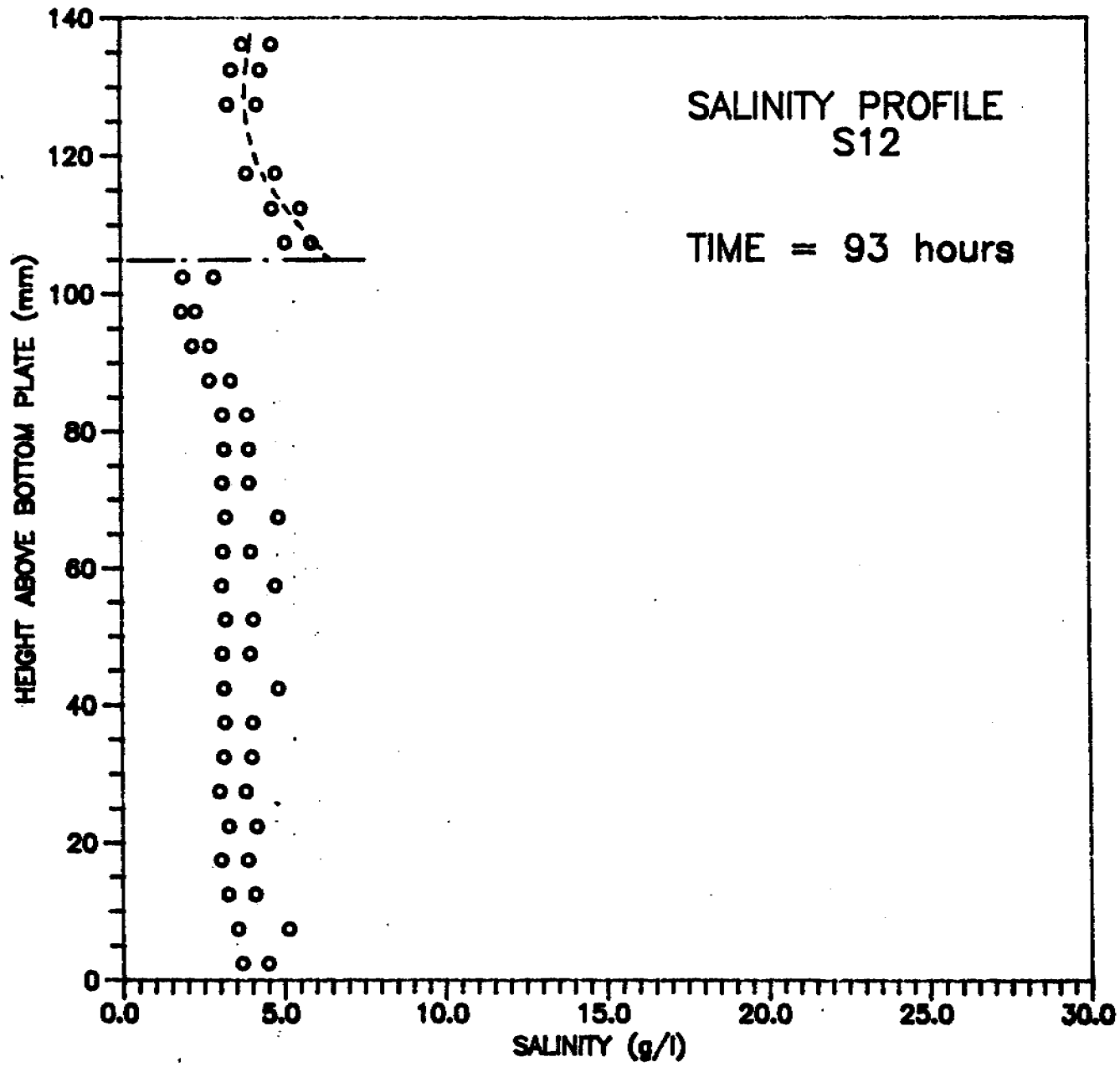
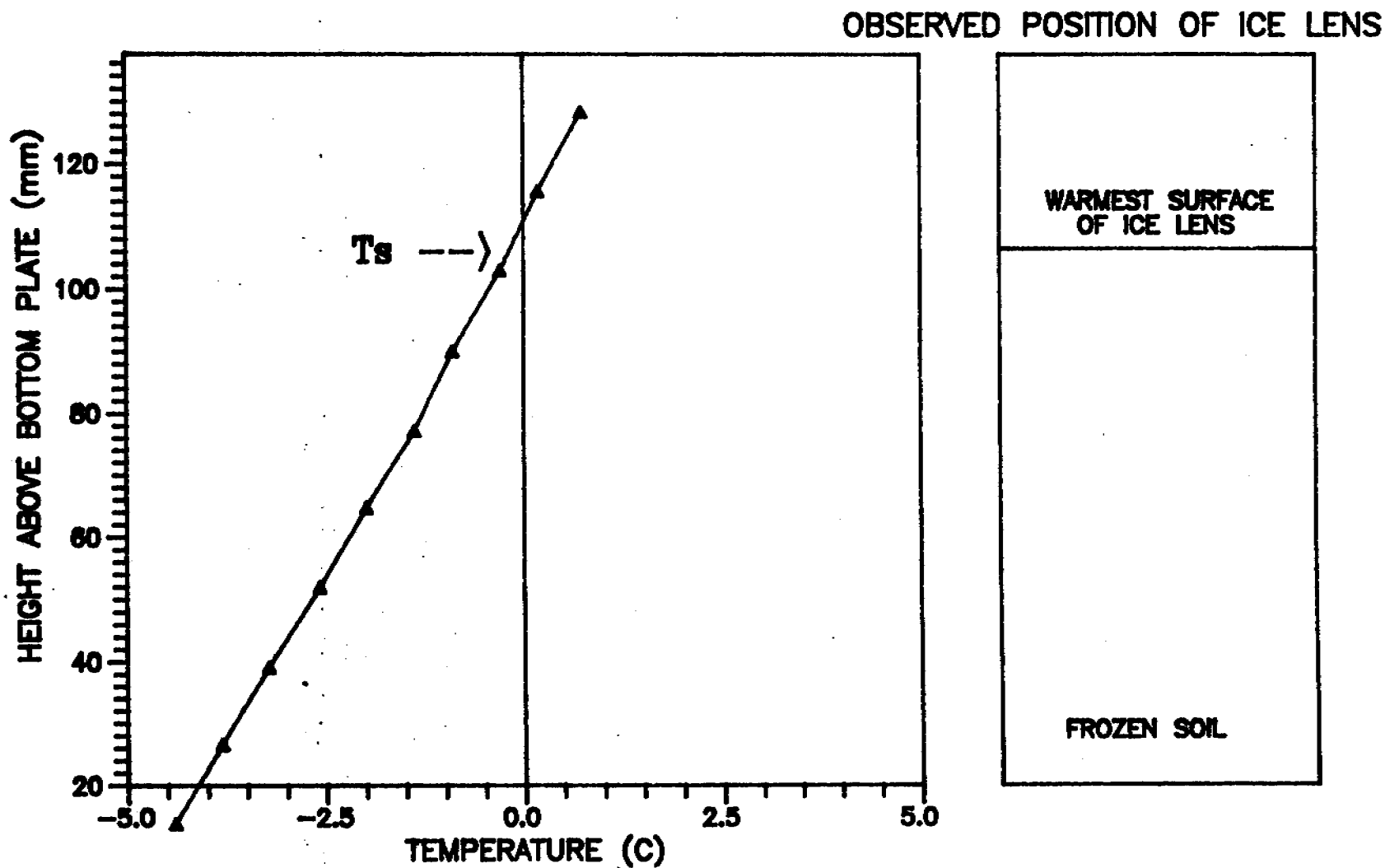


Fig. 18



TEMPERATURE PROFILE AT ONSET OF WARMEST ICE LENS -- S12

CONCENTRATION PROFILES IN UNFROZEN ZONE
for $z/l=0, dC/dz=0.001$
for $z/l=1, dC/dz=0$

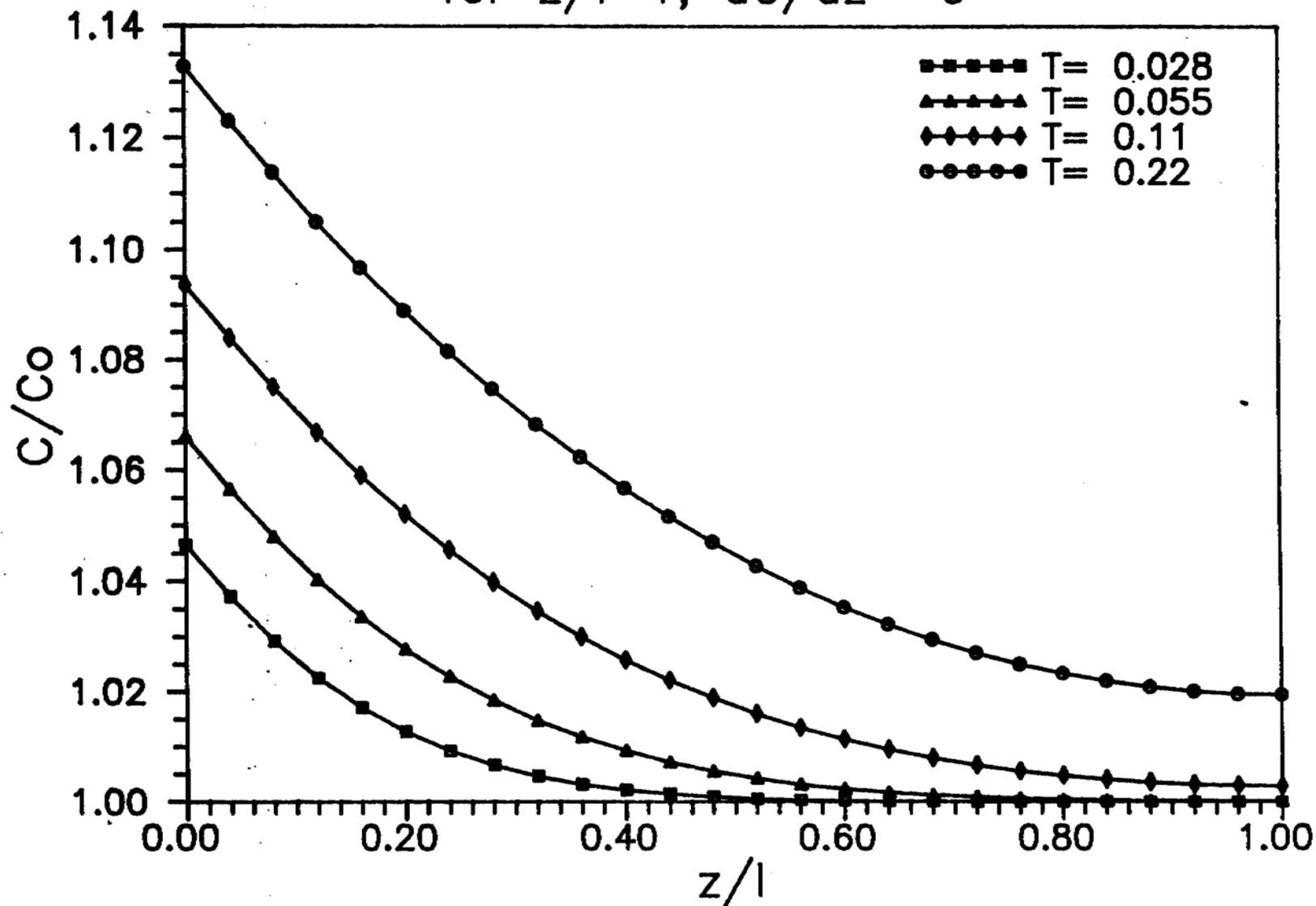
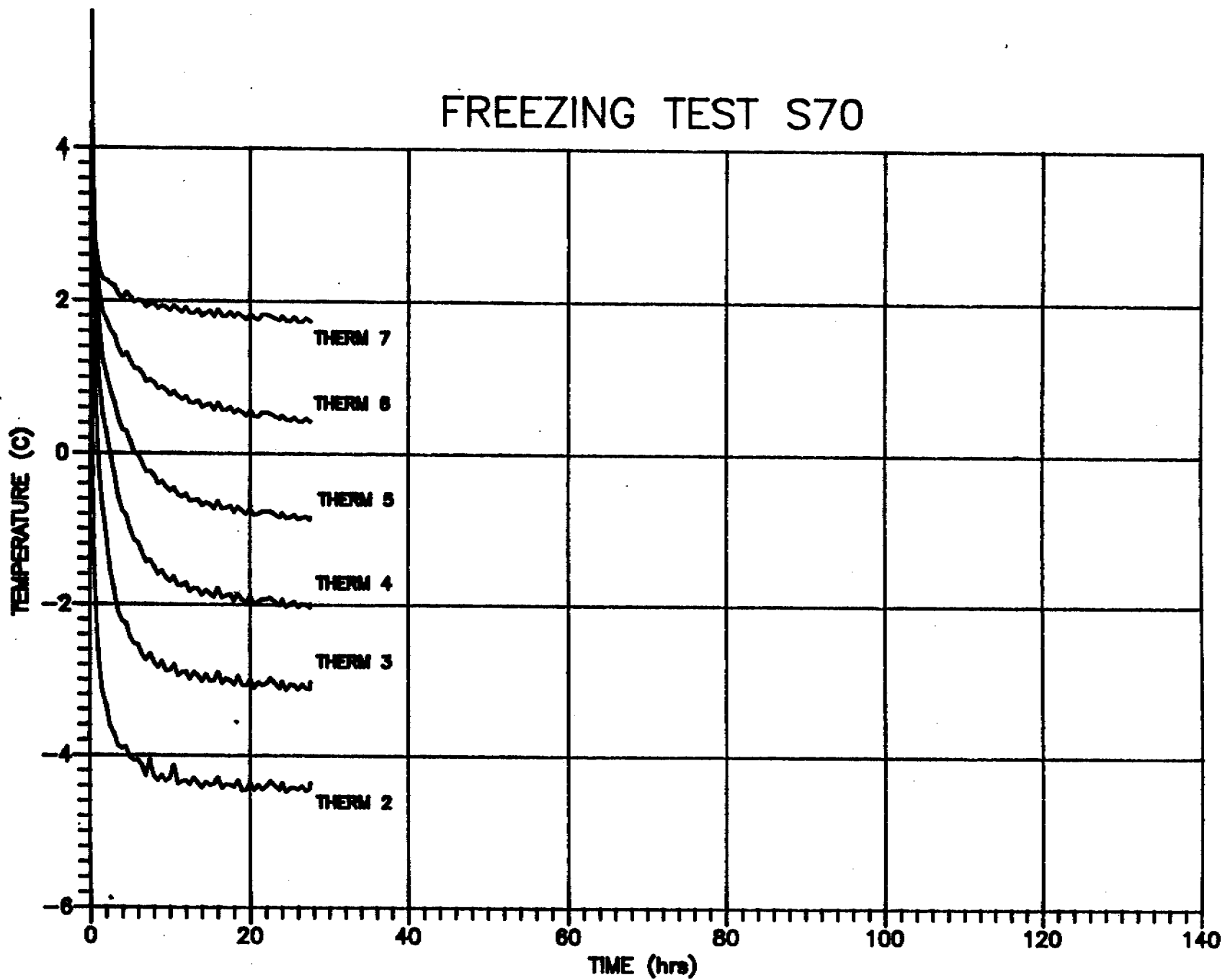


Fig. 20

FREEZING TEST S70



FREEZING TEST S70

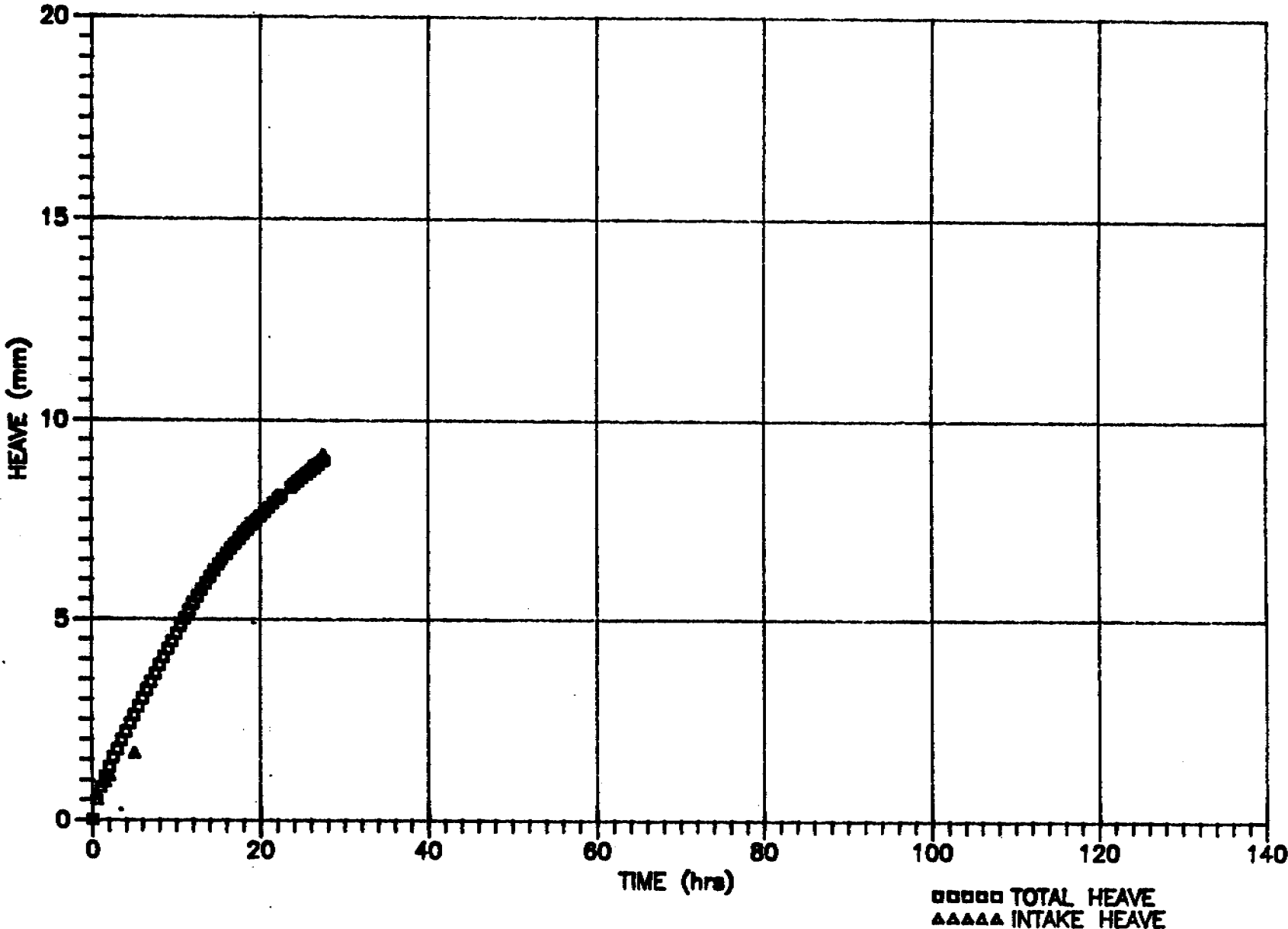


Fig. 22

TEST S70 FROST FRONT LOCATION

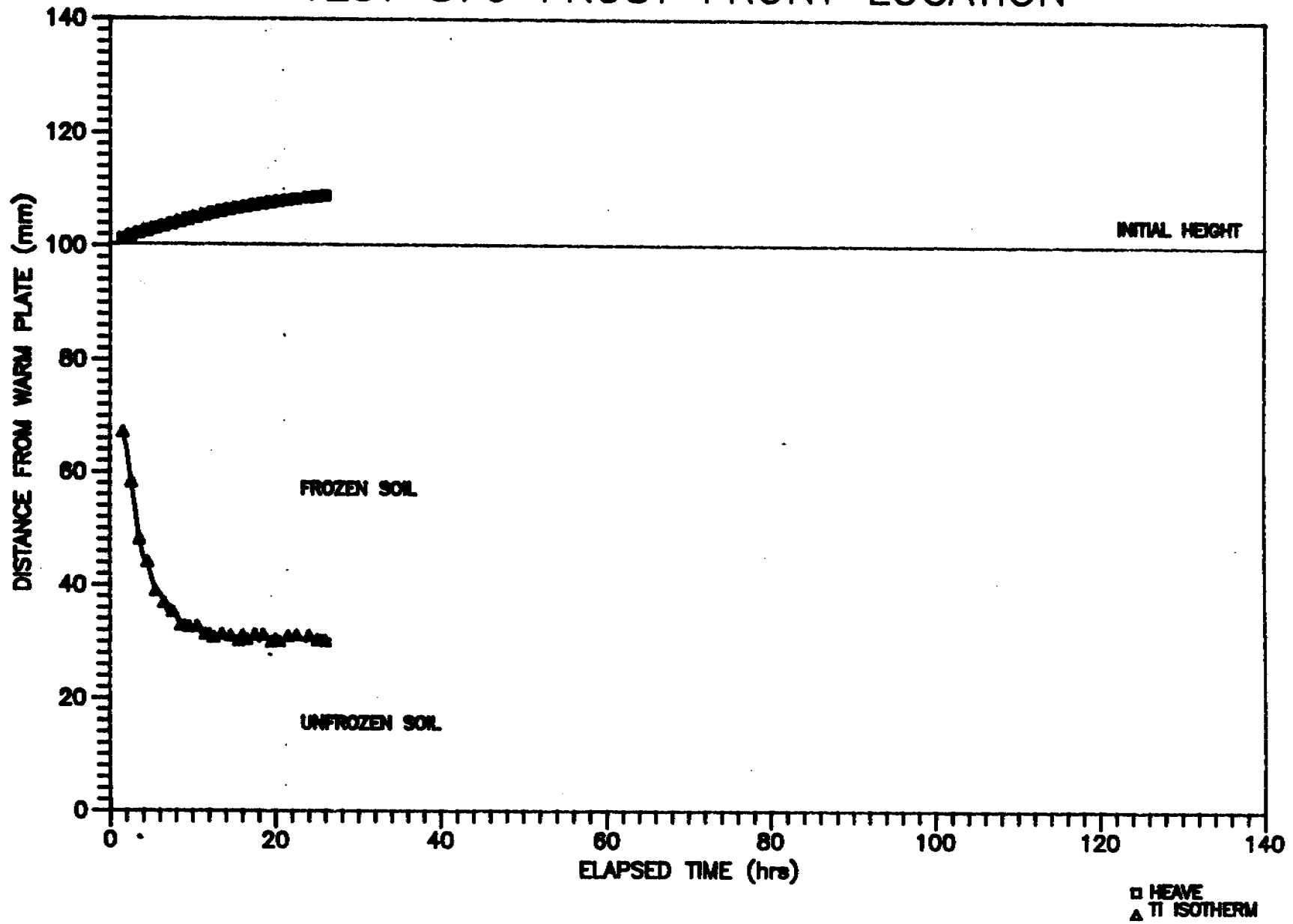


Fig. 23

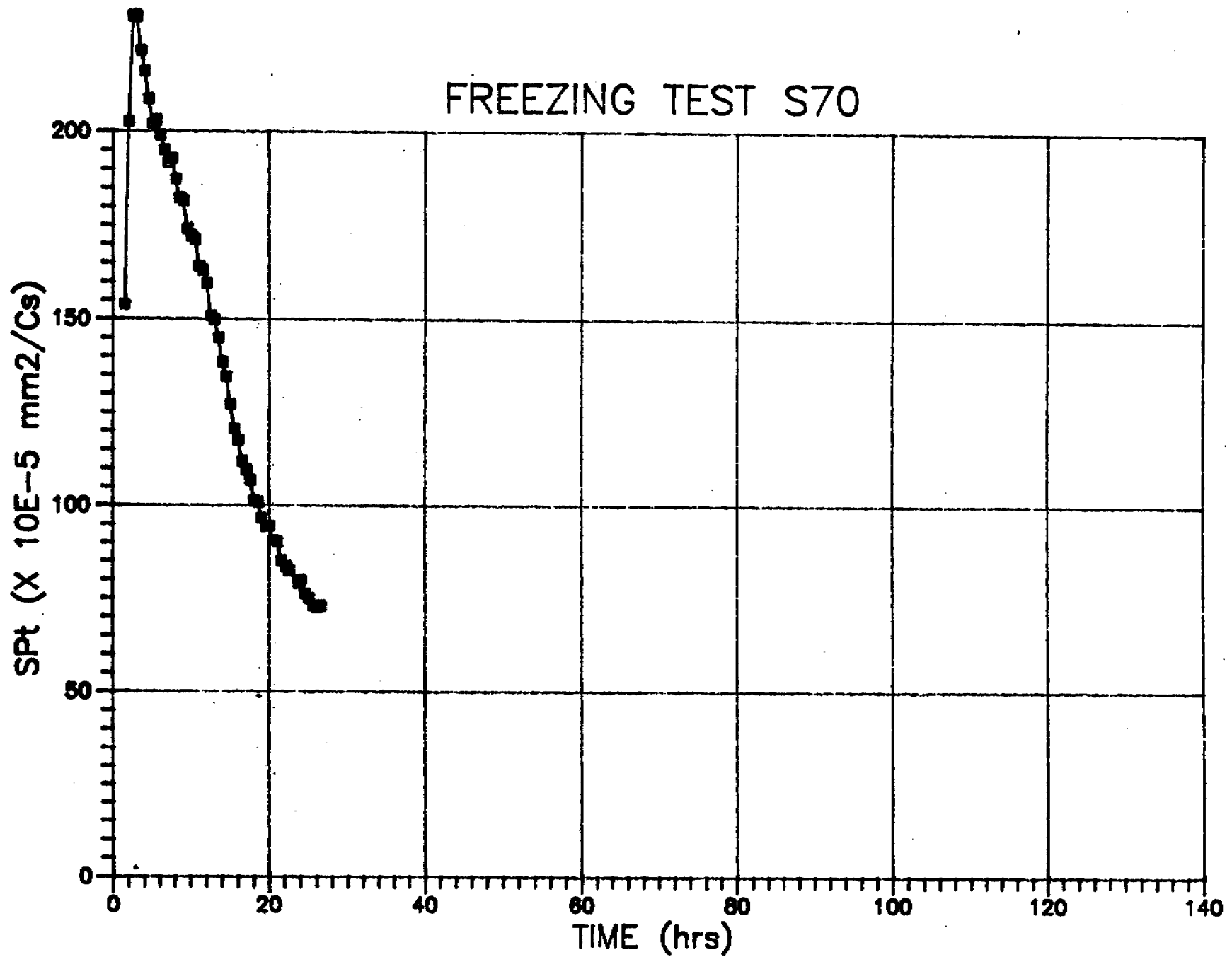


Fig. 24

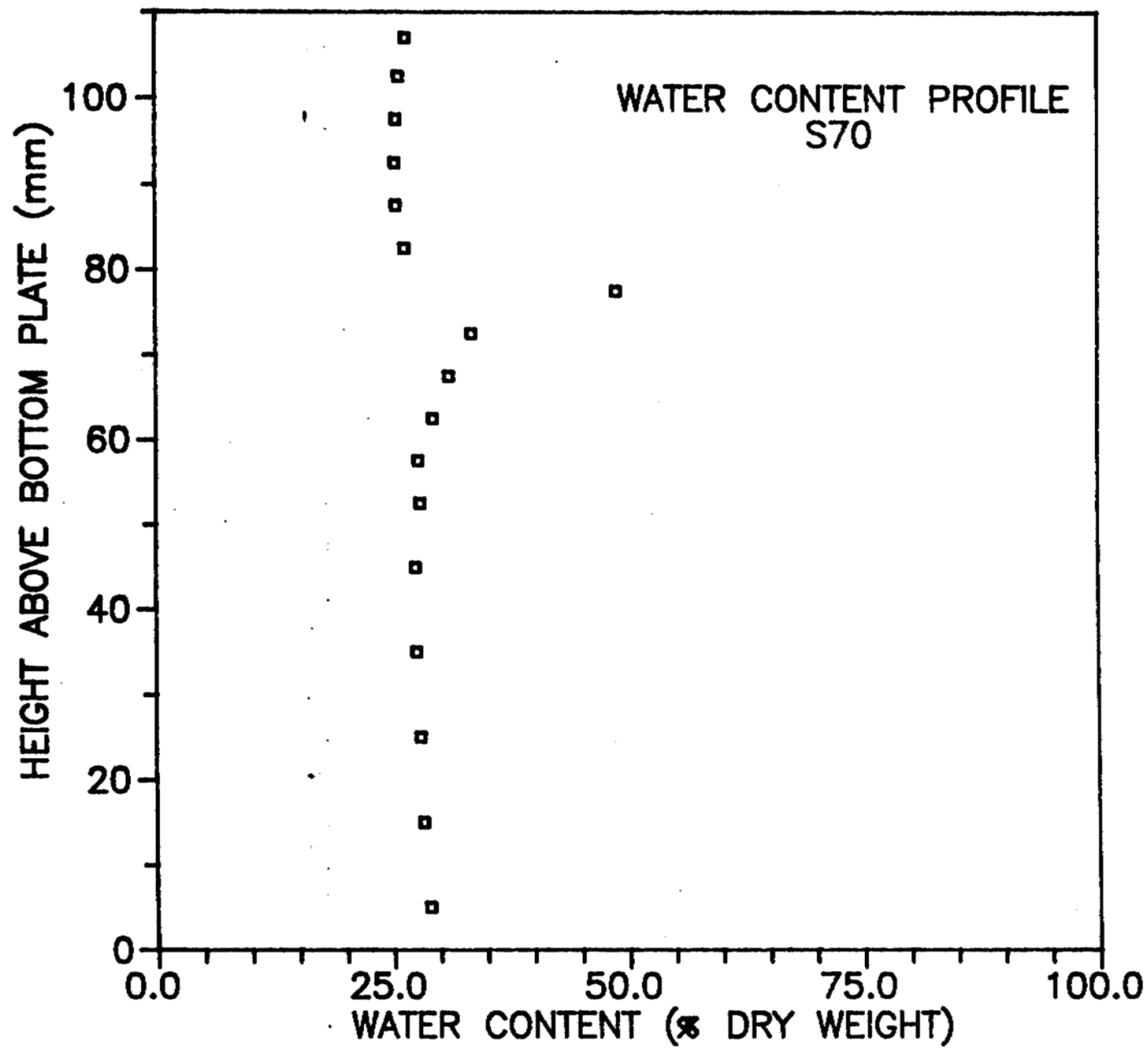


Fig. 25

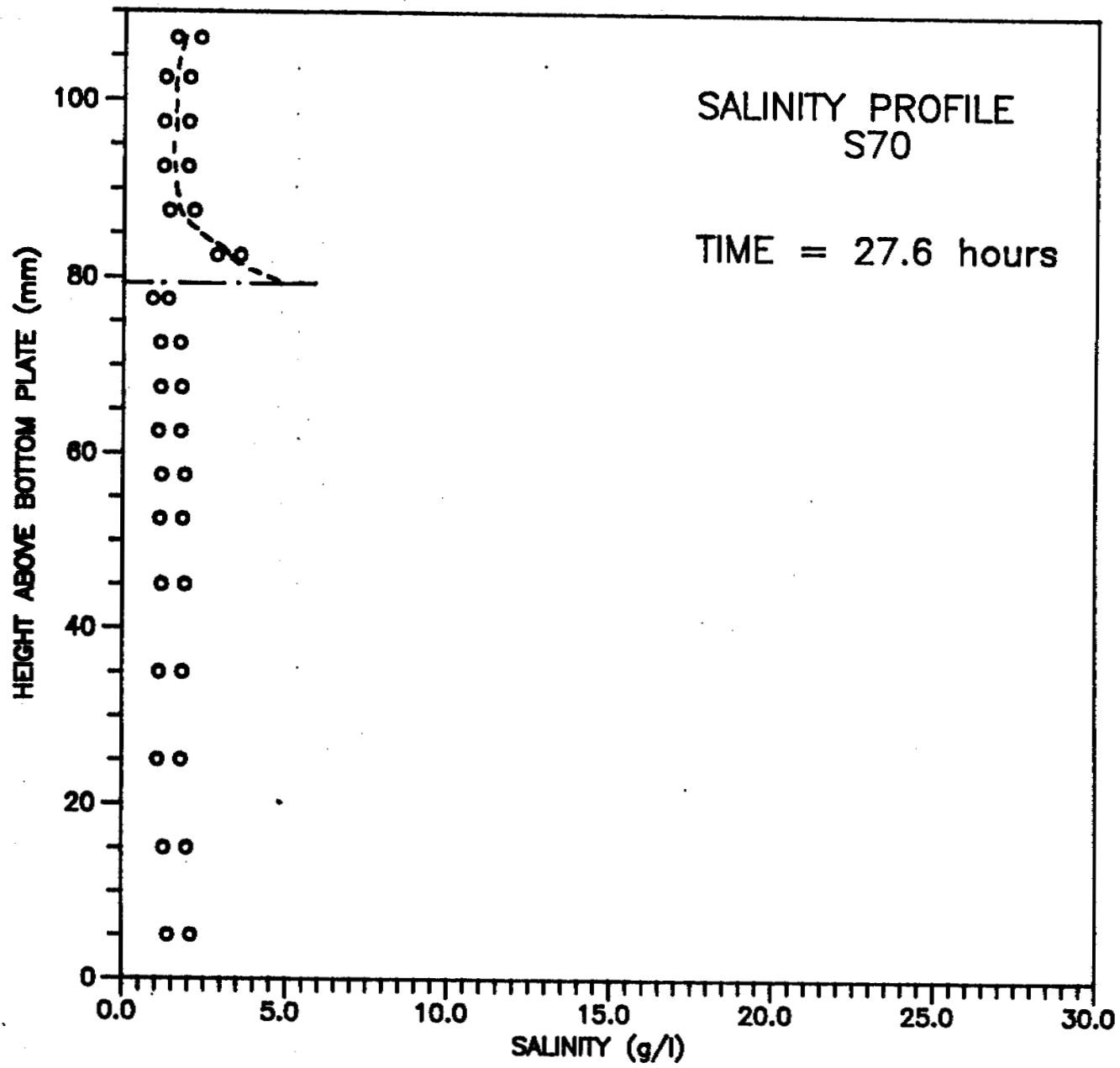
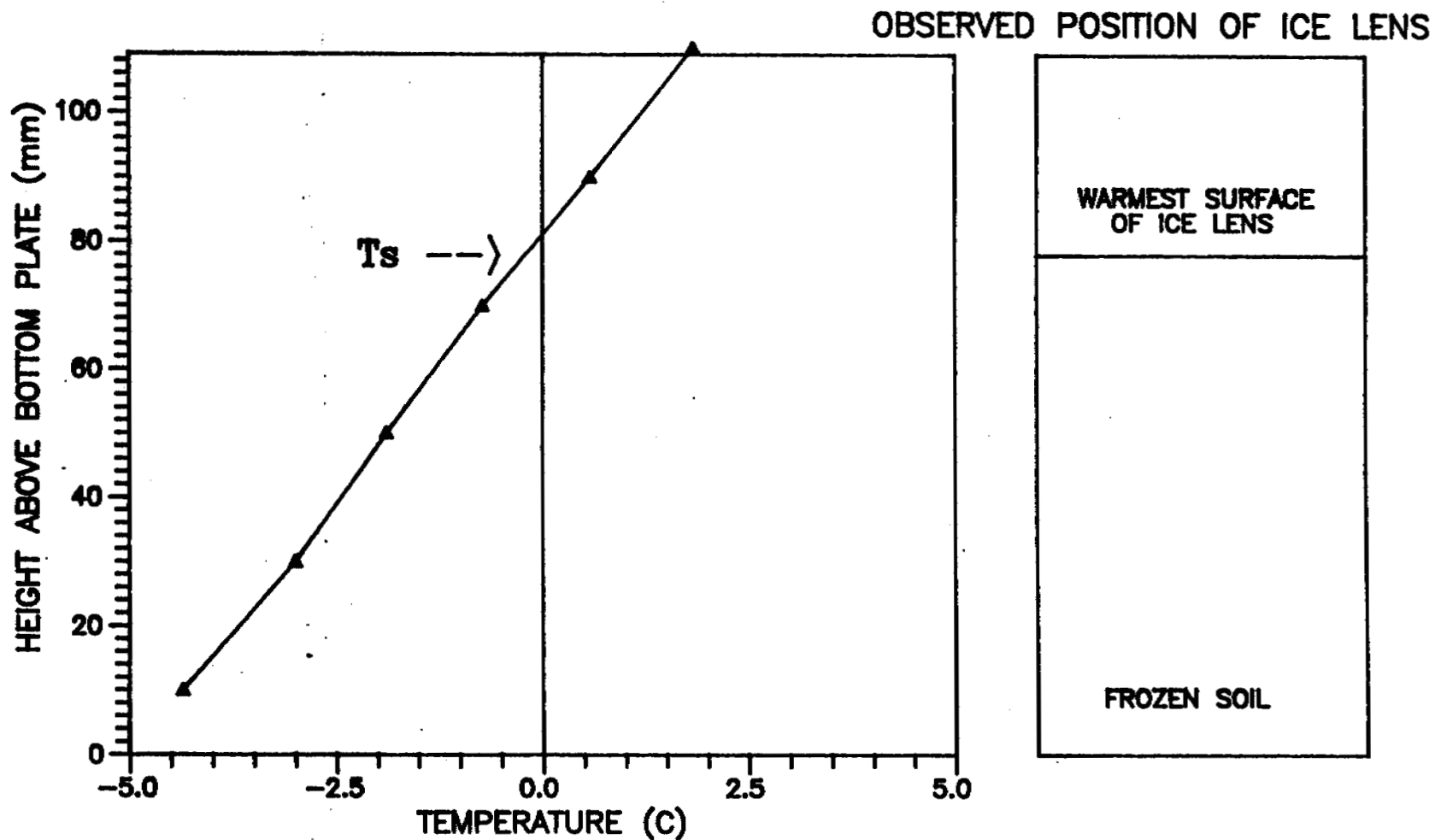


Fig. 26



TEMPERATURE PROFILE AT ONSET OF WARMEST ICE LENS -- S70

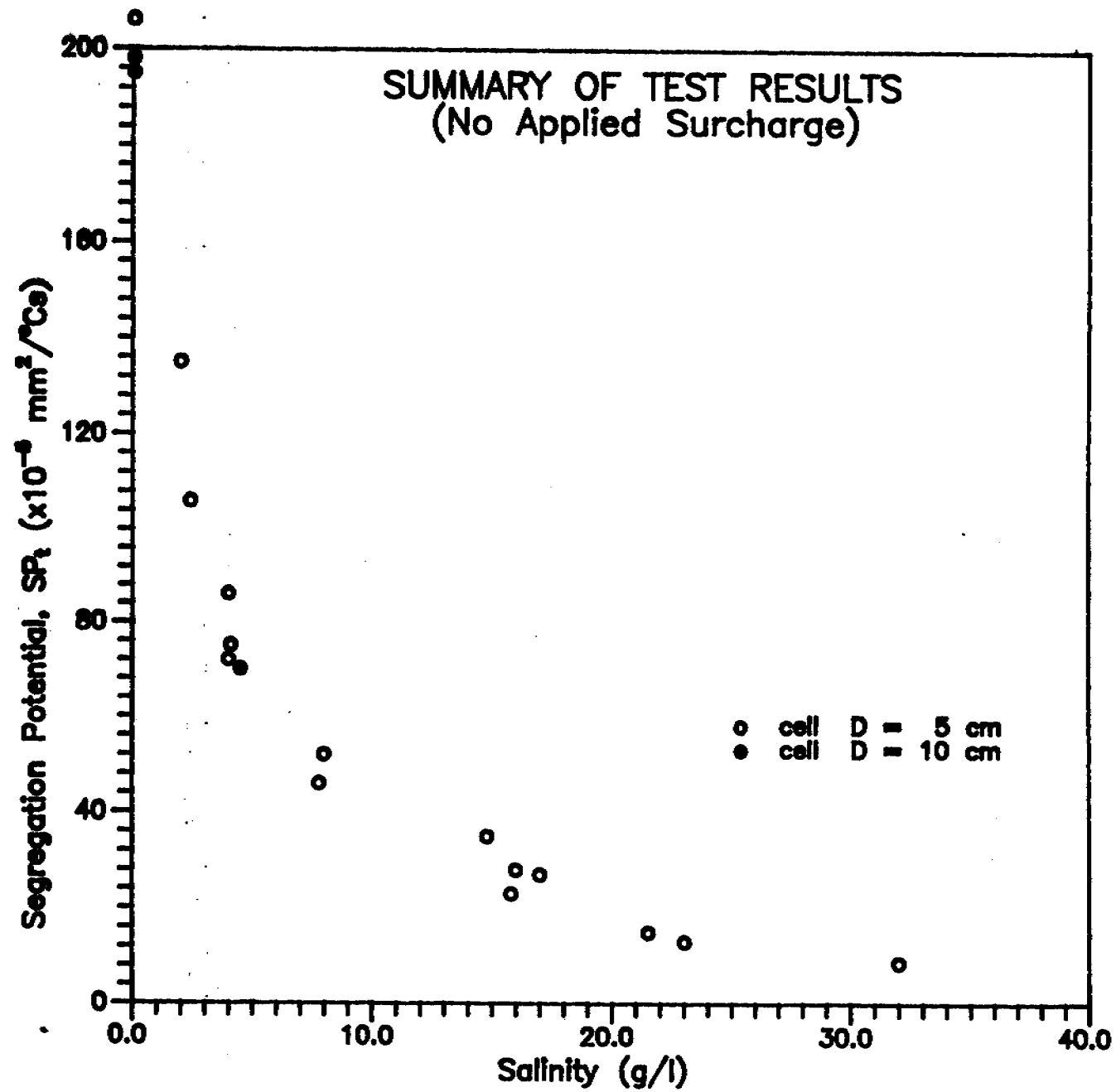


Fig. 28

FREEZING TEST SAP1

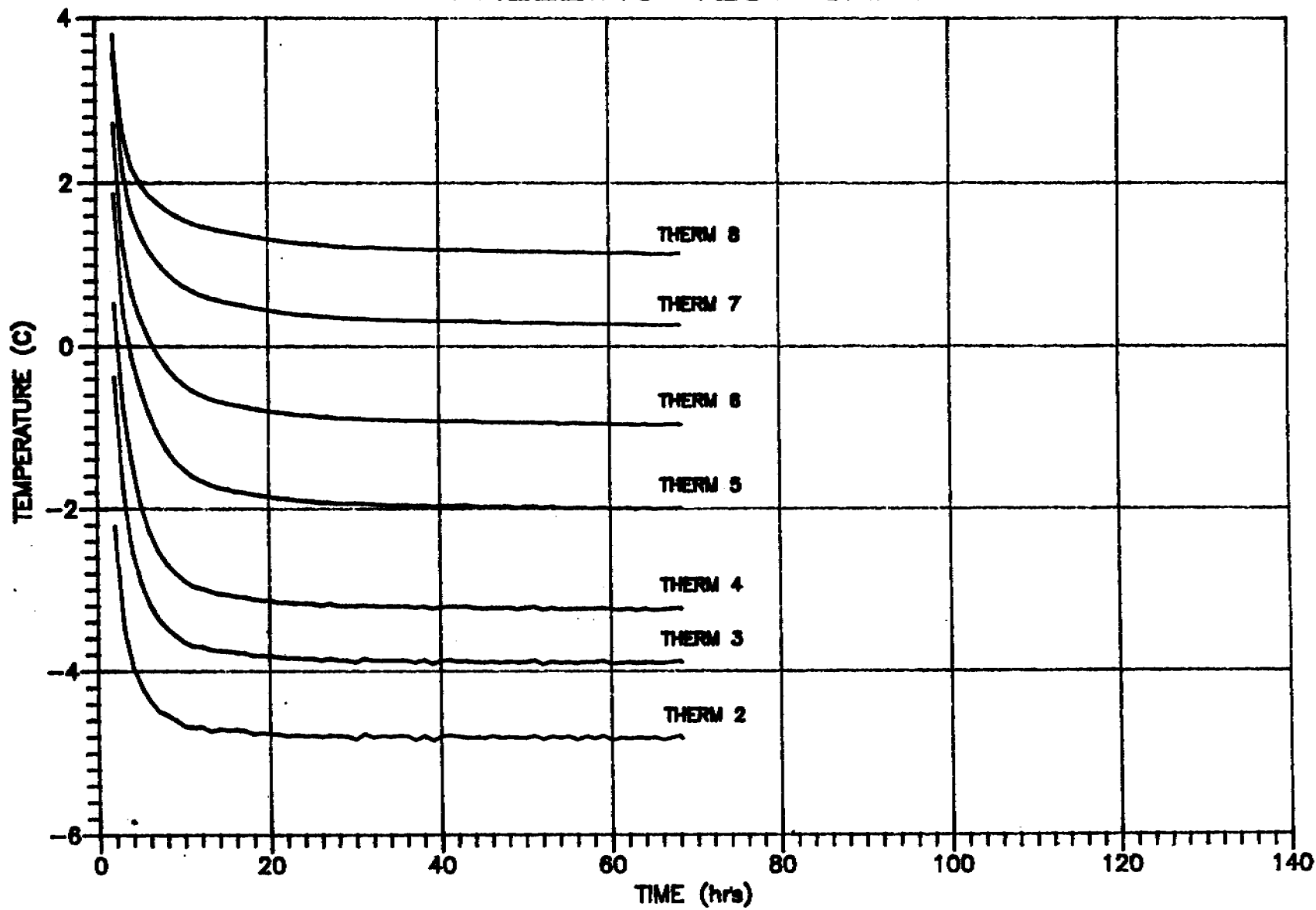


Fig. 29

FREEZING TEST SAP1

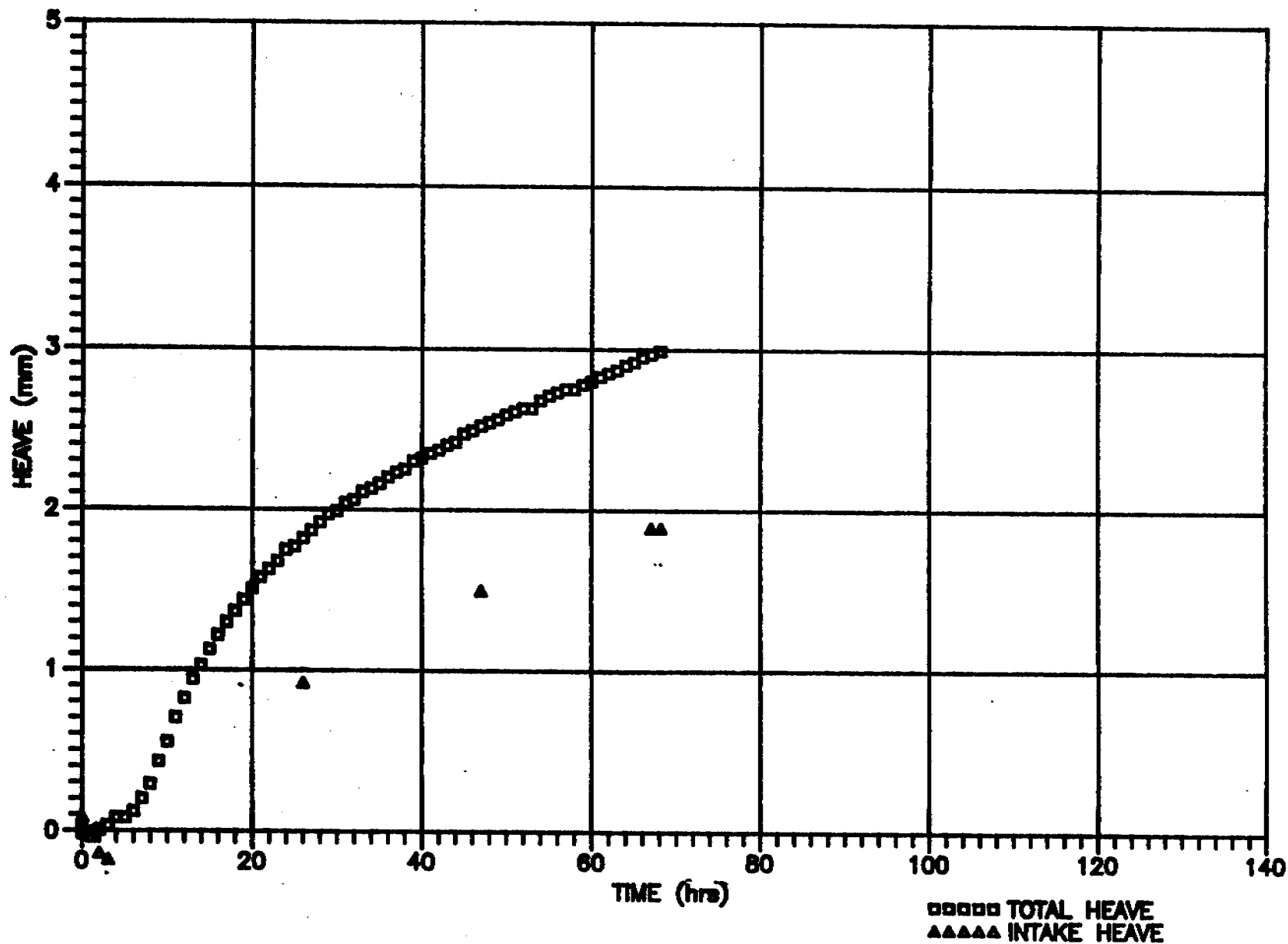


Fig. 30

TEST SAP1 FROST FRONT LOCATION

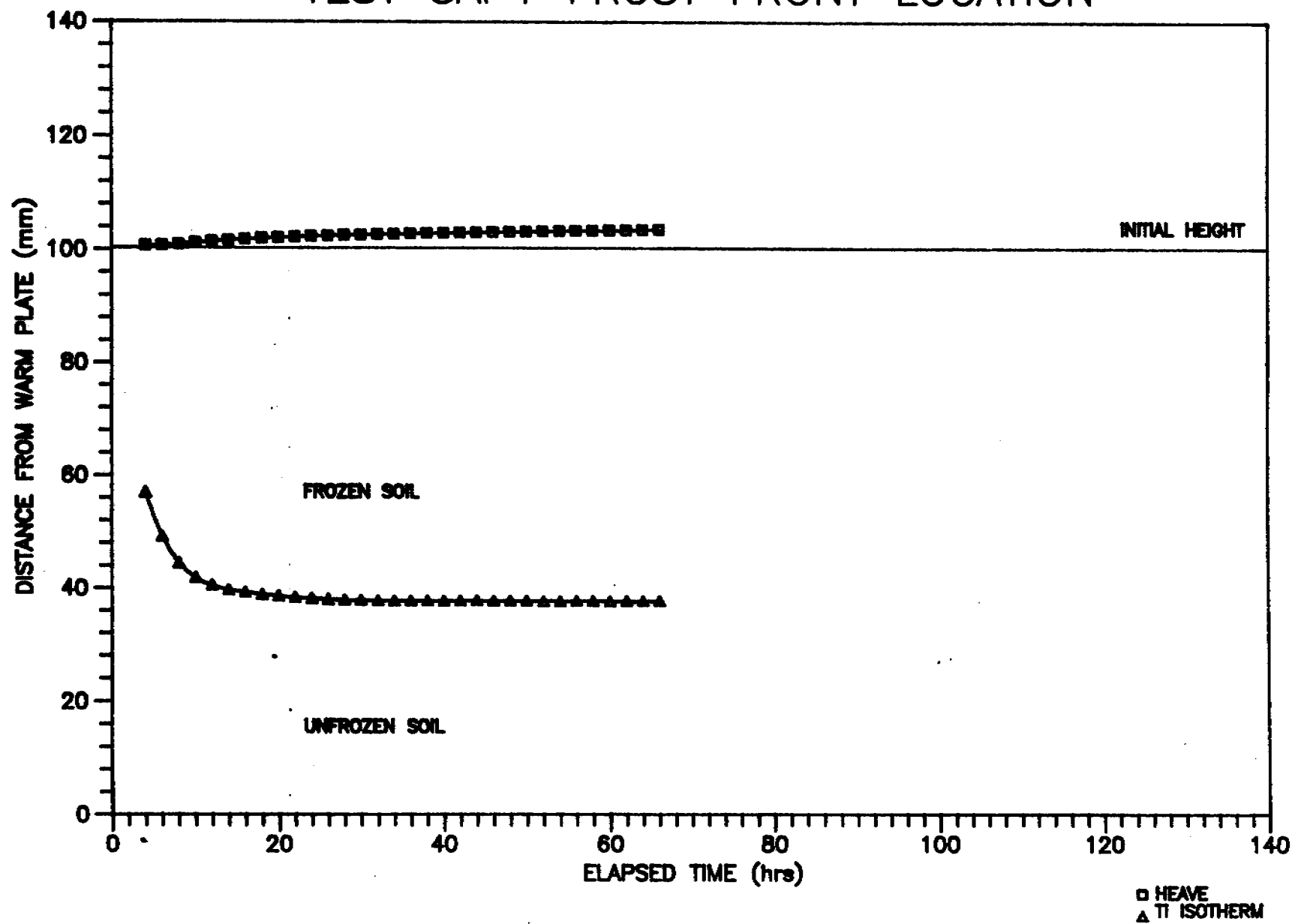


Fig. 31

FREEZING TEST SAP1

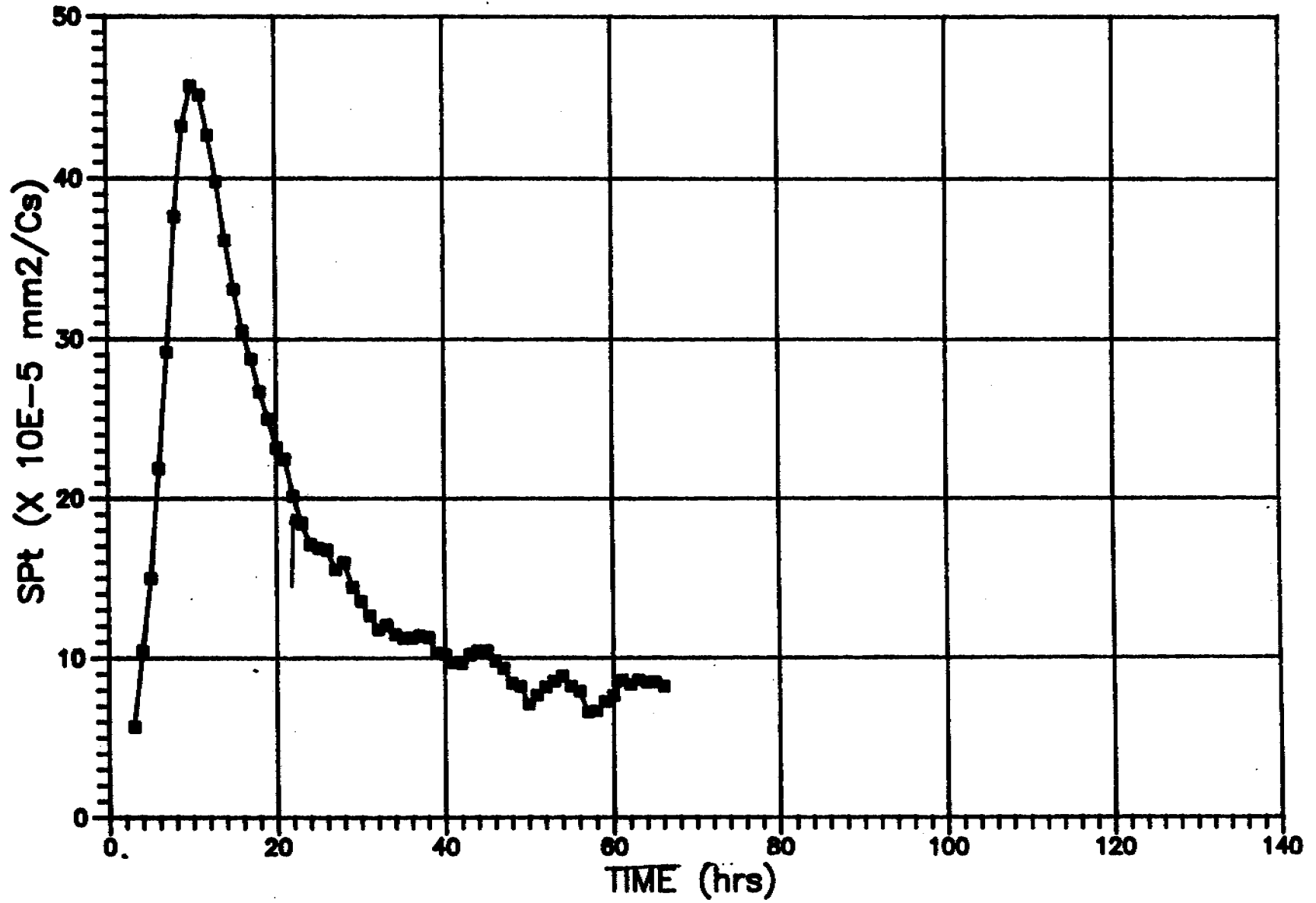


Fig. 32

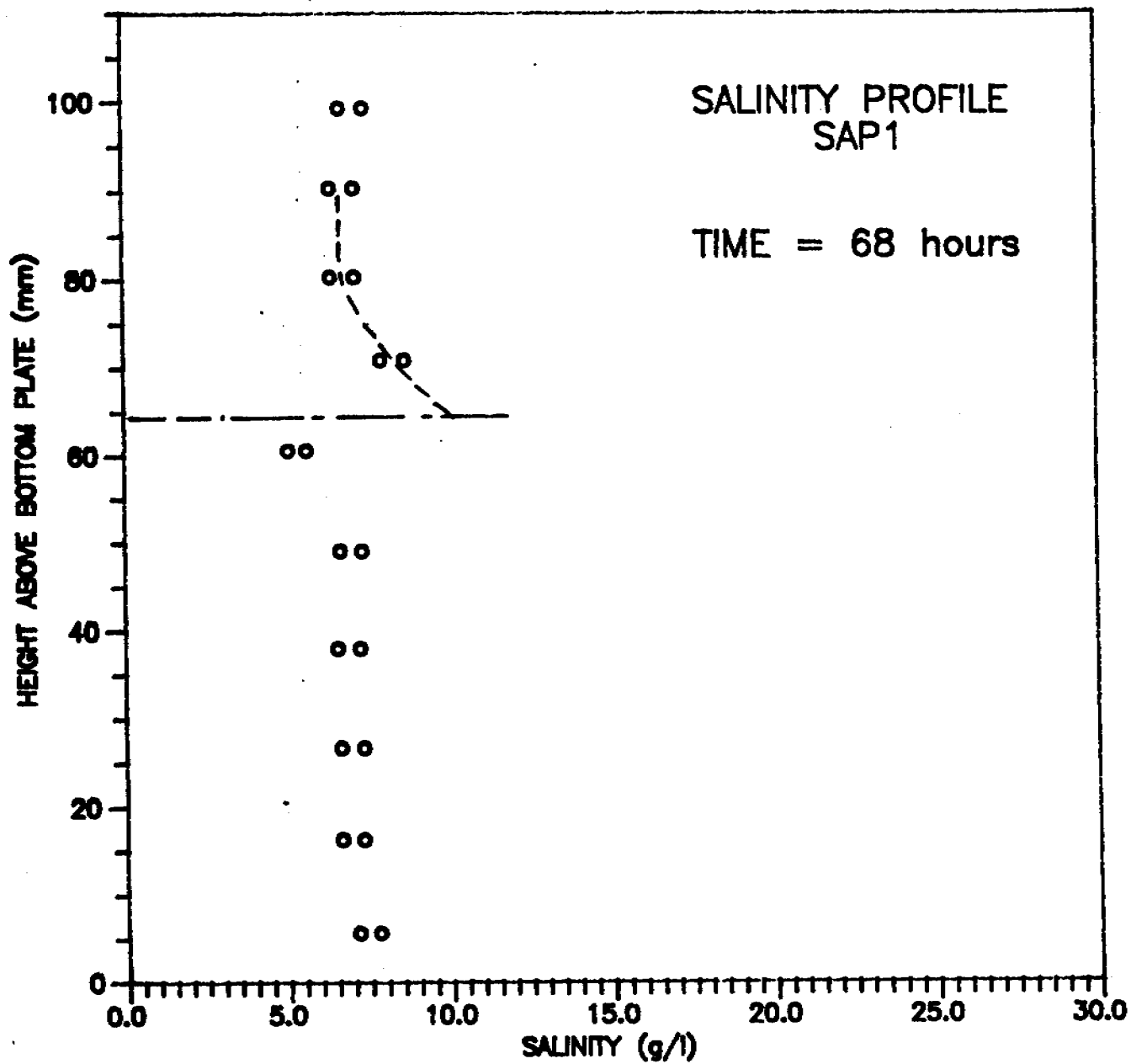


Fig. 33

FREEZING TEST SAP3

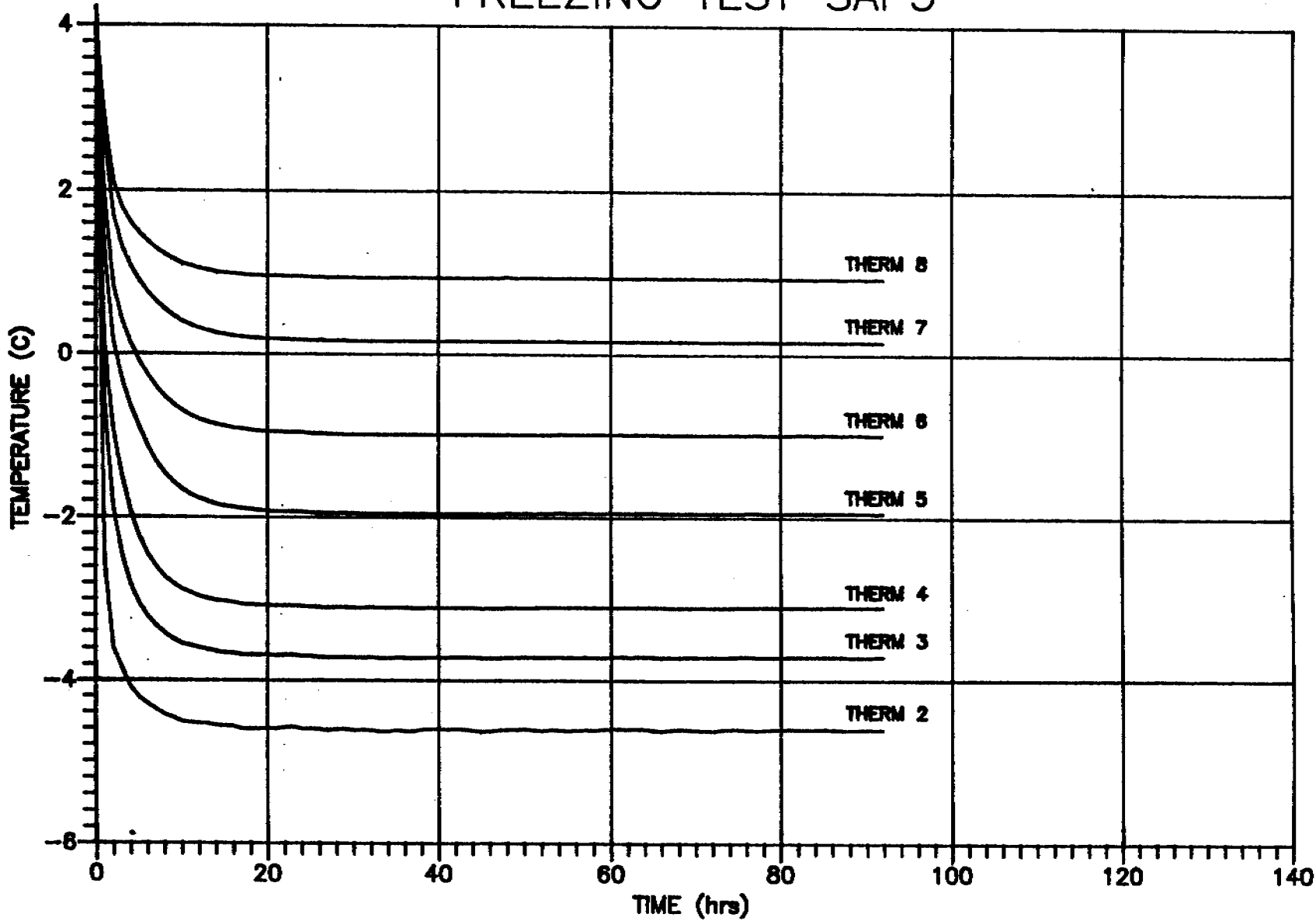


Fig. 34

FREEZING TEST SAP3

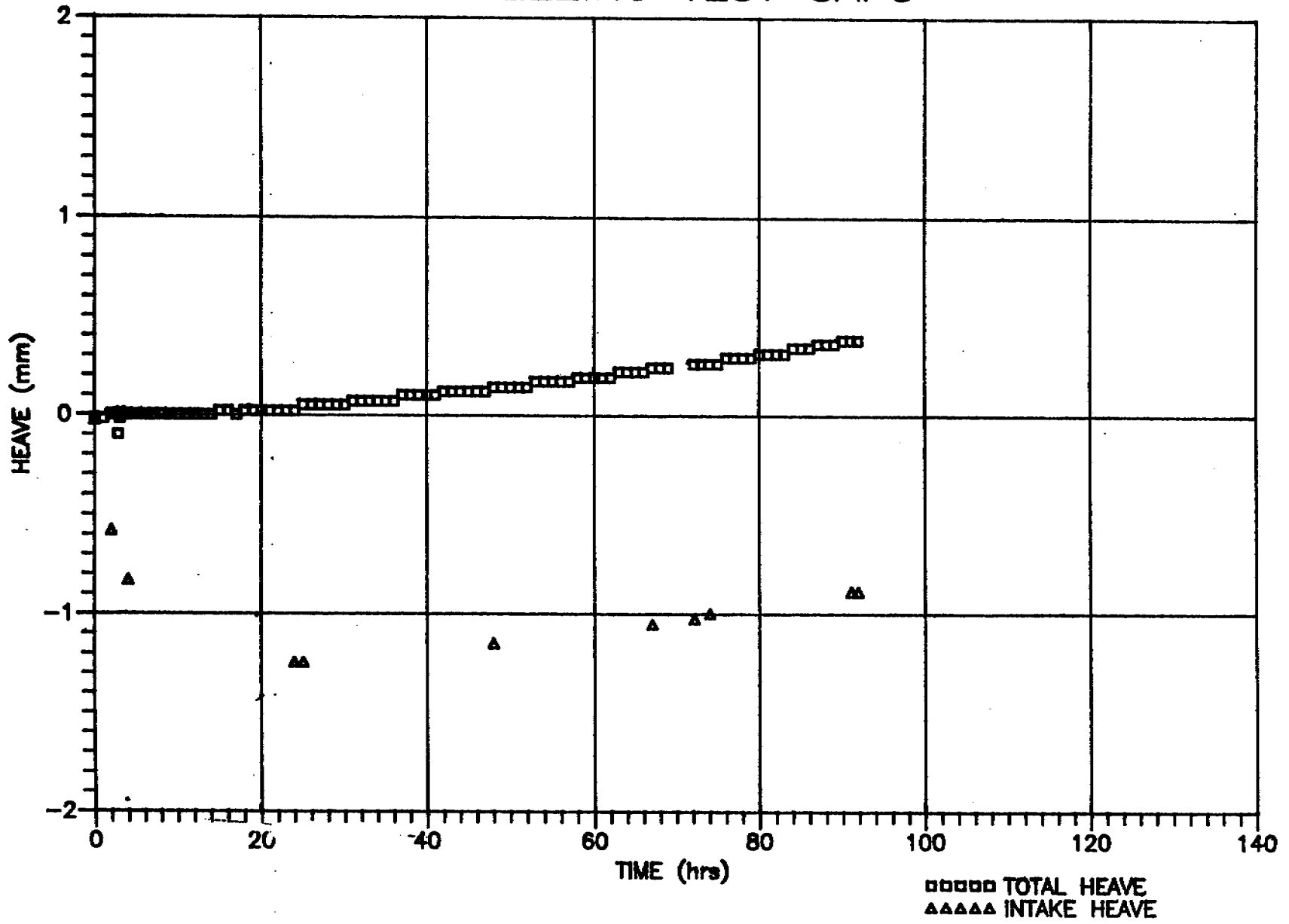


Fig. 35

TEST SAP3 FROST FRONT LOCATION

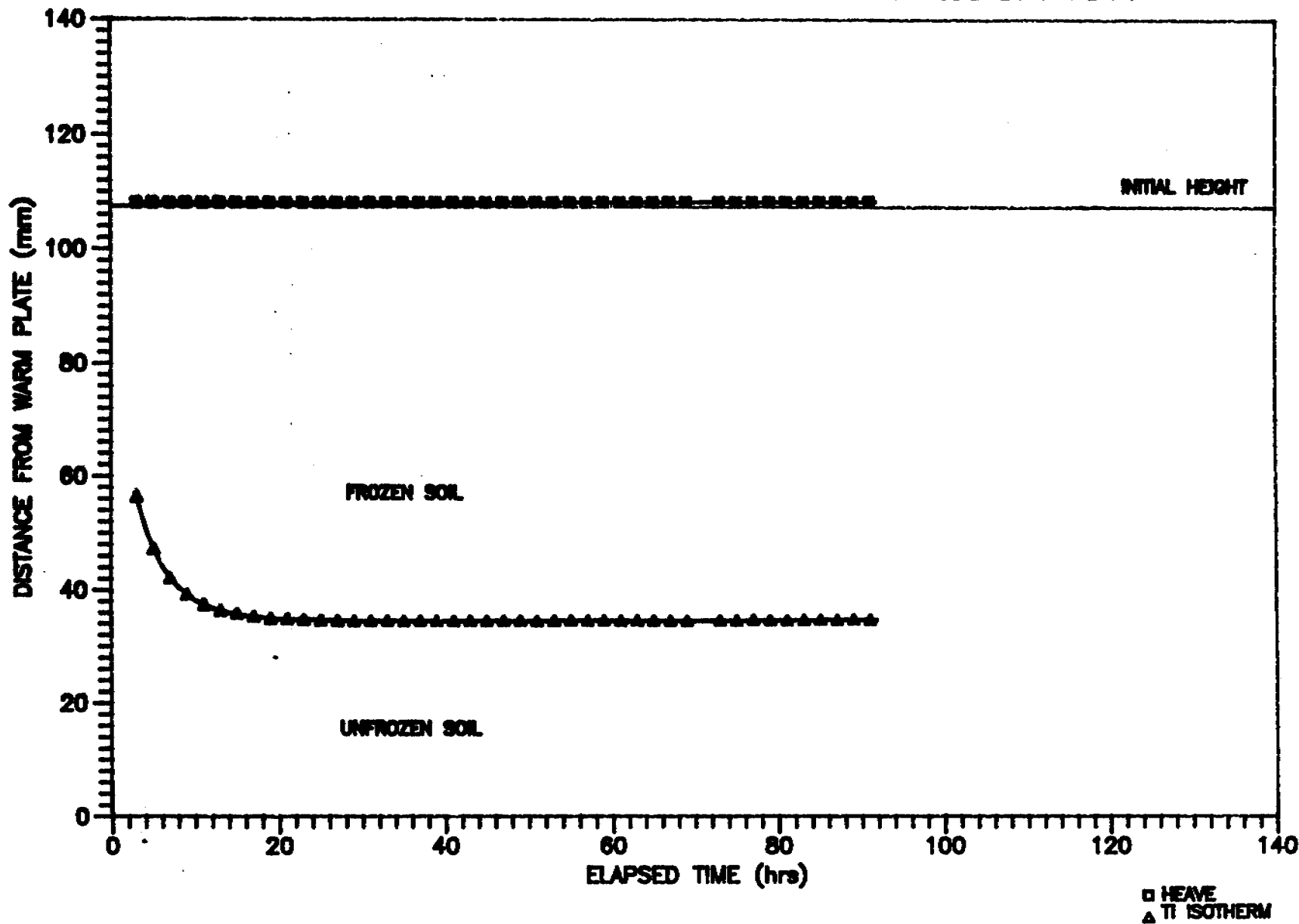


Fig. 36

FREEZING TEST SAP3

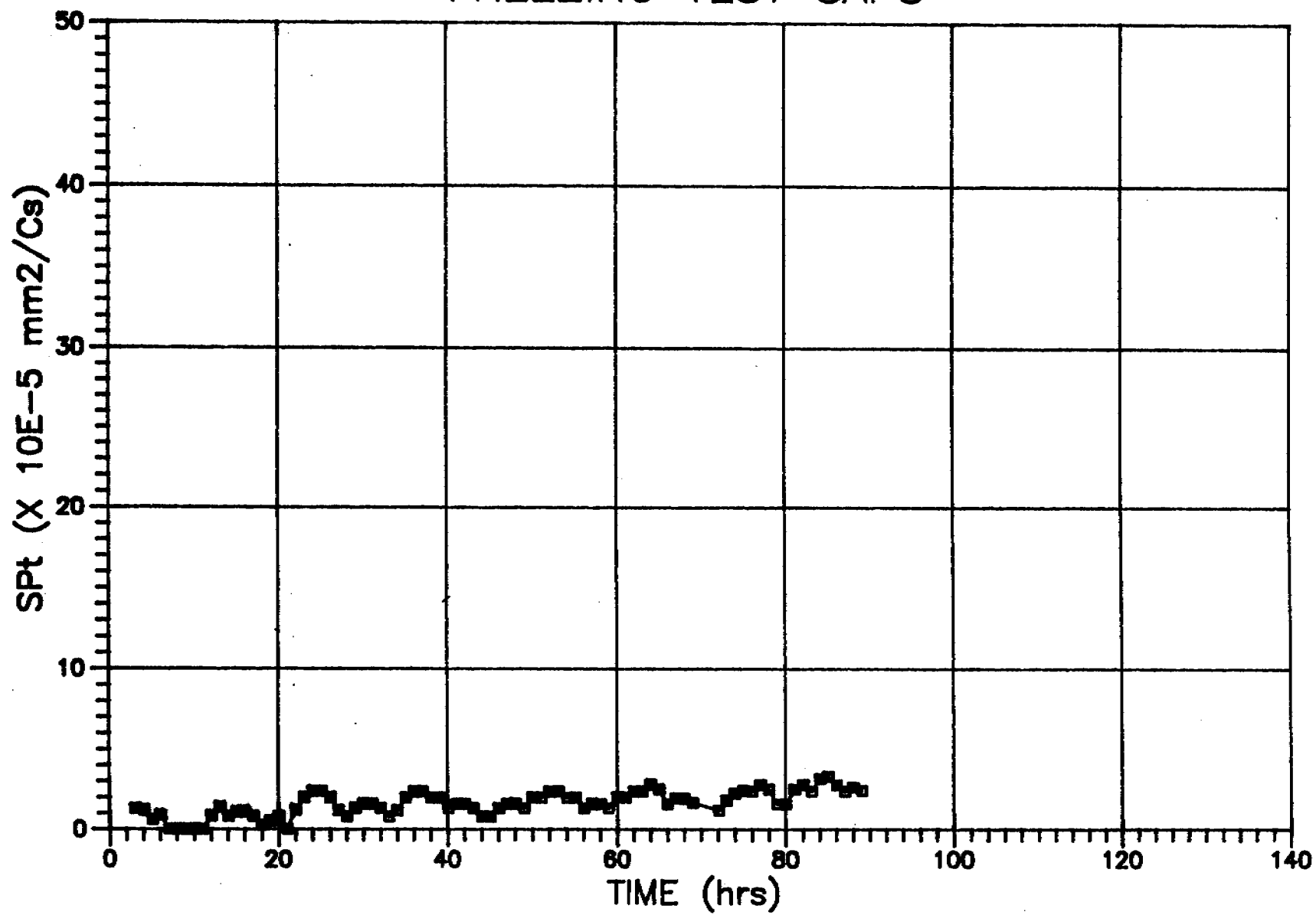


Fig. 37

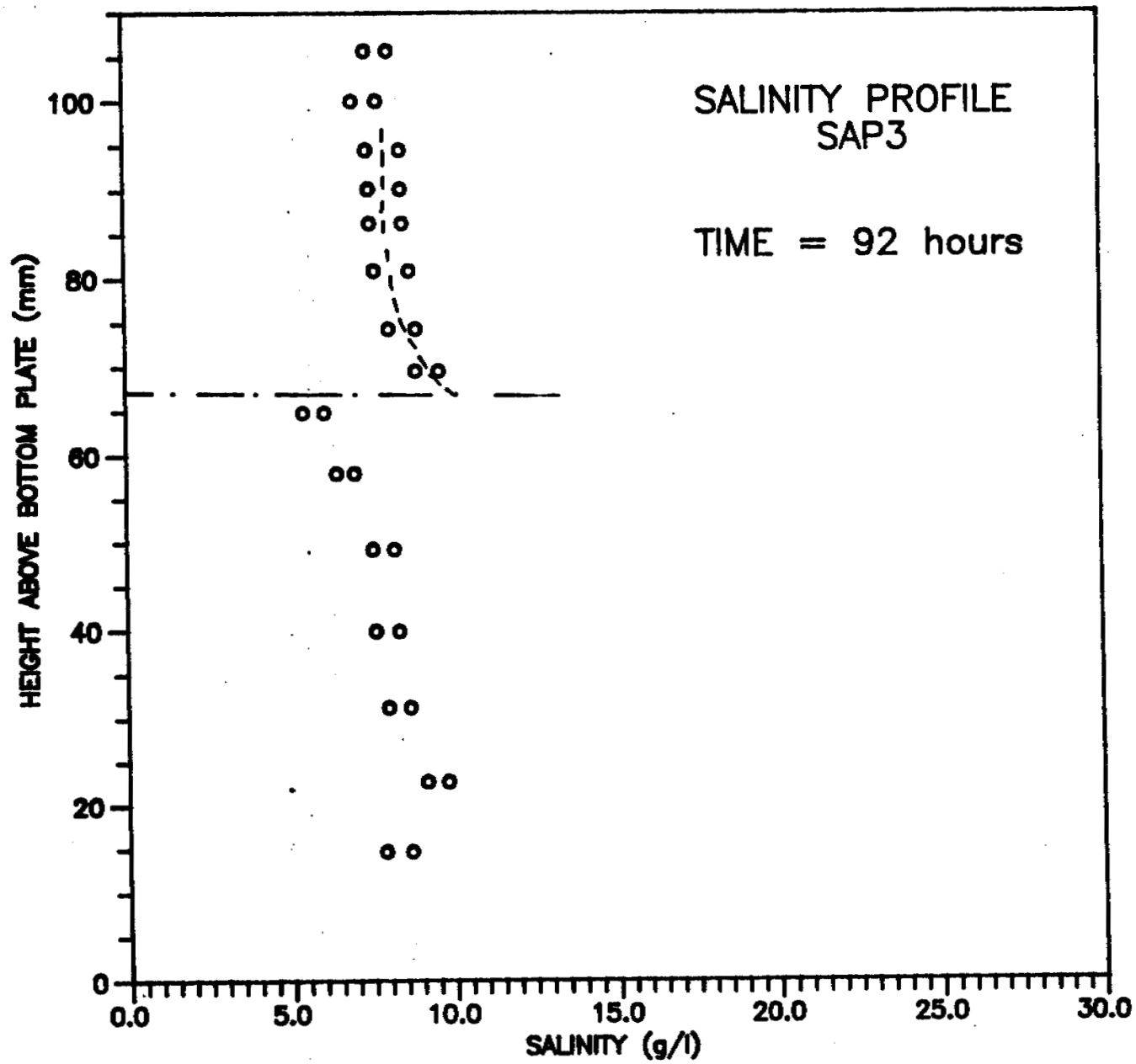


Fig. 38

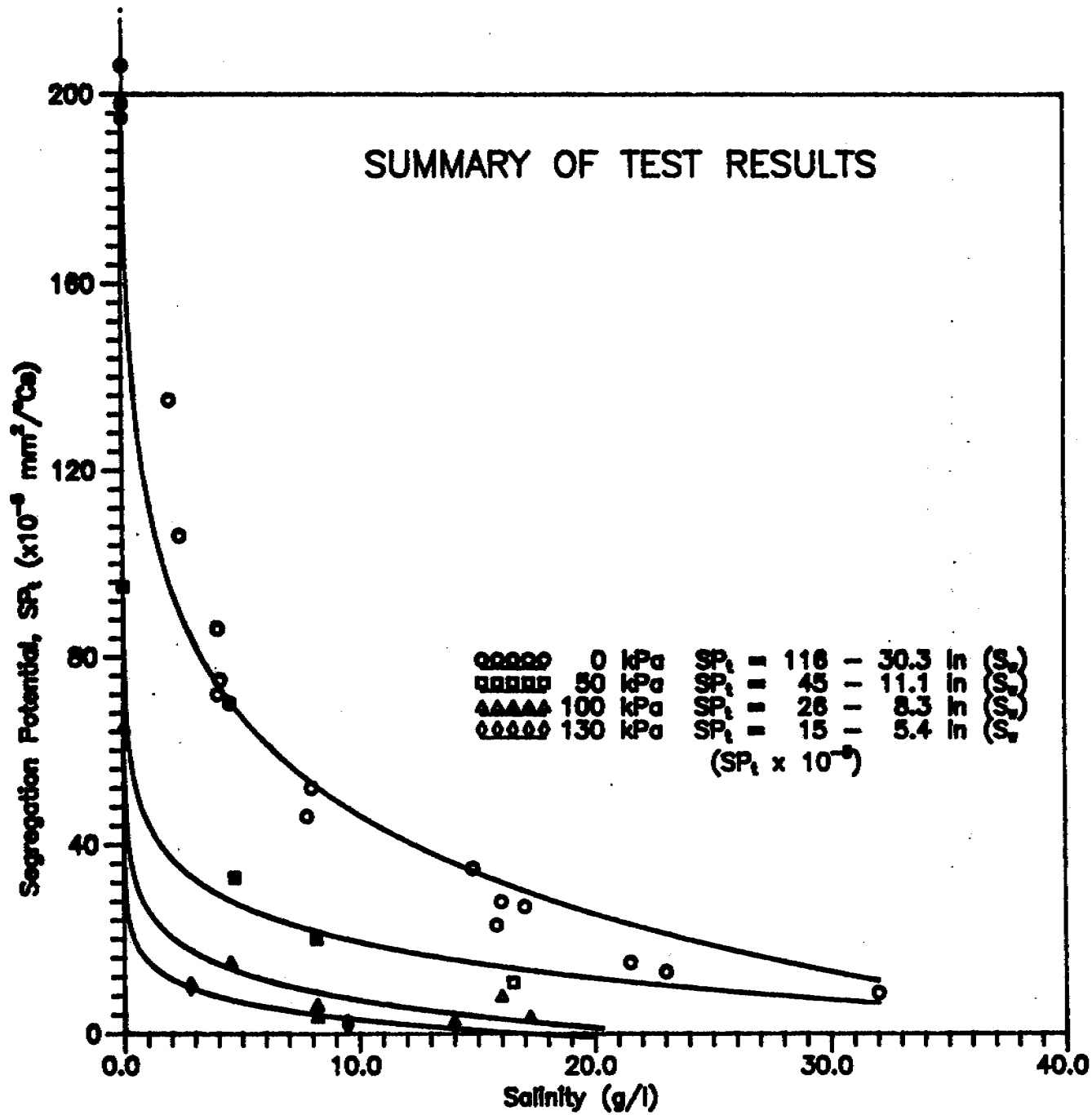
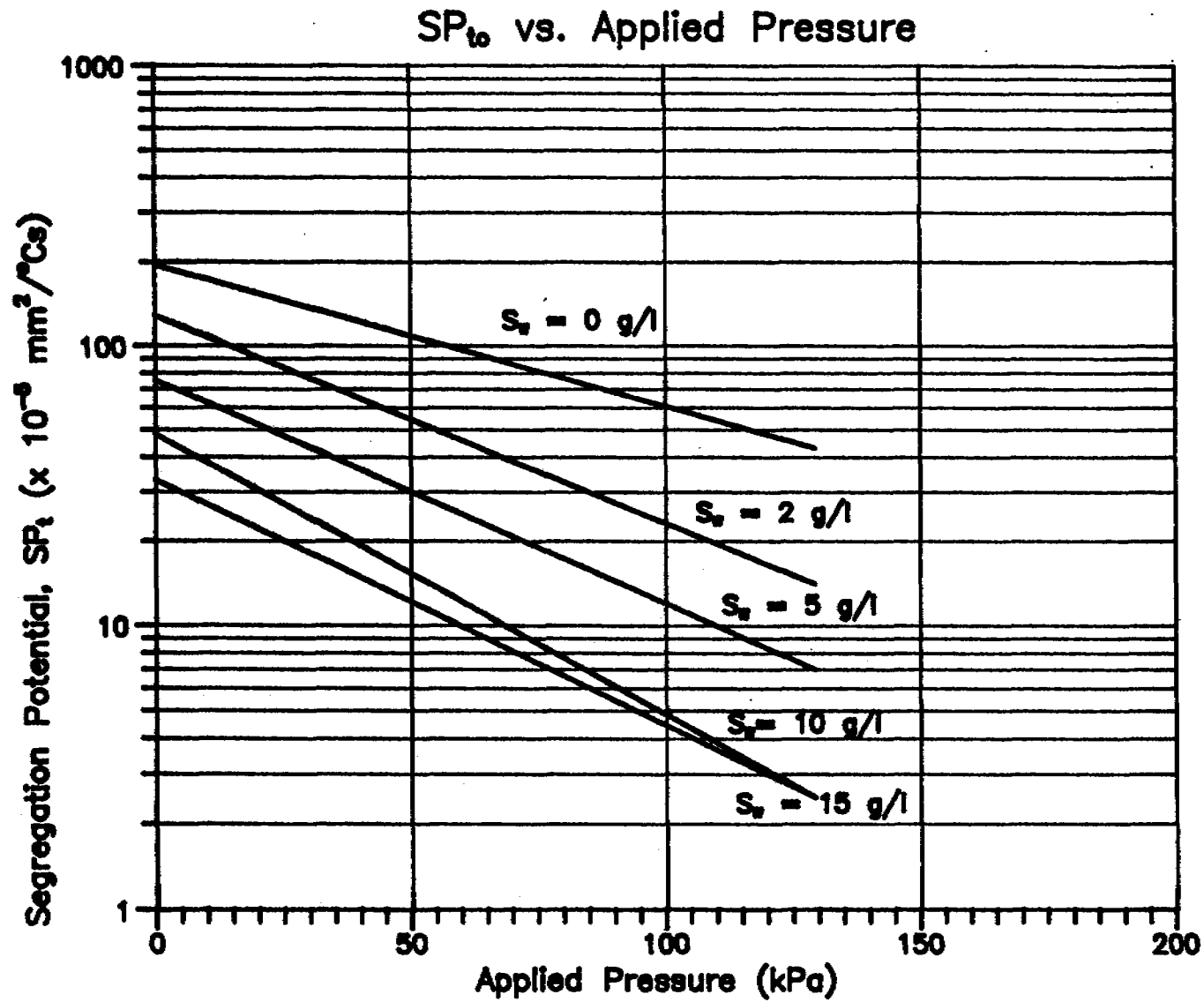


Fig. 39



S_v (g/l)	SP_t ($\text{mm}^2/^\circ\text{Cs}$)	
0	195×10^{-5}	$e^{-.0117P}$
2	128×10^{-5}	$e^{-.0171P}$
5	75×10^{-5}	$e^{-.0184P}$
10	48×10^{-5}	$e^{-.0229P}$
15	33×10^{-5}	$e^{-.0200P}$

FIG. 40

FREEZING TEST S50

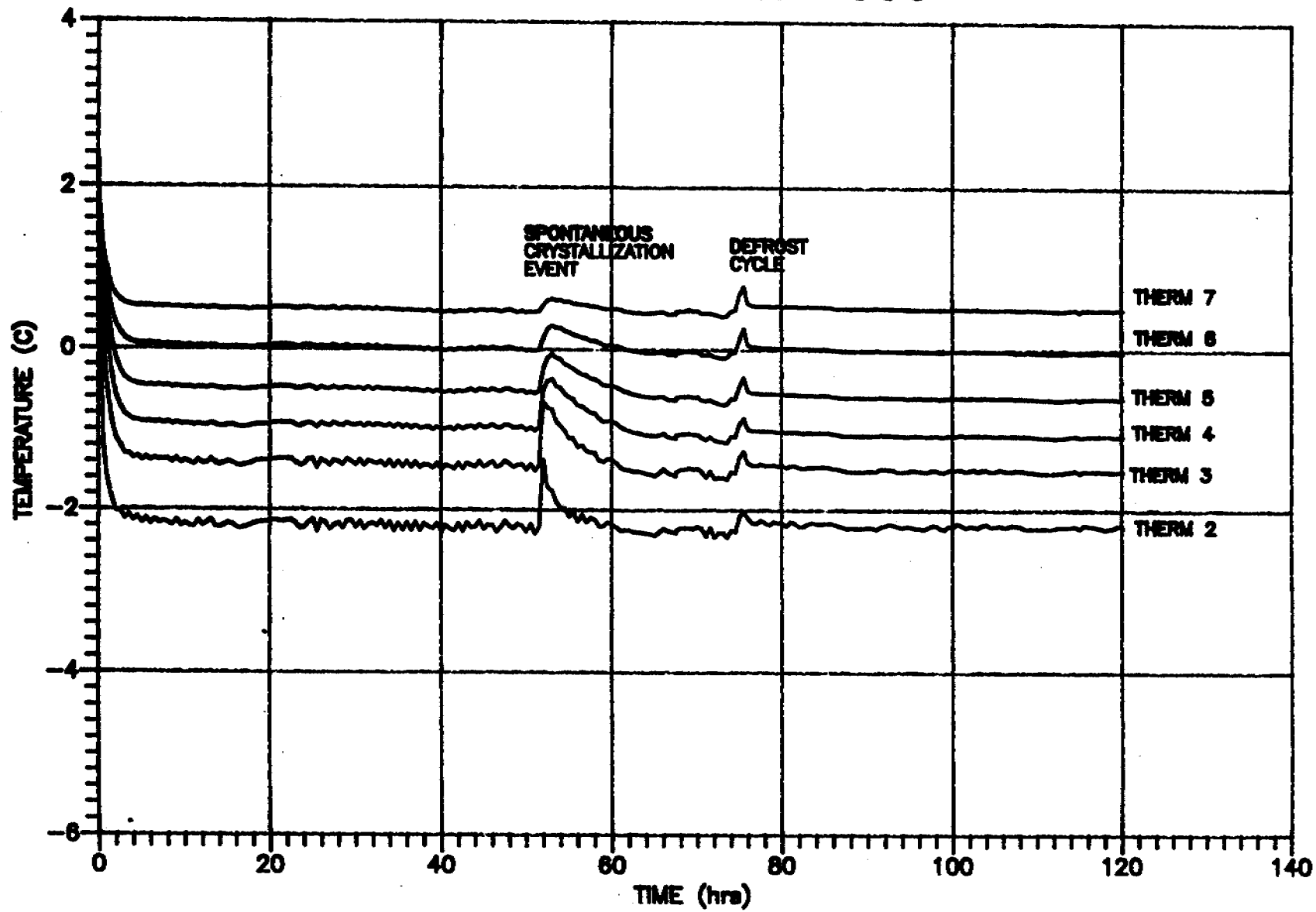


Fig. 41

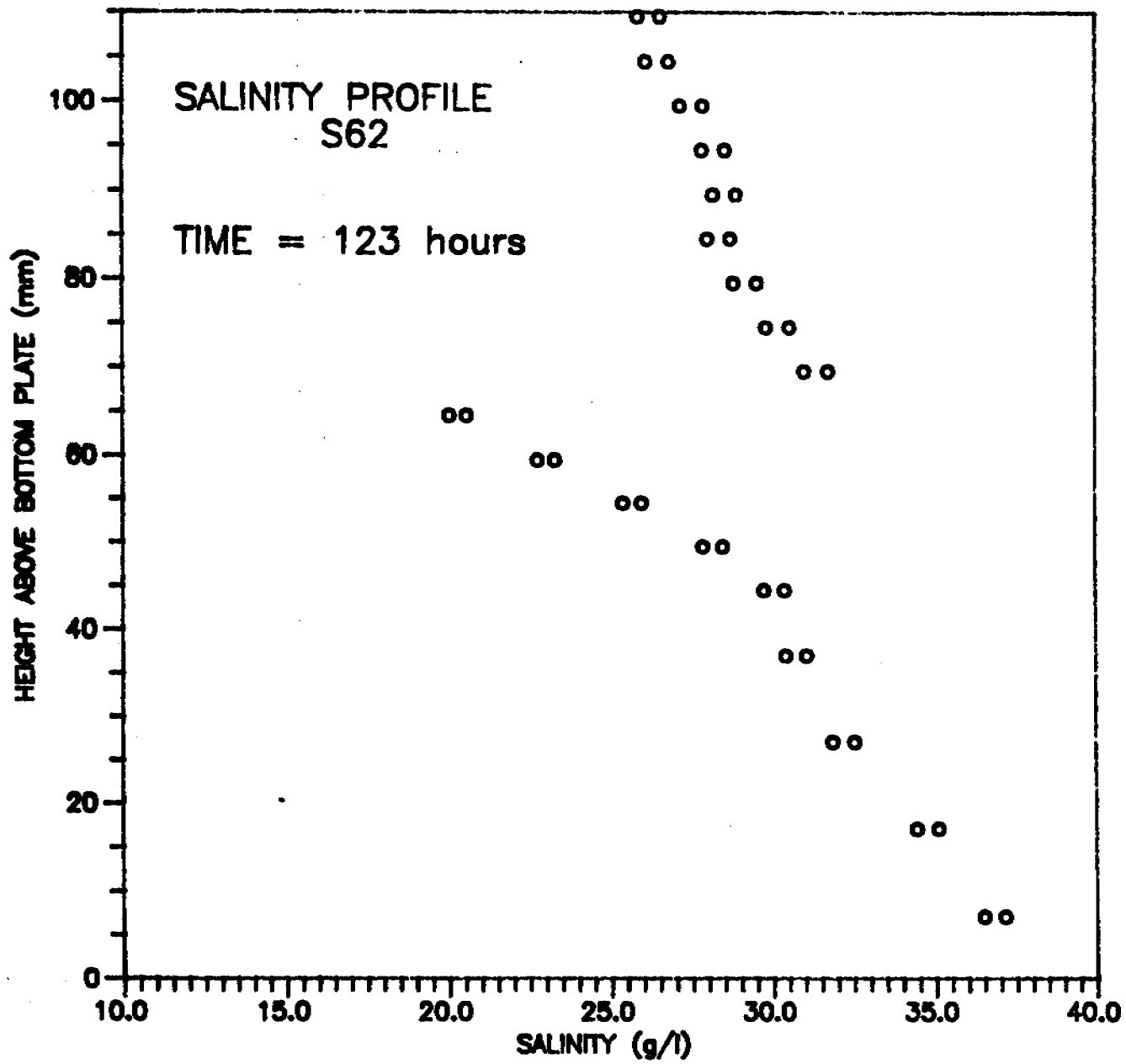
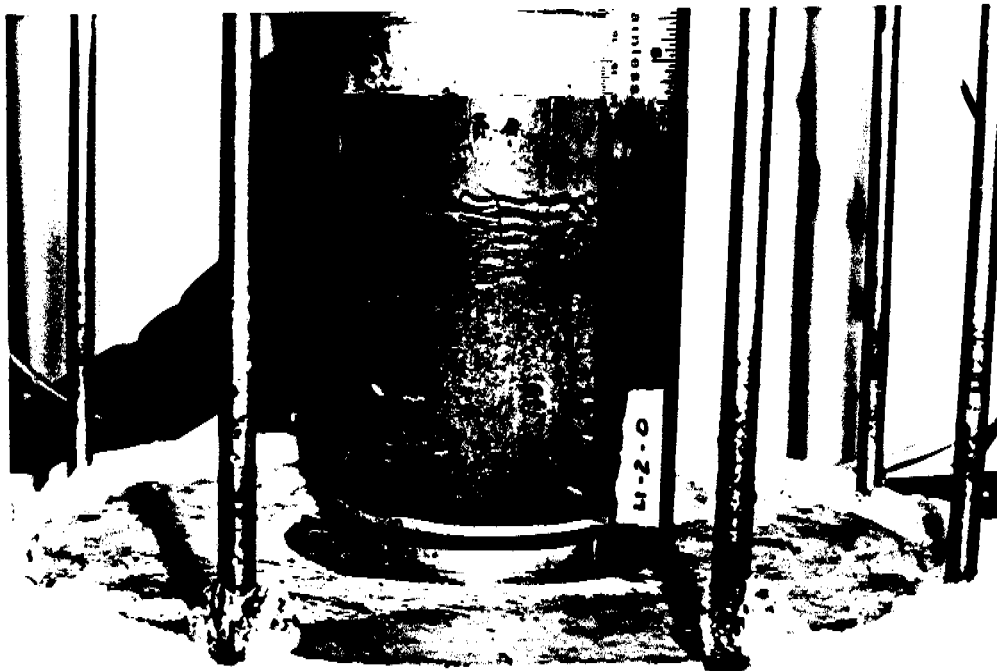


Fig. 42



Note: Original sample identification was changed in the report for reasons of simplicity.

PLATE 1 TEST S12

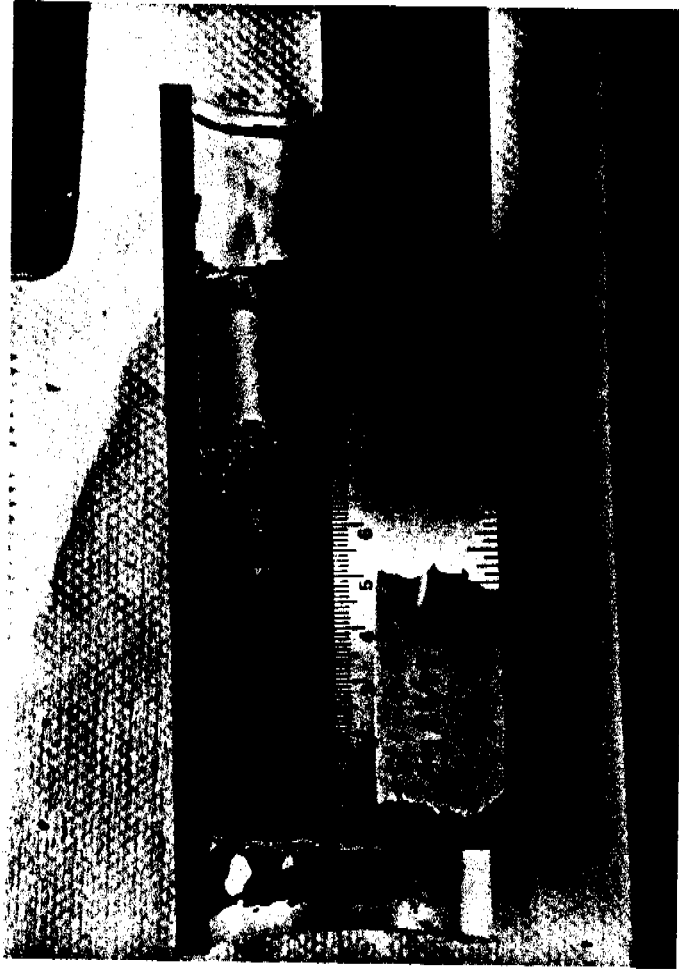


PLATE 2 TEST S70



PLATE 3 TEST SAP 1

ICE FORMATION IN SALINE SOILS

APPENCICES 1 - 3

SUPPLY AND SERVICES CANADA

HULL, QUEBEC

(DSS File No. 63SS.23233-7-1080)

March, 1989

APPENDIX 1 - Soil Properties

The soil used in the present investigation was clayey silt obtained from Devon, Alberta. The grain size distribution is shown in Fig. 1.1. The clay size fraction constitutes about 26 % by weight of dry soil and is mainly composed of quartz, feldspar and clay minerals such as smectite, dolomite with some traces of chlorite, illite and calcite.

The samples were consolidated from a slurry to 130 kPa and allowed to rebound under different applied surcharges of respectively 0, 50, 100 and 130 kPa. The water contents after rebound are plotted on Fig. 1.2 as a function of each surcharge and of the salinity of the pore water. As shown, salinity does not affect the final water content. The loading history, however, affects the water content. Samples allowed to rebound under zero applied surcharge display the highest water content while samples that were not allowed to rebound after primary consolidation was complete showed the lowest water content, i.e. about 23 %.

This figure confirms that the adopted procedure for sample preparation yielded reproducible properties and was therefore adequate.

APPENDIX 2 - Freezing Cells and Equipment

App. 2.1 Freezing cells

Plate 2.1 shows the frost heave cell used to perform freezing test with applied surcharge. The equipment displays the following key features:

- a) A sample container with a 10 cm i.d. and a wall thickness of 16.5 mm. The PVC container is split vertically in two halves and is teflon lined (white colour on photograph)
- b) Sample container barrel is 27 cm long.
- c) Insulation around the container is fiberglass pink over a thickness of about 9 cm contained by a steel cylinder. An additional layer of about 10 cm is installed around the outside cylinder as shown on Plate 2.2
- d) Soil sample temperature is measured by one array of thermistors installed flush with the cell wall at regular spacings of about 13 mm. The accuracy of the thermistors is about ± 0.02 C. Thermistor calibration procedure was done at 0 C using distilled water and ice-cubes made from distilled water. A digital high precision multimeter was used to obtain the off-sets and the slopes of the calibration curve for each thermistor.
- e) Heave is measured to within ± 0.001 mm by a DCDT
- f) The water supplied to the test sample is measured with an accuracy of ± 0.1 ml, which is equivalent to an accuracy of ± 0.0013 mm when translated to heave. The burette was adjusted regularly to maintain the external water level 10 cm above the top of the sample.
- g) Load is applied to the sample with a bellofram air pressure system which provides up to 700 kPa loading. Pressure is obtained with an air regulator and a Bourdon gauge accurate to 1 kPa. The pressure is checked daily.
- h) Porous end plates are installed at each heat exchanger.
- i) Heat exchangers are controlled with a Daytronic Advanced Data Acquisition and Control system.
- j) Temperature baths (Hot-Pack) were used to impose the temperature boundary conditions during freezing.

- k) Data was collected every hour. Dedicated software (developed at WATFROST,UW) is used for data processing. The key feature of the software is a 7-point regression model used to automatically estimate rates of change in time-dependent parameters from the experimental data. This is of significant value for the determination of heave rate, freeze rate and cooling rate. The same model is also used to calculate the temperature gradient in the frozen soil near the frost front (T_i °C) and obtain the segregation potential based on total heave data.

In the original proposal, the freezing tests were to be conducted in a 10-cm diameter freezing cell (described above). However, since two years of testing was to be produced in about 15 months, it was agreed that two additional freezing cells be built. Because soil contaminated with salt cannot be re-used, the size of these cells was reduced. Each of the cells has a diameter of 5 cm and a height of 15 cm. The design of these cells is illustrated on Plate 2.3.

Freezing tests on control samples showed that the freezing characteristics, i.e. SP, were independent of the size of the cells, see Fig. 28.

Tests with applied surcharge were thus conducted in the 10-cm freezing cell because the load was readily applied to the samples via the bellofram system, while most of the tests with zero applied surcharge were run on the 5-cm diameter cells.

App. 2.2 Controlled Environment

A walk-in temperature-controlled chamber maintained at $+2 \pm 2$ °C was used to minimize heat transfer to the sample during freezing.

APPENDIX 3 - Pore Water Salinity Measurements

App. 3.1 Concentration Units

To have a meaningful discussion of the chemical aspect of pore water, the relative amounts of solute (salts) and the solvent (water) must be specified. This is accomplished by means of concentration units. Various types of concentration units are in use.

Molarity is the number of moles of solute in 1 m³ of solution. It is usually designated as mol/m³, but moles per liter, with the symbol mol/l, is permitted in the SI system and is commonly used in groundwater studies.

Mass concentration is the mass of solute dissolved in a specific unit volume of solution. The most common mass concentration unit reported in the literature is milligrams per liter (mg/l).

Parts per thousand (ppt) is the number of grams of solute per thousand grams of solution. If the water does not have large concentrations of total dissolved solids and if the temperature is close to 4 C, 1 l of solution weighs 1 kg, in which case 1 g/l is equal to 1 ppt. If the water has a higher salinity or temperature, density corrections should be used when converting between units with mass and volume denominators.

To convert between molarity and milligrams per liter, the following relation is used:

$$\text{Molarity} = (\text{mg/l}) / (1000 \cdot \text{formula weight})$$

with formula weight of NaCl = 58.44 g

App. 3.2 Laboratory Procedure

By extracting pore water directly from a soil it is possible to determine solute concentrations via chemical analysis. Centrifuging or sample consolidation using high pressure squeezers allow extraction of pore water. A major disadvantage of this technique, however, is the relatively small volume which can be extracted from a small soil sample that is normally or over-consolidated.

Instead of collecting enough water from any soil volume, solutes were allowed to diffuse out of the soil. A saturated soil sample was placed in a closed container with distilled water and diffusion of solutes from the soil's pore water was allowed to proceed until equal salt concentration was established between the soil's pore water and the surrounding fluid. Electrical conductivity measurements were then performed on the diluted water and averaged. Original pore water salinity was back-calculated from the following data: 1) mass and water content of the soil sample, 2) the volume of distilled water added, 3) the electrical conductivity of the diluted water sample after equalization of the solute concentration, and 4) the relationship between ion concentration and conductance.

The advantage of this technique, referred to as soluble extraction, is the small amount of soil required to perform the analysis. A salinity profile at the end of each freezing test can readily be obtained for 5 mm thick soil slices. In the frozen soil, the slices were usually 1-cm thick.

The conductance function for Sodium Chloride (NaCl)

It has long been known that the electrical conductivity or conductance (the inverse of electrical resistance) of an electrolyte solution varies with concentration and

nature of the dissolved solute (s). From tables contained in "Handbook of Chemistry and Physics, 51 st Edition (1970)", the concentration-conductive properties of aqueous NaCl solutions were obtained and plotted on Fig. 3.1.

In order to verify the accuracy of the interpreted salinity from these tables, conductance of different NaCl aqueous solutions at known concentrations were compared to those obtained from the tables. As shown on Fig. 3.1, there is a slight difference, which increases with concentration. This may be caused by other ions present in the salt used at UW. It is therefore proposed to use the experimental relationship obtained at UW for the interpretation of conductance measurements in terms of pore fluid salinity.

Procedure for soil salinity measurements

The procedure for obtaining salinity profile data from a freezing test sample was as follows:

1) Starting from the warm end of the sample, soil was cut into disks between 5 and 10 mm thick. One half of each disk was used for salinity measurements and the other half yielded water content data.

2) A known volume of distilled water was added and time allowed for solute diffusion.

3) After approximately 3 to 4 days, a known volume of clear water was removed from the containers via a precision pipette.

4) Electrical conductivity for each water sample was then measured using a YSI Model 35 Conductance Meter with a probe featuring a 10 mm electrode spacing and approximately 0.75 ml volume requirement. The output is calibrated each time against a standard solution of KCl and the correction factor is applied to the subsequent readings. For each water sample, several successive conductance readings are made and then averaged.

5) Water samples were retained for possible re-sampling in the event a profile had doubtful points.

The mass of pore water in the soil fraction is derived from:

$$M_w = M_t \cdot w / (1 + w)$$

where:

M_w = mass of pore water

M_t = total mass of soil sub-sample

w = water content

It is assumed that concentrations of solutes are sufficiently low so that the density of these waters is approximately 1 g/cc and that the volume of water is thus readily obtained.

The salt concentration of the diluted solution is calculated via the conductance function as outlined above with the proper correction factor. NaCl concentration of the pore water is then back-calculated as the product of the dilution ratio and the diluted solution concentration. The dilution ratio is the ratio of total diluted water volume and pore water volume. Thus, the following equations were used:

$$C_d = (C_1 + C_2 + \dots + C_n) / n$$

S_d from conductance equation

$$D = (V_w + V_a) / V_w$$

$$S_w = D \cdot S_d$$

where: C_d = average conductance of diluted water (5 to 10 readings)
 S_d = Salinity of diluted water
 V_w = volume of pore water in soil sub-sample
 V_a = volume of distilled water added
 D = dilution ratio
 S_w = Salinity of pore water

It should be noted that the error in pore water salinity is related to the dilution ratio. Assuming that the accuracy in conductance of the diluted solution is ± 0.01 and ± 0.05 mmho, respectively the error on pore water salinity is ± 0.06 and ± 0.50 g/l for a dilution ratio of 30 while is ± 0.02 and ± 0.14 g/l for a dilution ratio of 10. This is summarized in Fig. 3.4. All salinity profiles incorporate the error related to the dilution ratio and an overall accuracy of conductance measurements of ± 0.05 mmho.

Verification

Natural Pore Water Chemistry

Use of the previous equations and procedure neglects conductance due to ions other than sodium and chloride. Chemical analysis on natural pore water of Devon clayey silt show that the amount of dissolved natural salts in the clay is very small. The following constituents were traced:

Na (10 mg/l or 10 ppm)
 K (3.2 mg/l)
 Ca (28.1 mg/l)
 Mg (12.8 mg/l)
 Cl (28.1 mg/l)
 SO₄ (24.2 mg/l)

The total amount of dissolved salt in the natural environment is thus 106.4 mg/l or 0.1 g/l and can be neglected in the salinity analysis with NaCl salt.

Salinity Profiles after Consolidation

To verify that consolidation of the slurries at various initial salinities does not affect the salinity of the consolidated samples, the following experiment was performed. Three samples were consolidated to 130 kPa from slurries at different initial salinity concentrations. After consolidation was complete, each sample was sliced in 5 mm thick horizontal sections and water content and salinity measurements were performed resulting in the data shown in Figs. 3.3 to 3.9. The initial conditions are given in Table 3.1. In all cases, the water content profile was uniform throughout the samples, indicating that the consolidation procedure is adequate and that wall friction is negligible. The salinity distribution is also very uniform and the pore water salinity of the consolidated sample was equal to that of the slurry for each sample. The results are summarized in Table 3.1.

This test series thus demonstrates that the sample preparation is adequate since uniform conditions (water content and pore water salinity) are obtained prior to freezing.

APPENDICES 4 & 5 Freezing Test Results See Volumes 2 and 3.

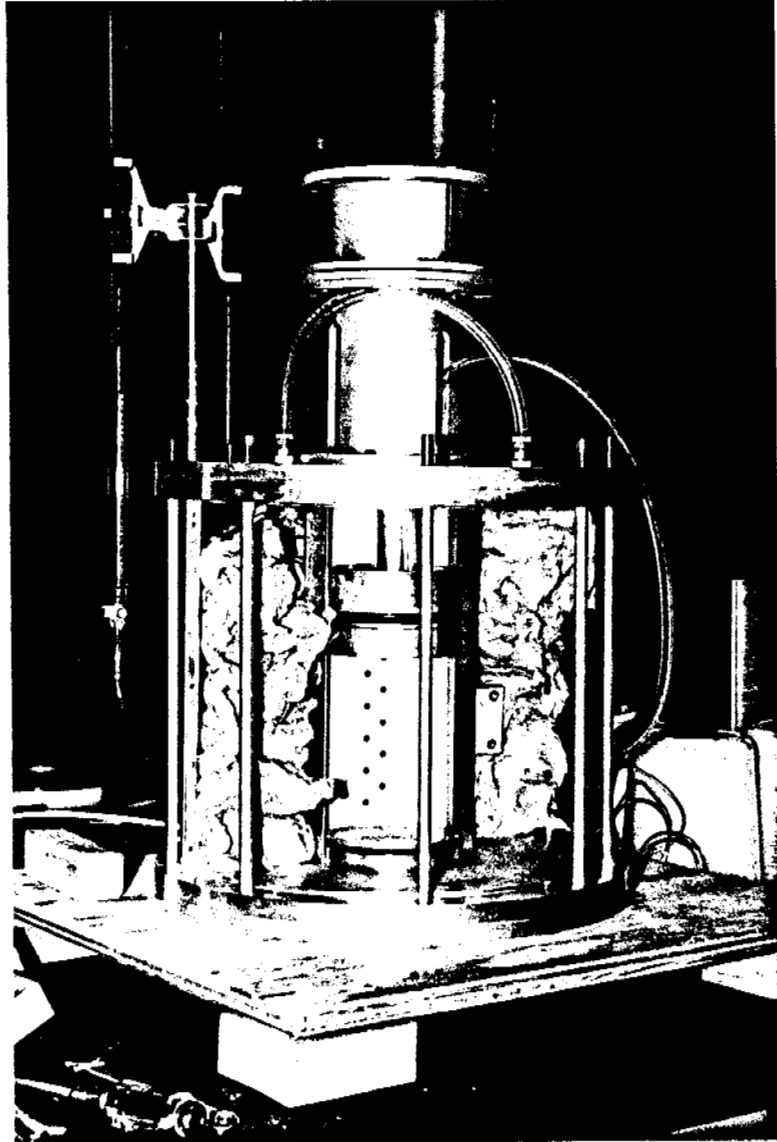


PLATE 2.1 FREEZING CELL (D=10 cm)

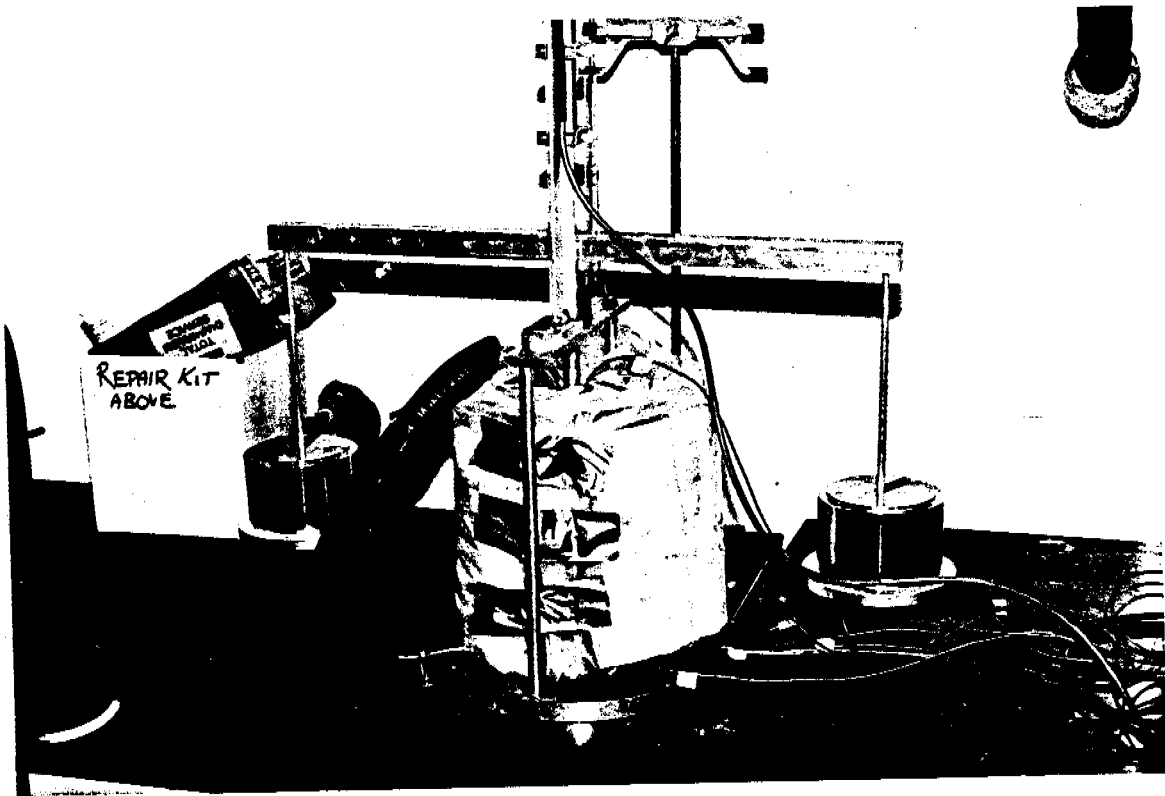


PLATE 2.2 FREEZING CELL IN COLD ROOM

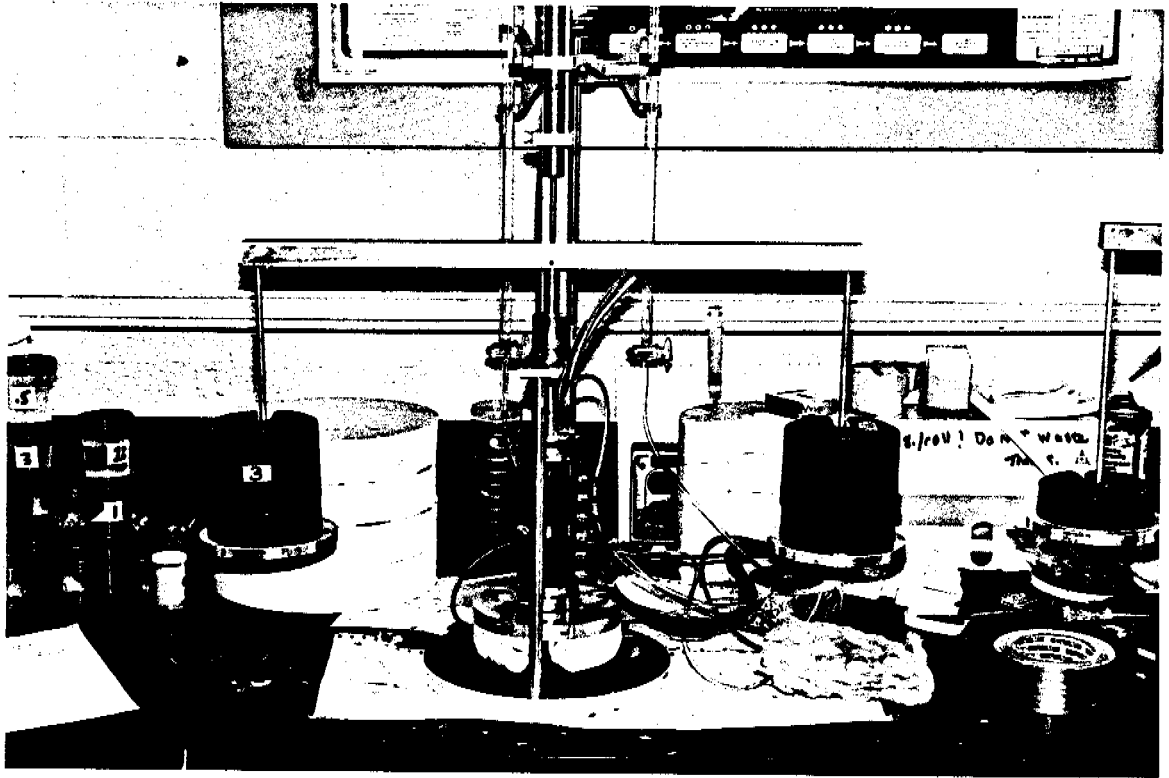


PLATE 2.3 FREEZING CELL (D = 5 cm)

Table 1.1 Physical Properties of Devon Clayey Silt at Different Salinities.

Salinity g/l	Liquid Limit	Plastic Limit
0	31.3	23.8
1.0	32.2	23.3
2.0	31.1	22.6
3.0	32.5	22.2

Table 3.1 Summary of Control Tests of Salinity Profiles after Consolidation

Test #	Water Salinity Mol/l	g/l	Slurry g/l	Water Content % Dry Weight
S22	0.06	3.44	3.6	26.0
S34	0.15	8.65	8.5	26.0
S48	0.29	17.0	16.8	27.8

GRAIN SIZE DISTRIBUTION
UNIFIED SOIL CLASSIFICATION SYSTEM
Devon Silt, Alberta

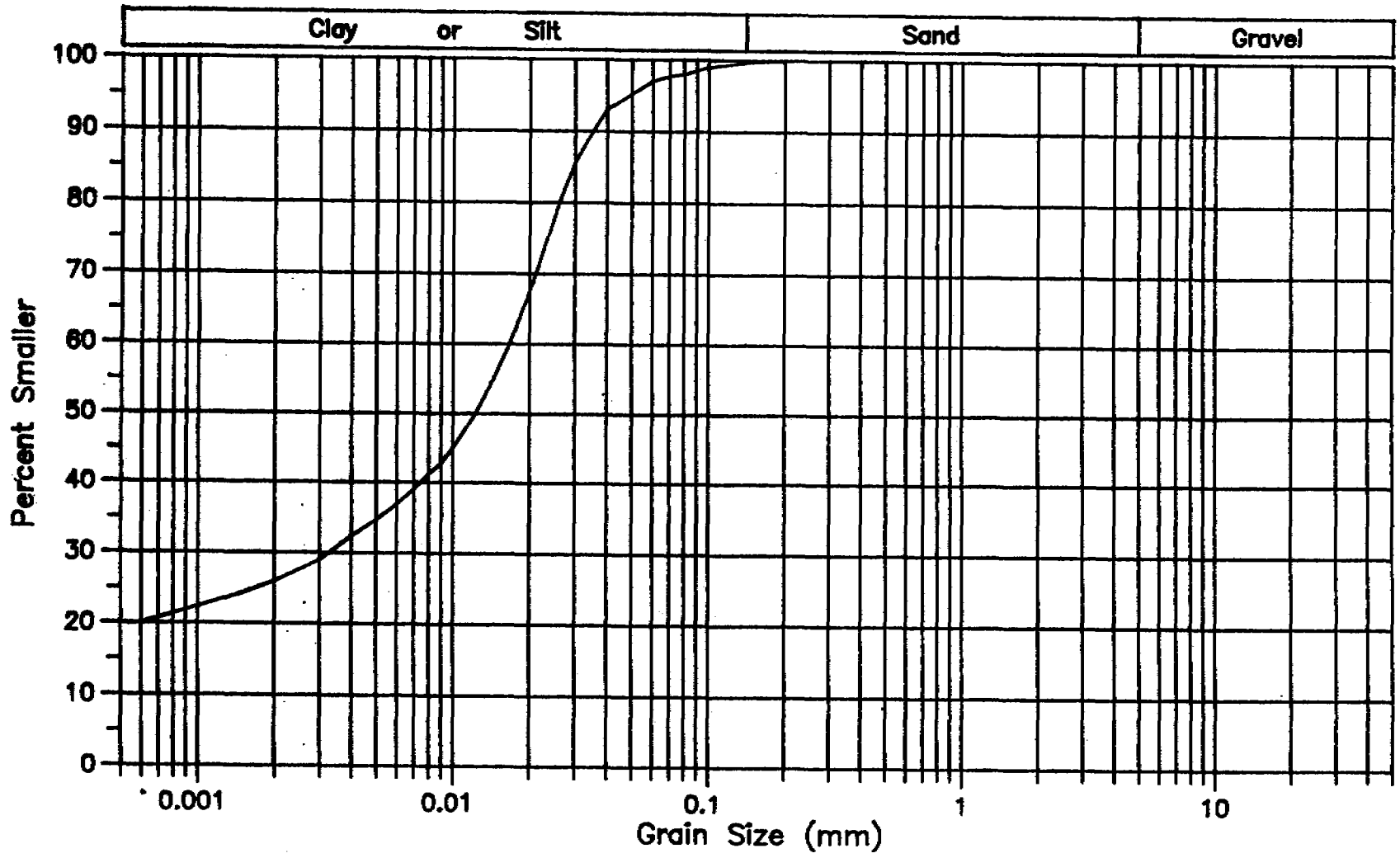


Fig. 1.1

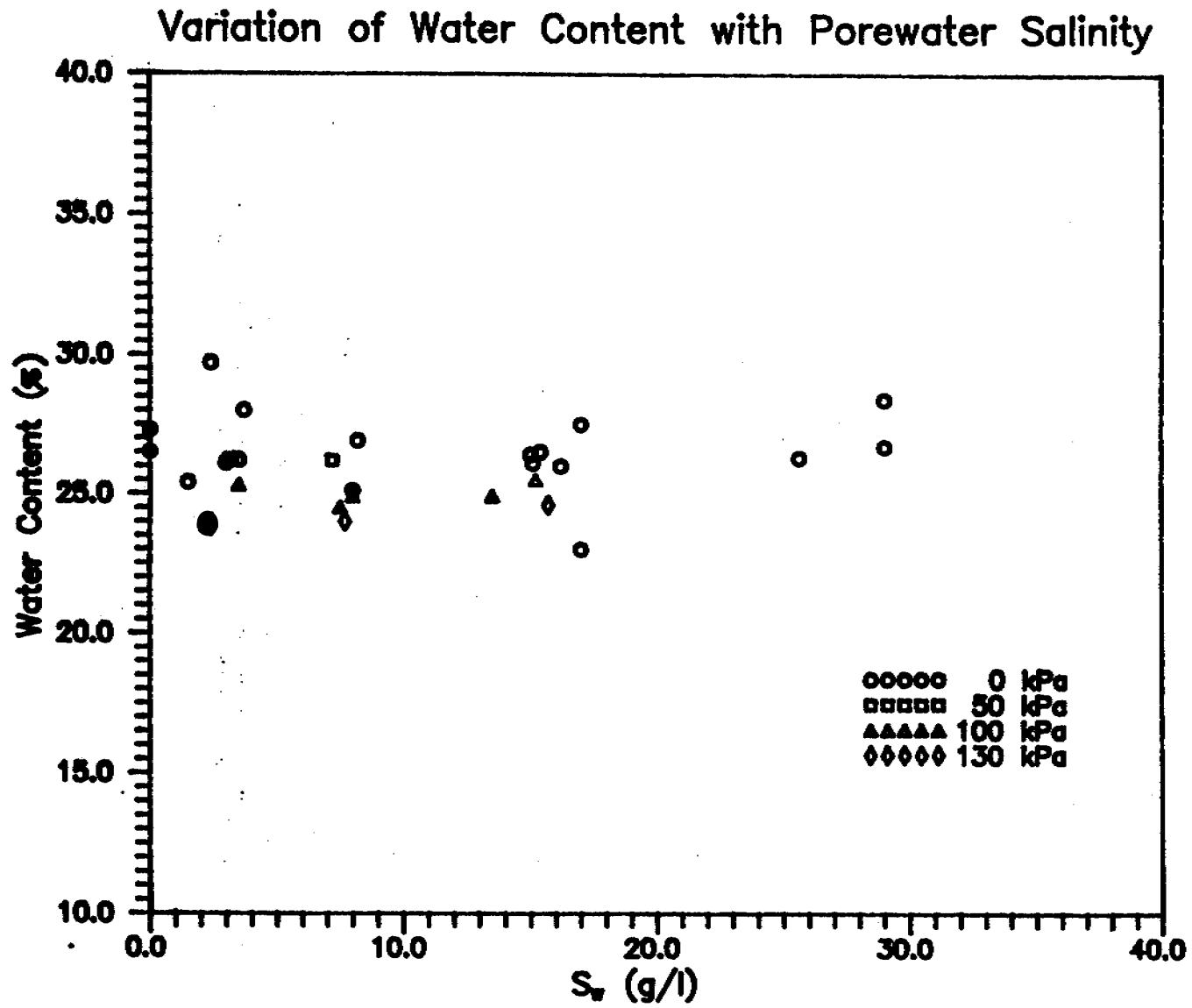


Fig. 1.2

SALINITY vs. CONDUCTANCE (NaCl)

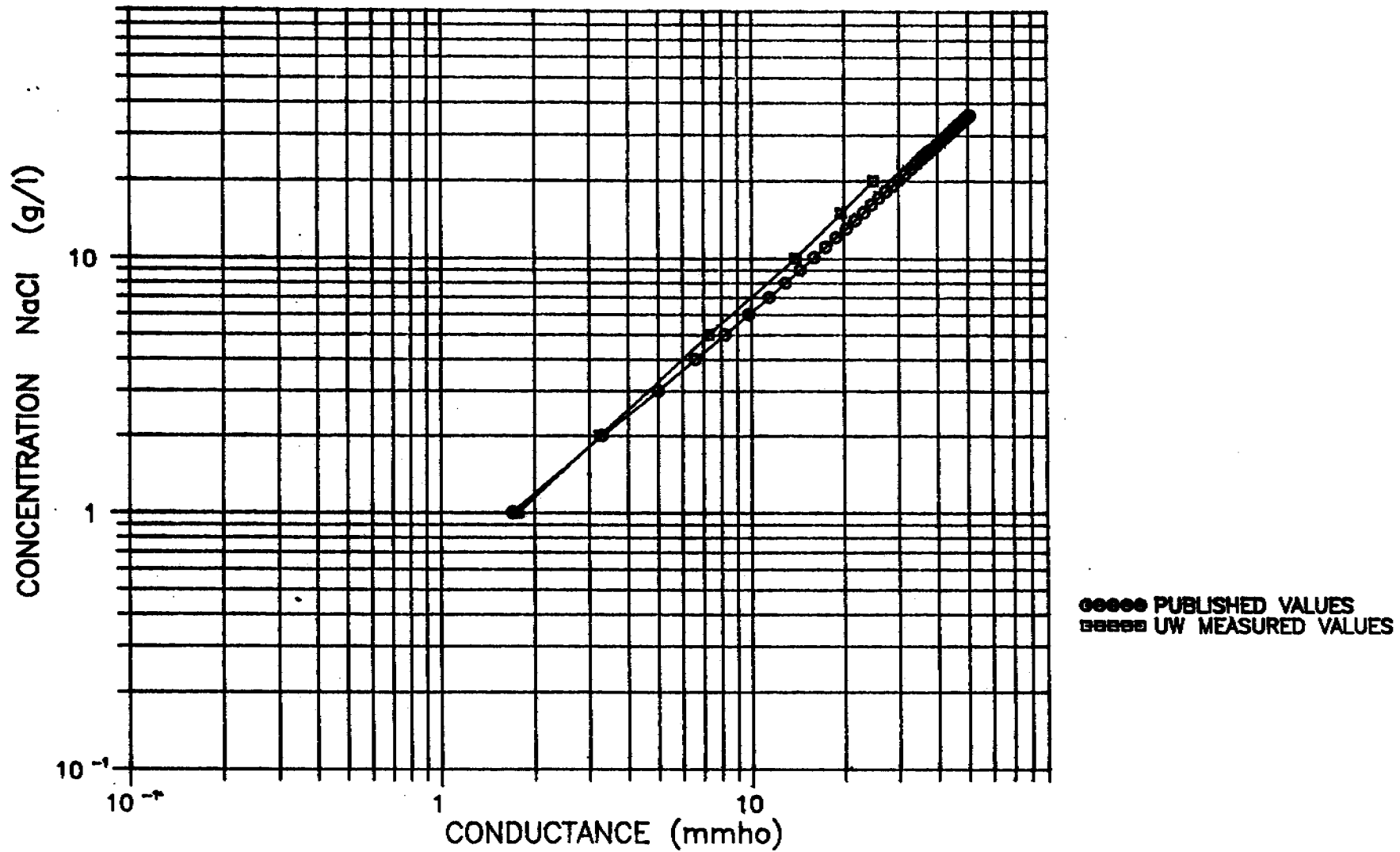


Fig. 3.1

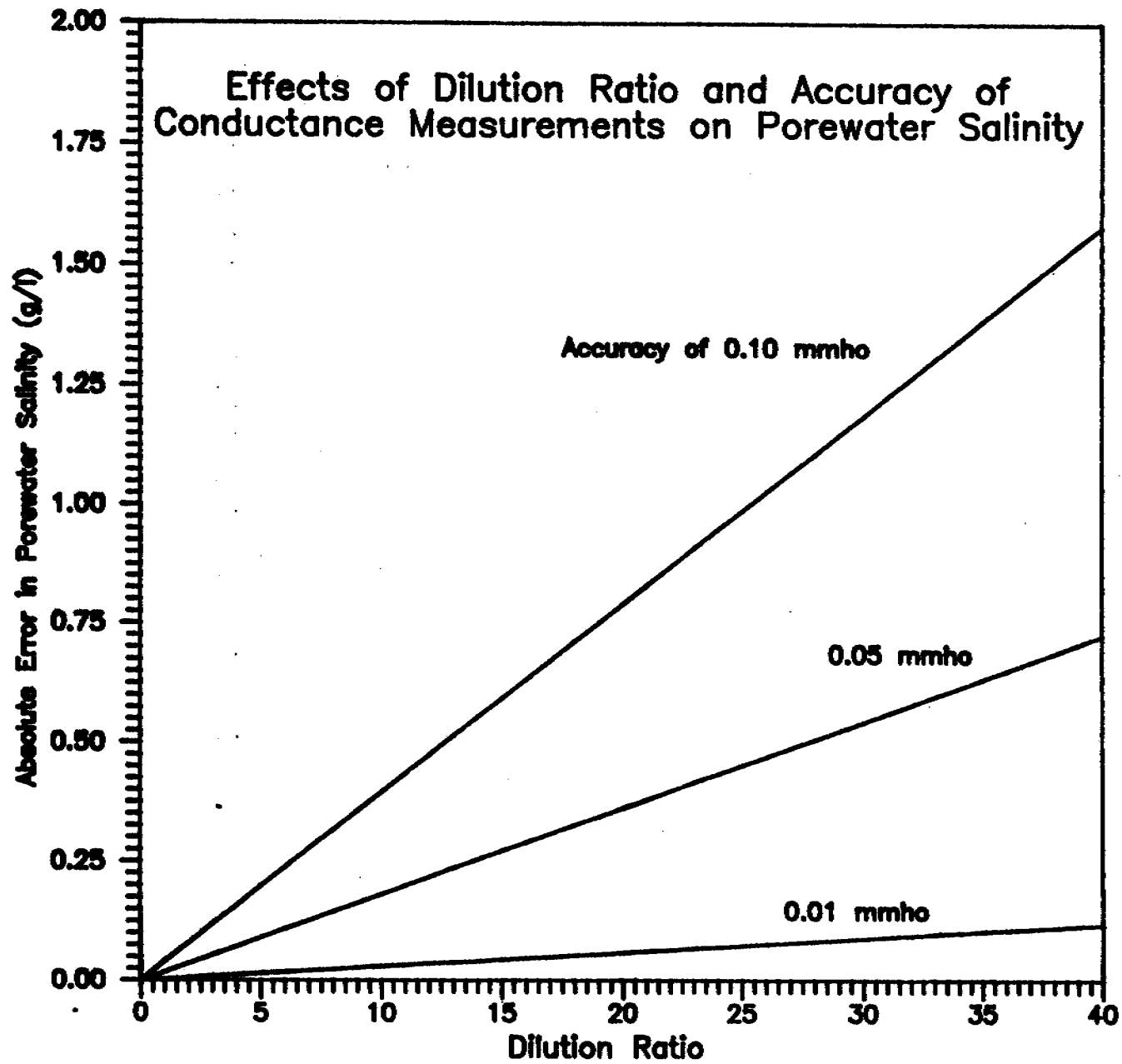


Fig. 3.2

CONSOLIDATION TEST S22

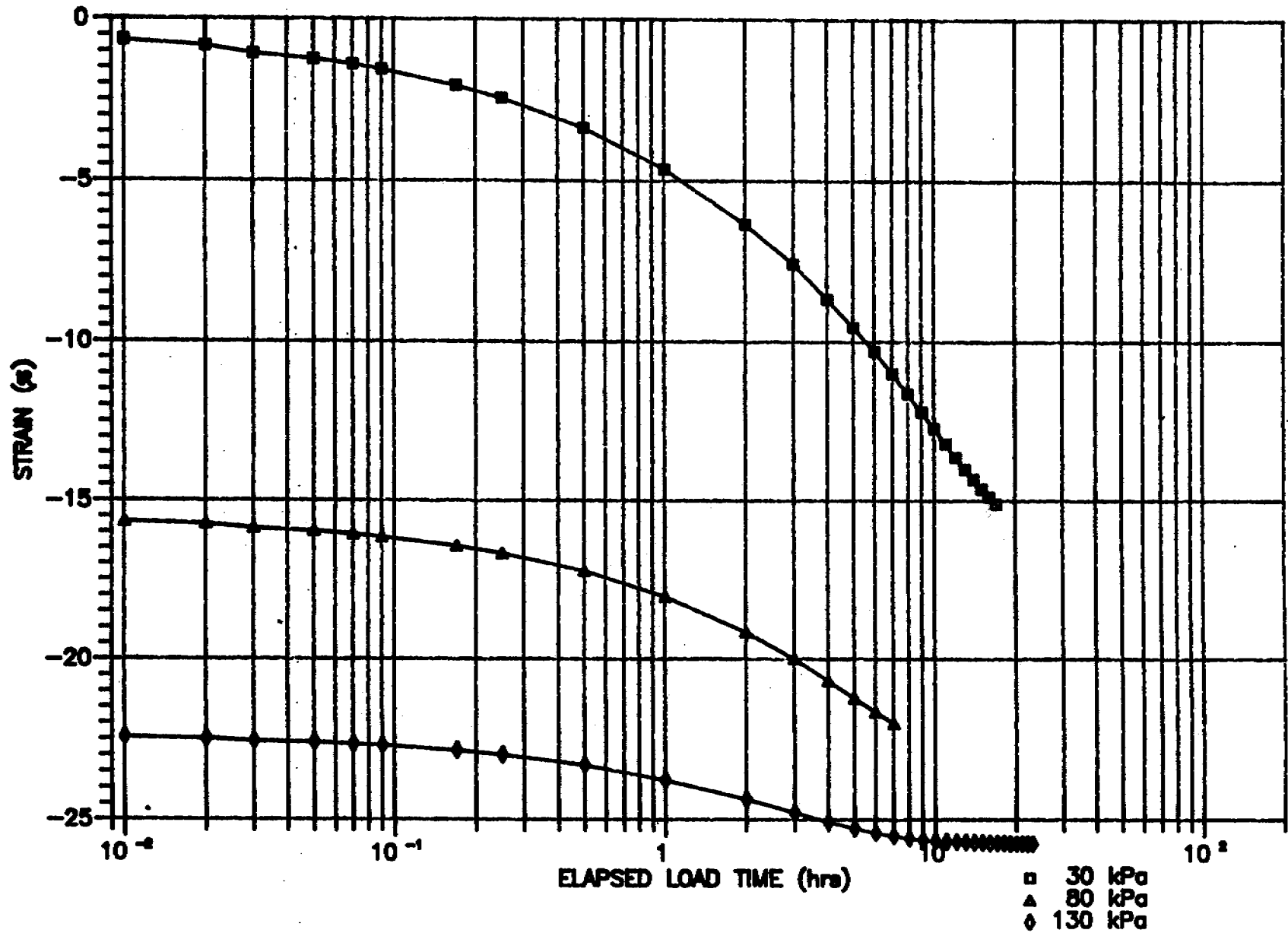


Fig. 3.3

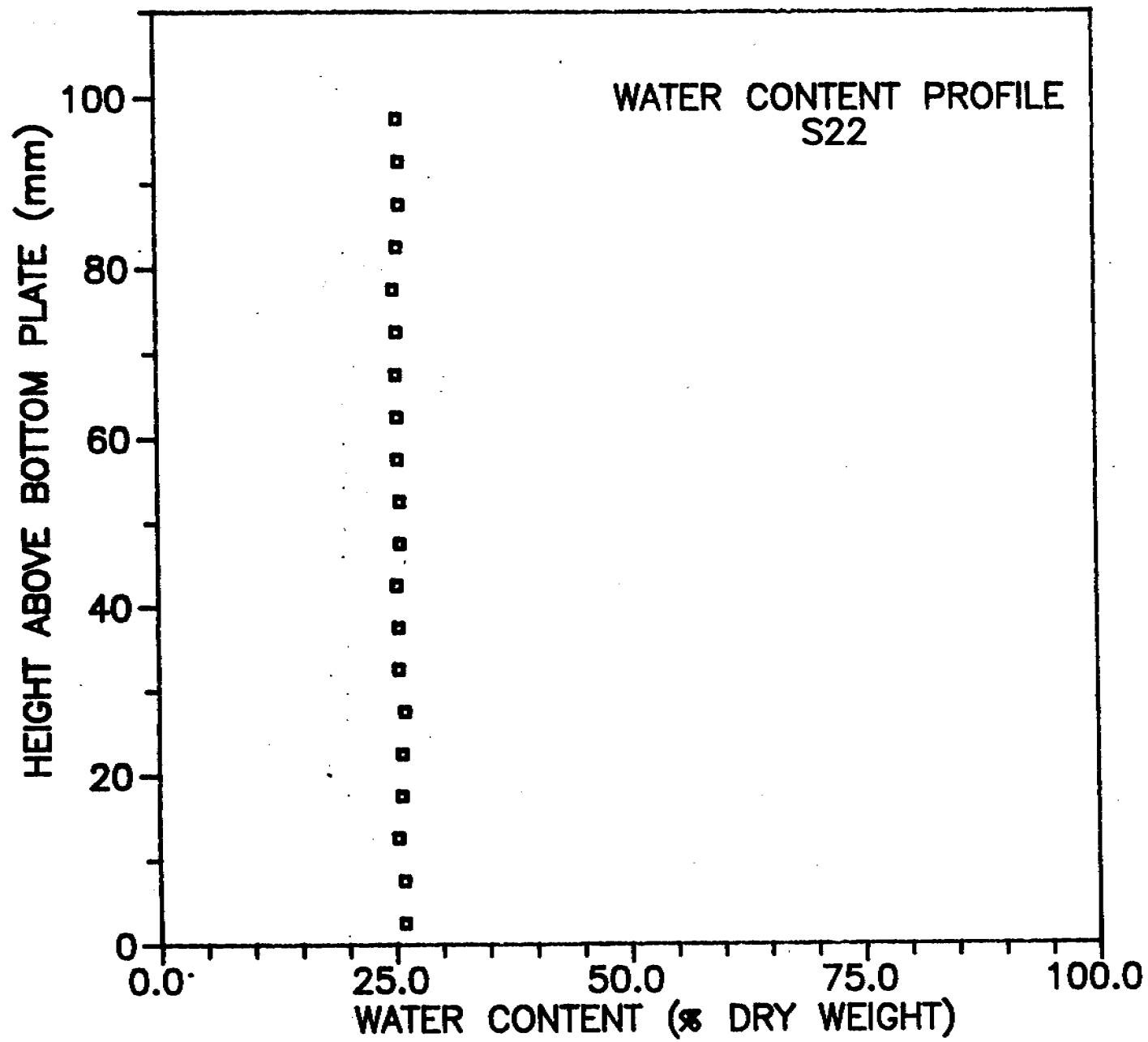


Fig. 3.4

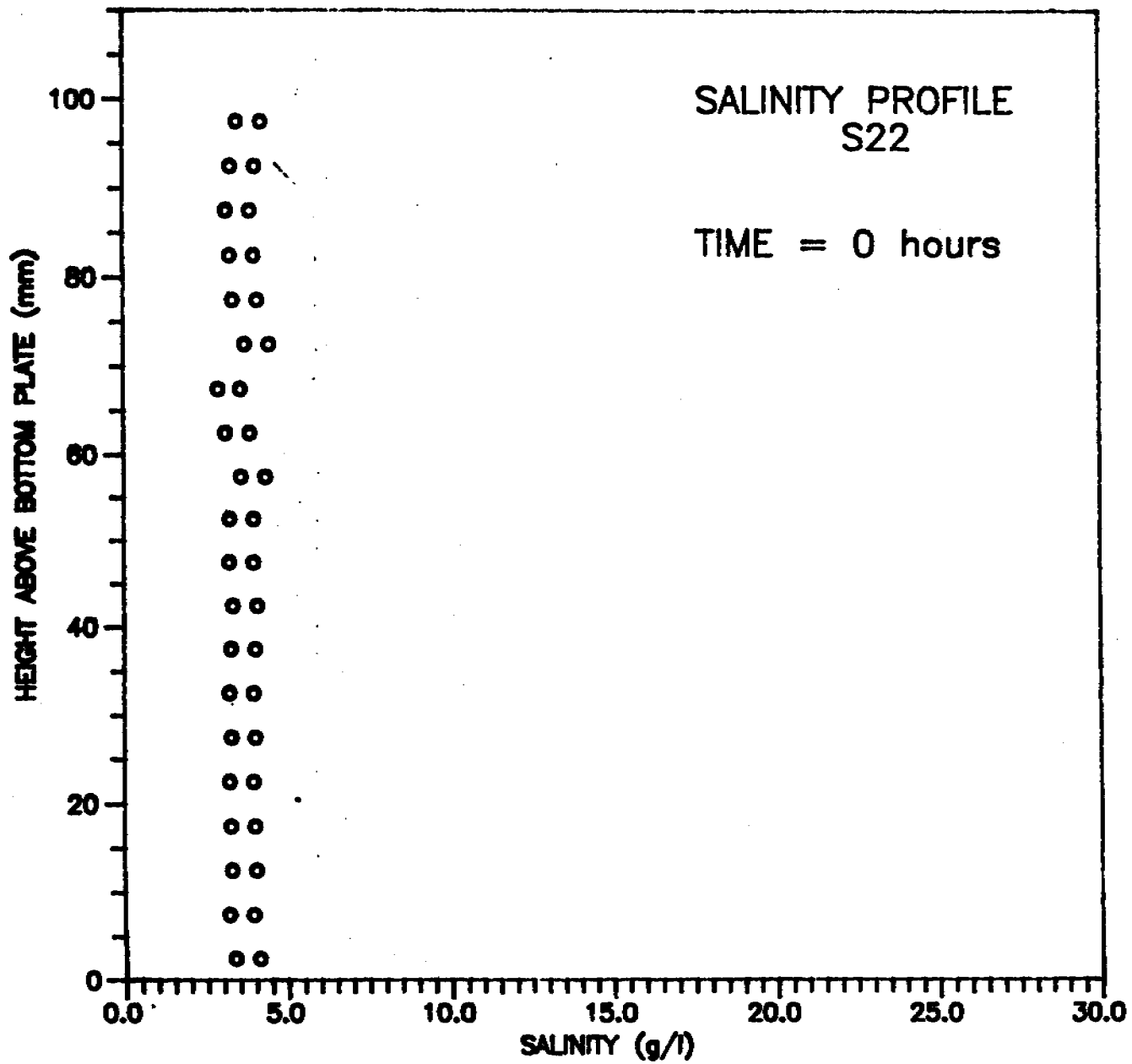


Fig. 3.5

CONSOLIDATION TEST S34

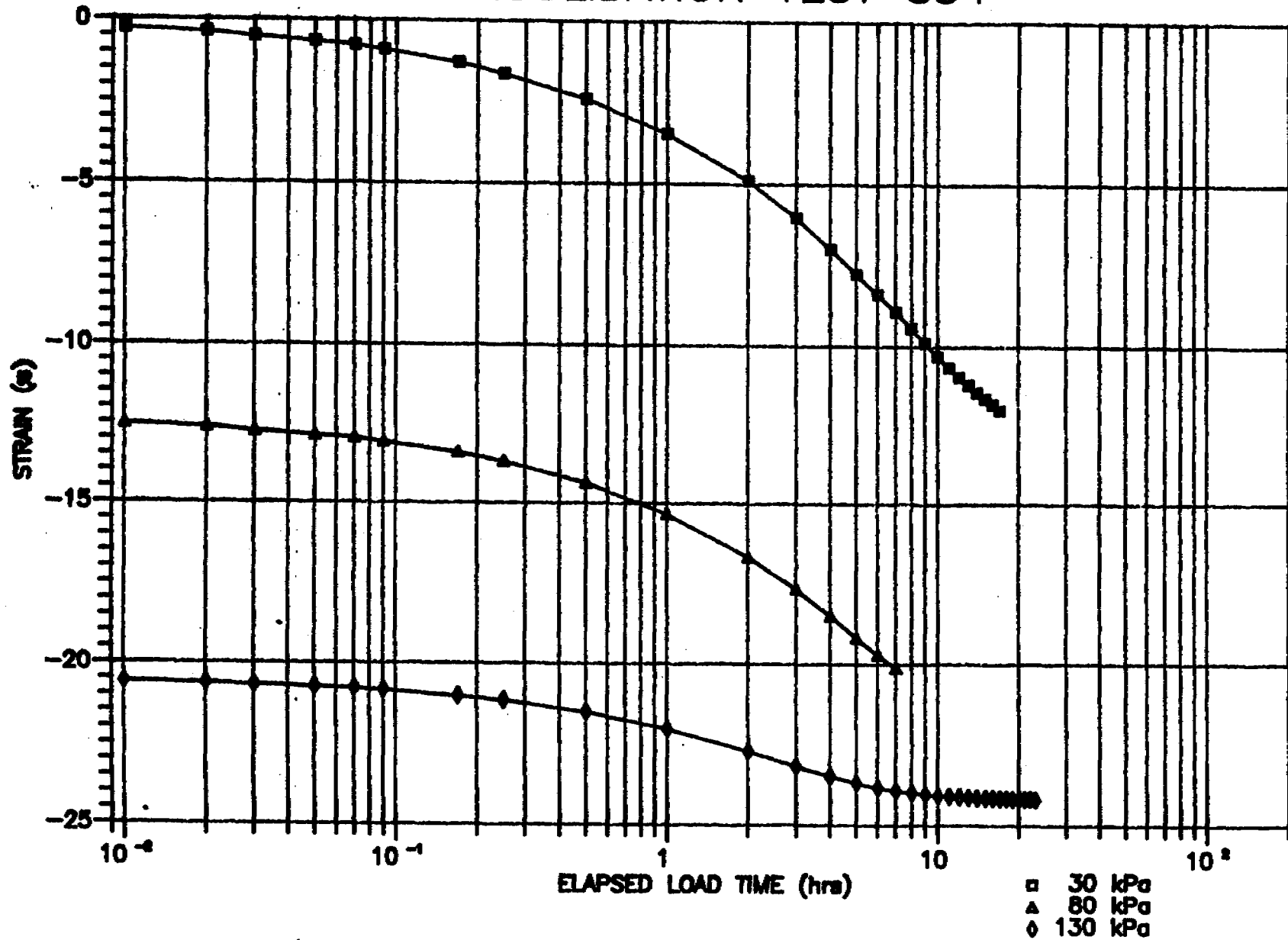


Fig. 3.6

CONSOLIDATION TEST S48

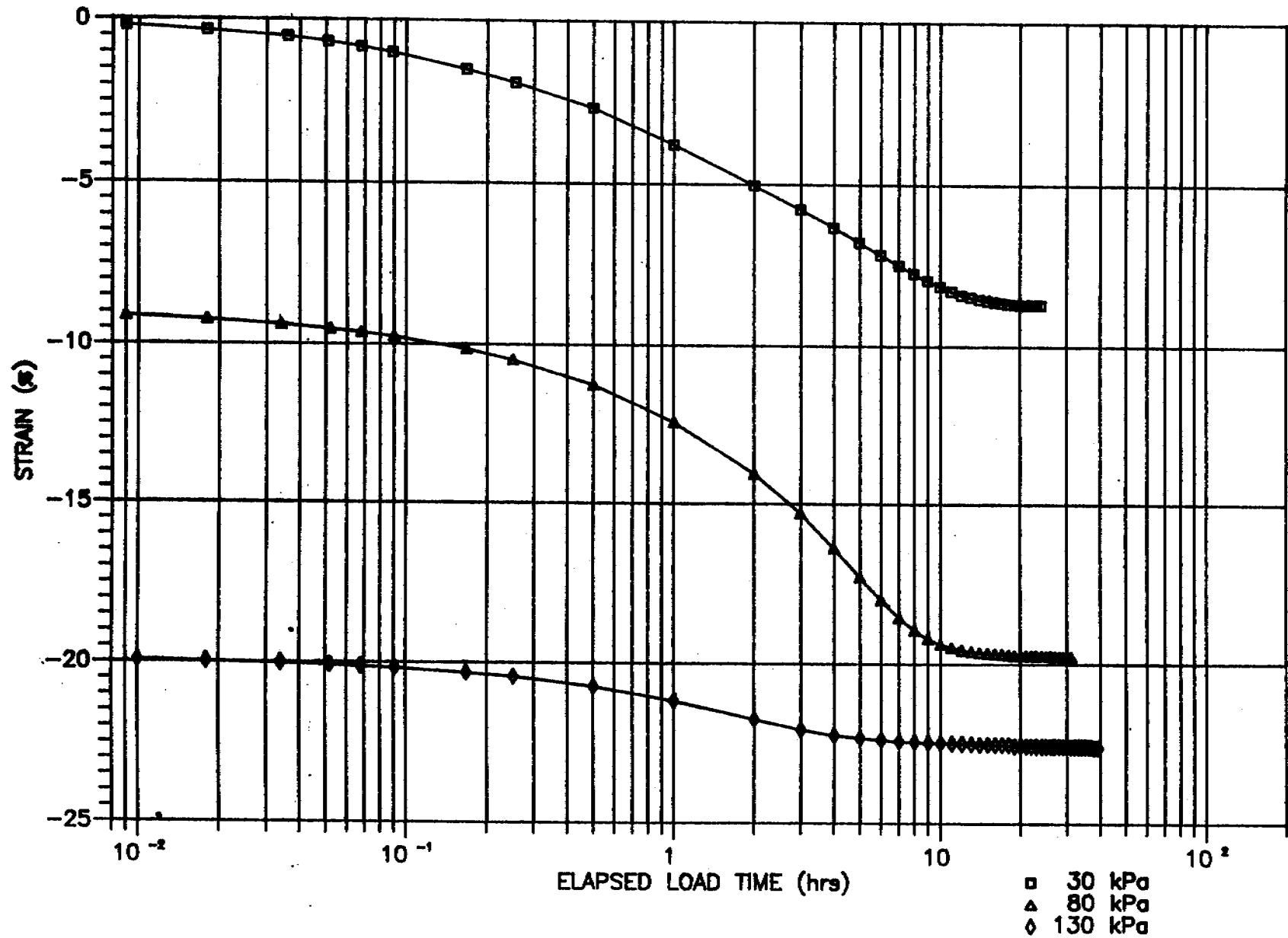


Fig. 3.7

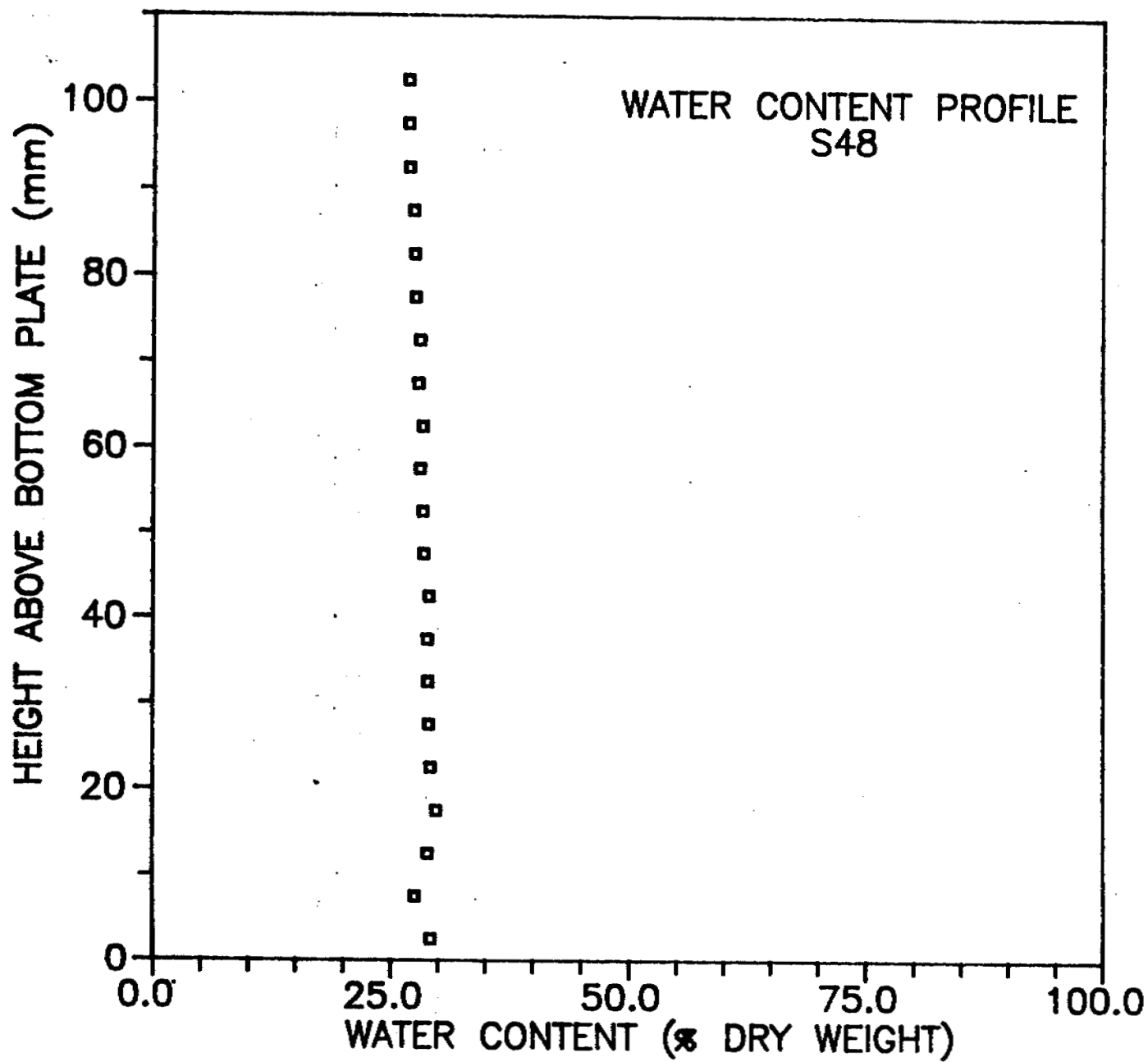


Fig. 3.8

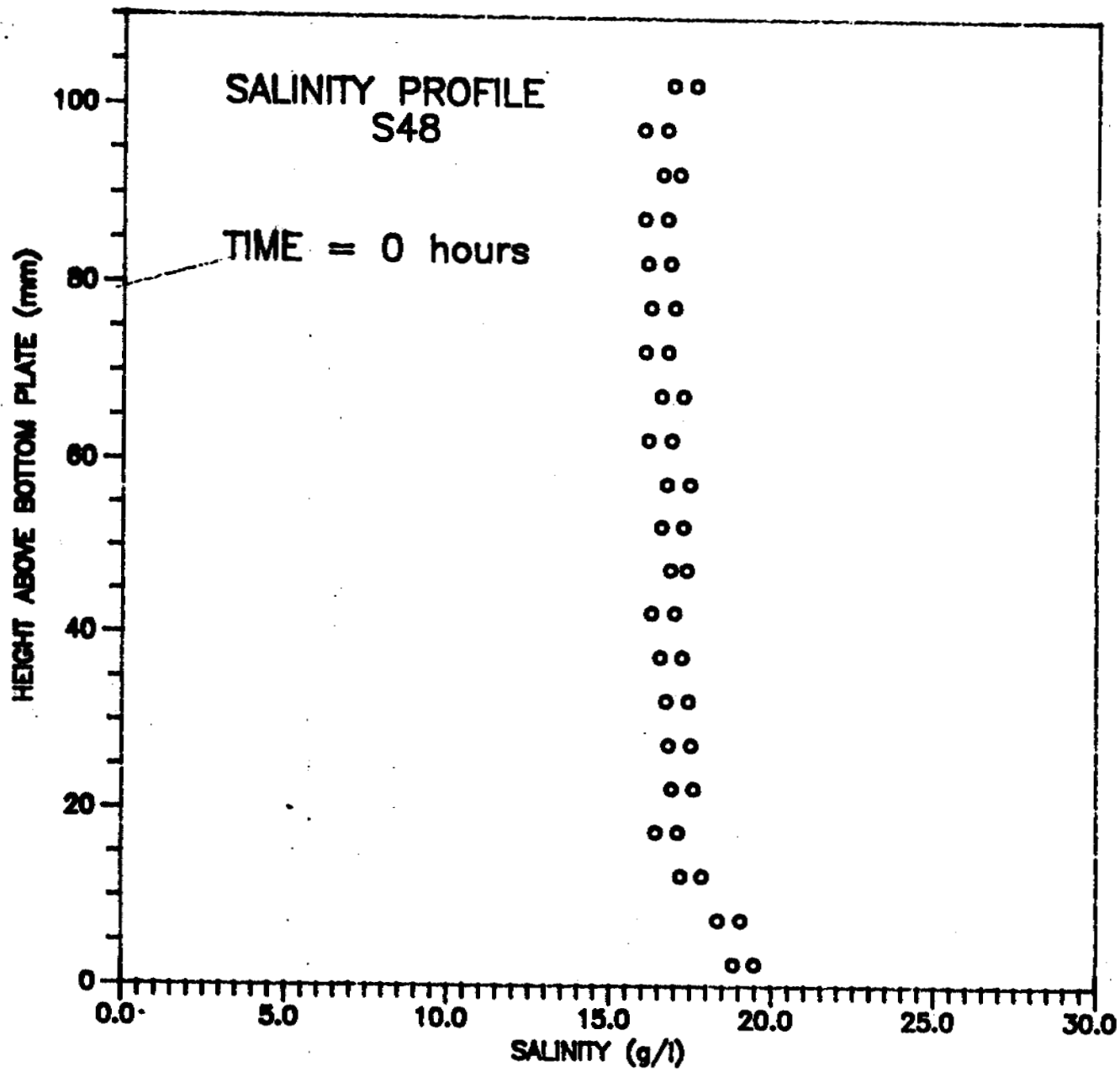


Fig. 3.9